UNIVERSITY OF CAMBRIDGE

Investigating CD8+ T-cell gene expression signatures as disease prognostic biomarkers in paediatric inflammatory bowel disease

Marco Gasparetto

Supervised by Prof Matthias Zilbauer

Hughes Hall College

HUGHES HALL
UNIVERSITY OF CAMBRIDGE

November 2018

This dissertation is submitted for the degree of Doctor of Medicine

Preface

DECLARATION OF ORIGINALITY

This dissertation is the result of my own work and includes nothing which is the outcome of work done in collaboration except as declared in the Preface and specified in the text.
It is not substantially the same as any that I have submitted, or, is being concurrently submitted for a degree or diploma or other qualification at the University of Cambridge or any other University or similar institution except as declared in the Preface and specified in the text. I further state that no substantial part of my dissertation has already been submitted, or, is being concurrently submitted for any such degree, diploma or other qualification at the University of Cambridge or any other University or similar institution except as declared in the Preface and specified in the text.

This project was conducted between July 2014 and July 2018. The research took place within the Department for Paediatric Gastroenterology, Cambridge University Hospitals NHS Foundation Trust under the supervision of Dr. Matthias Zilbauer. Patients were consented and recruited in accordance with the study protocol “Genomics and Epigenetics in Paediatric Gastrointestinal and Immune Mediated Diseases (GEPAEDGI)”.
Preparation of samples for microarray analysis was carried out under the supervision of Komal Nayak. Bioinformatic data analysis was supervised by Felicity Payne.
Preliminary results from a limited group of patients from the same project were submitted in 2017 by my colleague Claire Lee, clinical research nurse in the same Department, as part of her Master’s Degree thesis at the University of Cambridge. I was a co-supervisor in that project.

This thesis does not exceed the word limit 60,000 words set by the Degree Committee of the School of Clinical Medicine.

Name: Marco Gasparetto
Date: 29/11/2018
Signature:

Main Publications

- **Gasparetto M**, Wong-Spracklen V, Torrente F, Howell K, Brennan M, Noble-Jamieson G, Heuschkel R, Zilbauer M. Early Treatment Response Predicts Outcome in Paediatric Ulcerative Colitis. J Pediatr Gastroenterol Nutr. 2018 Feb 23. doi: 10.1097/MPG.0000000000001941. PMID: 29481442.

- Howell KJ, Kraiczy J, Nayak KM, **Gasparetto M**, Ross A, Lee C, Mak TN, Koo BK, Kumar N, Lawley T, Sinha A, Rosenstiel P, Heuschkel R, Stegle O, Zilbauer M. DNA Methylation and Transcription Patterns in Intestinal Epithelial Cells from Pediatric Patients with Inflammatory Bowel Diseases Differentiate Disease Subtypes and Associate with Outcome. Gastroenterology 2017 Oct 11. pii: S0016-5085(17)36241-8. doi: 10.1053/j.gastro.2017.10.007.

- Zilbauer M, Zellos A, Heuschkel R, **Gasparetto M**, Kraiczy J, Postberg J, Greco L, Auricchio R, Galatola M, Embleton N, Wirth S, Jenke A. Epigenetics in Paediatric Gastroenterology, Hepatology, and Nutrition: Present Trends and Future Perspectives. J Pediatr Gastroenterol Nutr. 2016 Apr;62(4):521-9. doi: 10.1097/MPG.0000000000001053. Review. PMID: 26628441.

- **Gasparetto M**, Guariso G, Visona' Dalla Pozza L, Ross A, Heuschkel R, Zilbauer M. Clinical course and outcomes of diagnosing Inflammatory Bowel Disease in children 10 years and under: retrospective cohort study from two tertiary centres in the United Kingdom and in Italy. BMC Gastroenterol. 2016;16(1):35. doi: 10.1186/s12876-016-0455-y. PMID: 26976427

- Kraiczy J, Nayak K, Ross A, Raine T, Mak TN, **Gasparetto M**, Cario E, Rakyan V, Heuschkel R, Zilbauer M. Assessing DNA methylation in the developing human intestinal epithelium - potential link to Inflammatory Bowel Disease. Mucosal Immunol 2015, Sep 16. doi: 10.1038/mi.2015.88. Epub 2015 Sep 16. PMID: 26376367.

Main Poster Presentations and Talks

- 51st Annual Meeting of ESPGHAN (European Society of Gastroenterology Hepatology and Nutrition). Geneva, Switzerland. Palexpo. May 2018.

  Oral presentation: **Gasparetto M**, Nayak K, Lee C, Kraiczy J, Payne F, Torrente F, Heuschkel R, Lyons P, Zilbauer M. Investigating CD8 + T-cell gene expression signatures as potential prognostic biomarkers in paediatric inflammatory bowel disease.

  Oral presentation: Hensel K, Cunion D, **Gasparetto M**, Brennan M, Folan A, Lee C, Torrente F, Zilbauer M, Heuschkel R. Looking the truth in the eye - benchmarking care and outcomes against the world's largest paediatric IBD registry.

  Poster presentation: Orfei M, **Gasparetto M**, Hensel K, Heuschkel R, Zilbauer M, Torrente F. Headache and active IBD: think centra vein! Case report and review of the literature.

- The Hughes Hall Life Sciences Research Symposium 2018. Pavillion Room, Hughes Hall College, University of Cambridge, United Kingdom. March 2018.

  Oral presentation: **Gasparetto M**. Investigating CD8+ T-cell gene expression signatures as potential prognostic biomarker in paediatric inflammatory bowel disease.

- 50th Annual Meeting of ESPGHAN (European Society of Gastroenterology Hepatology and Nutrition). Prague Congress Centre, Prague, Czech Republic. May 2017.

  Poster presentation: Alterio T, Torrente F, Brennan M, Zilbauer M, Heuschkel R, **Gasparetto M**. Management and outcomes of children with localised ileo-caecal Crohn's disease: survey from a tertiary-level centre. Cambridge University Hospitals, Addenbrooke's, Department of Paediatric Gastroenterology, Hepatology and Nutrition, Cambridge, United Kingdom

  Poster presentation: Lee C, **Gasparetto M**, Brennan M, Folan A, Cunion D, Maidment M, Torrente F, Heuschkel R, Zilbauer M. Implementation of an international quality improvement initiative for children with inflammatory bowel disease (IBD) - A UK site perspective of ImproveCareNow (ICN). Cambridge University Hospitals, Addenbrooke's, Department of Paediatric Gastroenterology, Hepatology and Nutrition, Cambridge, United Kingdom.

- 5th World Congress of Paediatric Gastroenterology, Hepatology and Nutrition. October 5-8, 2016. Montreal, Canada. Palais des Congres.

  Poster presentation: **Gasparetto M**, Wong-Spracklen V, Torrente F, Heuschkel R, Brennan M, Noble-Jamieson G, Zilbauer M. Clinical outcomes in pediatric ulcerative colitis: a single-centre cohort study.

- 48th Annual Meeting of ESPGHAN (European Society for Paediatric Gastroenterology, Hepatology and Nutrition). 6-9 May, 2015. The Amsterdam RAI Exhibition and Convention Centre, Amsterdam, The Netherlands.

  Poster presentation: **Gasparetto M**, Guariso G, Visona' Dalla Pozza L, Torrente F, Brennan M, Heuschkel R, Zilbauer M. Assessing phenotype and disease course in children with earlier onset of IBD (< 11 years). Data from two tertiary centres in the United Kingdom and in Italy.

Acknowledgments

These Cambridge years have been the most exciting, revealing and challenging of my whole life.
I will never forget the chances I have been given, and the difficult times I have managed to overcome. All of it made me a stronger and better person, and I now feel more than ready as a professional to embrace the next career step with competence and enthusiasm.
I would like to dedicate this thesis to the following people, who have supported me in many significant ways:

Matthias Zilbauer, my Academic Supervisor, for his input and guidance in this project through the good and difficult times. Thank you for leading me throughout this overwhelming experience.

Robert Heuschkel, my Clinical Supervisor, for allowing me to refine my clinical skills whilst having protected time to undertake this research project.

CICRA (Crohn's in Childhood Research Association) for giving me the opportunity of a three-year fellowship that made this research work possible.

My Mum and Dad, and my sister Anna, for supporting my passion for this job and my dream of pursuing a career, no matter how far from home that may lead you.

Graziella Guariso, for teaching me paediatric gastroenterology and for giving me the chance to start this professional experience in Cambridge.

Paul Lyons and Eoin McKinney, for their precious guidance in this project.

Felicity Payne, for her huge support in the final rounds of data analysis and for her friendship.

Komal Nayak, for her very hard work in preparing the samples for microarray analysis and for her kind support throughout.

Claire Lee, Judith Kraiczy, Gabi Noble-Jamieson, Franco Torrente, Camilla Salvestrini, Alexander Ross, Gina Stravou, Tom Dennison, and all my colleagues and friends in the Paediatric Gastroenterology Team and in the Paediatric Gastroenterology Laboratory at Addenbrooke's. Working together has been a grate pleasure.

Claire Leivers, Megan Roberts, Daniel Ohayon and all my Cambridge friends for welcoming me and making me feel like home from day one. Special thanks to Sam Ivell for her excellent job in proof-reading this work.

My dear friends in Cambridge University Musical Society (CUMS), in particular Sacha Lee, Harry Perkin, Millie Newis, Tanya Kundu, Rita Hess, James Downs and Er-Gene Kahng, for their invaluable friendship and for supporting me along this journey.

Julia Hwang and Bertie Baigent for sharing with me their immeasurable talents and for participating in charity concerts in support of paediatric IBD. Thanks for your friendship, thanks for making those concerts happen and for giving such high-quality performances … I will never forget how great it was to combine my passion for music and for my job.

Thank you all for being there for me throughout and for making my Cambridge years unforgettable.

Summary

Background: Currently, it is not possible to predict disease behaviour for children with inflammatory bowel disease (IBD), which is a major obstacle in an era where we strive to deliver personalised, tailored therapy. Previous investigation of gene expression profiles from CD8+ T-cells in adult IBD cohorts identified promising signatures, including a T-cell exhaustion signature, to predict disease outcome in these patients.

Hypothesis and aim: We hypothesised that adult CD8+ T-cell prognostic signature and T-cell exhaustion signature would also predict outcome in paediatric IBD. We also hypothesised that CD8+ methylation profiles would underpin changes in gene expression, hence providing an alternative potential predictor. The aim of this project was to test whether CD8+ T-cell gene expression and methylation signatures can predict disease outcome in children with IBD.

Methods: Purified CD8+ T-cells from a prospective cohort of 112 children newly diagnosed (treatment naïve) with IBD were subjected to cellular genome-wide RNA and DNA profiling (affymetrix and epic methylation microarrays). Detailed clinical information from each patient was recorded in a clinical database (1.5 years follow-up). First, the adult CD8 prognostic signatures were applied to the paediatric data in order to test for their ability to differentiate children according to their disease behaviour. Subsequently, the paediatric data was analysed on its own through unsupervised clustering analysis and Weighted Gene Co-expression Network Analysis (WGCNA) to test for correlations between gene expression data and clinical outcome parameters. Survival analysis (kaplan meyer) was used to compare patient groups for disease outcomes, including number of treatment escalations, use of biologic treatments and surgical intervention.

Results: Applying the adult CD8 prognostic signature and the T-cell exhaustion signature to the paediatric dataset did not generate groups with significant differences in disease outcomes. Furthermore, the clinical data collected from the paediatric cohort showed that two thirds of the children had at least two treatment escalations, compared to less than 40% of the adult patients from the previous study. The analysis of the paediatric data per se identified correlations with clinical outcomes including use of biologics in Crohn's (WGCNA correlation index (CI) < 0.4) and surgical intervention in ulcerative colitis (top CI: +0.38 and – 0.59). Preliminary analysis of the CD8 methylation profile did not show any correlation with clinical outcomes in this paediatric cohort.

Conclusion: The adult prognostic CD8 signatures did not prove to be effective in children with IBD. We speculate that this could be due to the paediatric IBD phenotype being homogeneously more severe. Our findings hint the hypothesis that absent T-cell exhaustion in paediatric CD8+ T-cell could underlie a more severe disease phenotype in children. Further understanding of the mechanism of T-cell exhaustion in children has the potential to open up to future target options in paediatric IBD.

Table of contents

List of Figures

List of Tables

List of abbreviations used

5-ASA: 5-aminosalicylates

5mC: 5-methylcytosine

6-MP: 6-mercaptopurine

6-TGN: 6-thioguanine nucleotide

ADA: adalimumab

APC: antigen presenting cell

AZA: azathioprine

CD: Crohn's disease

CH3: methyl group

CpG: 5'-cytosine-phosphate-guanin-3'

CRP: C-reactive protein

EEN: exclusive entral nutrition

EIM: extra-intestinal manifestations

ESR: erythrocyte sedimentation rate

FBC: full blood count

LFTs: liver function tests

IBD: Inflammatory Bowel Disease

IFX: Infliximab

MTX: methotrexate

PCDAI: paediatric Crohn's disease activity index

PSC: primary sclerosing cholangitis

PUCAI: paediatric ulcerative colitis activity index

RT-PCR: real time polymerase chain reaction

TDM: therapeutic drug monitoring

TNF-a: tumor necrosis factor alpha

UC: ulcerative colitis

WGCNA: Weighted Gene Co-Expression Network Analysis

CHAPTER 1

INTRODUCTION

1.1 Paediatric inflammatory bowel disease (IBD)

The term inflammatory bowel disease (IBD) covers a heterogeneous group of chronic disorders of the digestive tract, causing relapsing inflammation of the intestinal mucosa. The two main entities in IBD are Crohn's disease (CD) and ulcerative colitis (UC). While in UC the inflammation is generally restricted to the mucosa of the large bowel, CD can spread throughout the entire gastrointestinal (GI) tract and affects all layers of the bowel wall (i.e., trans-mural inflammation). A third entity describes patients whose diagnostic features do not fully qualify for either CD or UC and are therefore diagnosed with IBD-unclassified (IBD-U) [1,2]. In IBD, the disease onset can range from early childhood to beyond the sixth decade of life, and over the past few decades there has been a significant increase in the incidence of this condition [1]. This increase has been particularly noticeable in children and young adults, who currently constitute almost 30% of all patients diagnosed with IBD [3-6]. In the absence of any curative treatment, patients are faced with a lifelong, often severely disabling condition.

Managing IBD in children is particularly challenging for several reasons such as body growth, puberty and the need to attend school during a crucial phase of their lives. Growth failure and impaired nutritional status are seen in 65-85% of children and adolescents diagnosed with CD, and 15-40% of these patients continue to suffer from growth deficiency throughout the course of their disease [7,8]. Delayed growth may precede any clinical evidence of bowel disease, and can severely affect the quality of life of children and adolescents with CD [9-12]. Because of its relevance to the care of children with IBD of developmental age, growth assessment was included in the Paris classification of paediatric CD, which replaced the previous Montreal classification [13].

1.2 Epidemiology of IBD

The incidence of IBD is increasing worldwide, and over the past few decades, advances have been made in understanding its evolving epidemiology. This rising pattern may be due to improvement in disease detection and recognition, as well as environmental alterations and exposure that impact the disease onset. IBD was once considered to be a "Western" disease, principally affecting patients in North America and Western Europe, but it is now clear that the incidence and prevalence of this condition are both rapidly rising in other parts of the world, with dramatic increases noted in India, Japan, China, and the Middle East [14]. IBD is, in fact, emerging in previously low-prevalence areas such as the developing world, as well as among migrant populations moving to industrialised westernised countries [14-16]. (Figure 1.1)

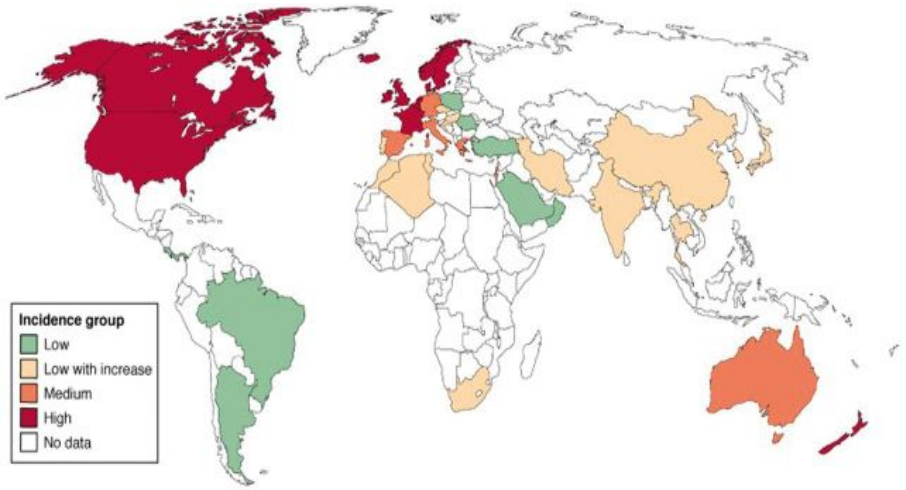

Figure 1.1 Global map of IBD in established and emerging populations. (Taken from: Cosnes J, et al. Gastroenterology 2011 [16])

The changing epidemiology of IBD across time and geographies (north-south and west-east gradients) suggests that environmental factors play a major role in modifying disease expression, and its rising incidence in developing societies seems to be linked to industrialisation and the Western lifestyle [14-19]. Individual, familial, community-, regional- and country- based environmental risk factors could, in isolation or in association, contribute to IBD's pathogenesis. Urbanisation in developing countries, diet changes, antibiotics, hygiene status, microbial exposure and pollution have all been implicated as potential environmental risk factors for IBD [20,21].

The geographical variability in IBD incidence and prevalence may, in turn, reflect a variety of underlying genetic patterns in different populations [20]. The current mean prevalence of IBD in the general population of Western countries is estimated at 1/ 1,000 inhabitants [22,23]. IBD primarily affects the Western world and the highest incidence rates are observed in North America and Europe [17, 24-26]. Recent studies in the UK indicate that the incidence of paediatric IBD is 5.2 per 100,000, where 3.1 of those cases are CD, 1.4 are UC and 0.6 are IBD-U [27]. Although there is limited epidemiology data available regarding developing countries, the incidence and prevalence of this disease have both been increasing over the past 50 years in practically all regions of the world, indicating its emergence as a global disease [14,28]. The trend appears to have stabilised in the adult population but not in children, especially in central and southern Europe where it still appears to be rising [17,18]. Incidence and prevalence of childhood-onset IBD has almost doubled over the last decade, and children currently constitute almost 30% of all patients diagnosed with IBD [14,28]. Patients can be diagnosed with IBD at any age, but peak incidences are observed in childhood (between 10-15 years of age) and early adulthood (i.e., the second to third decades of life) [17,18,29,30]. Estimates of the incidence of paediatric-onset IBD reported around the world vary considerably [31] as do its patterns and distributions in the various age brackets of the paediatric population [32,33].

The disease distribution by gender shows a slight male preponderance (1.5:1) in CD patients before puberty, whereas a female preponderance is reported in adults [34-36]. While initially relatively low, CD incidence has gradually risen to levels that are similar to those of UC [16]. CD incidence rates seem to have been stable in most industrialised countries since the 1980s, whereas an increase in childhood-onset IBD continues to be observed [37-39].

Accordingly, this disease represents an increasing burden upon global health, which is likely to continue to grow in the future.

1.3 Current models of IBD pathogenesis

The molecular patho-physiology of IBD remains largely obscure. Experimental studies and genetic evidence suggest that chronic intestinal inflammation is triggered by various environmental factors in genetically susceptible individuals. During the last decade, several genome-wide linkage and association studies have revealed over 200 genetic polymorphisms associated with an increased susceptibility to CD and UC [40-45]. (Figure 1.2)

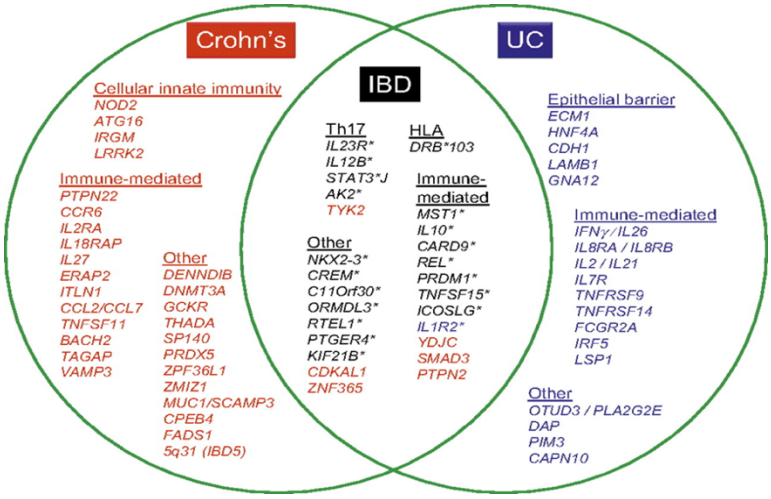

Figure 1.2 Mutations in genes implicated in the pathogenesis of IBD regulate various biological functions such as immunomodulation, mucosal barrier integrity and microbial homeostasis. (Taken from: Lees CW et al. Gut 2011. [44])

Major efforts have focused on investigating the role of genetic factors in IBD pathogenesis. A number of disease-predisposing genetic variants (i.e., Single Nucleotide Polymorphisms (SNPs)) have been identified, but these can, at best, explain up to 30% of IBD cases [46,47], which suggests that other factors make a substantial contribution to IBD pathogenesis.

Genes that are implicated in the pathogenesis of IBD regulate various biological functions such as immunomodulation, mucosal barrier integrity and microbial homeostasis [48,49].

However, despite extensive research in the field of adult and paediatric IBD using increasingly sophisticated tools, our understanding of disease pathogenesis remains incomplete for the majority of cases. Hence, the most widely accepted general hypothesis to explain the development of IBD continues to include three main factors: genetic predisposition, environmental influences and the homeostasis between the intestinal microbiome and host immunity [50] (Figure 1.3). The complex interaction of these factors is ultimately considered to cause chronic relapsing inflammation of the intestinal mucosal lining and the well-described phenotypes.

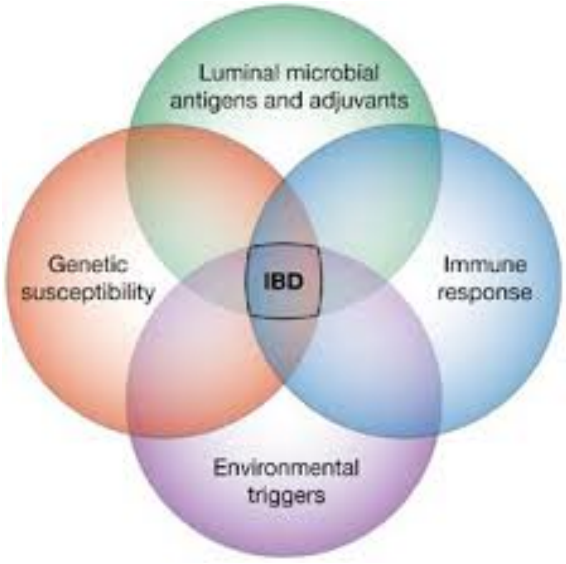

Figure 1.3 Interaction of various factors contributing to chronic intestinal inflammation in a genetically susceptible host. (Taken from: Sartor BR, et al. Nature Clinical Practice Gastroenterology & Hepatology 2006.[50])

In the absence of a major genetic factor, the environment has moved back into the focus of researchers as the possible main causative factor. Epigenetics can be defined as heritable changes to phenotype (e.g., gene expression) that are due to mechanisms other than changes to the underlying DNA sequence. These mechanisms operate at the interface between environmental stimuli and long-lasting molecular, cellular and even behavioural phenotypes that are acquired during periods of developmental plasticity [51,52]. The study of epigenetic mechanisms in IBD aims to address questions currently unanswered about the processes mediating the effects of environmental factors on the intestinal mucosa. Unlike our genetic code, which remains stable throughout life, epigenetic profiles are influenced by exposure to environmental factors (e.g. smoke), diet or even behaviour. Nevertheless, as such environmentally induced epigenetic changes are passed on during cell division, they can ultimately determine a newly acquired phenotype in offspring [53,54].

Epigenetics could therefore provide the missing link in explaining clearly heritable complex, but non-Mendelian, diseases such as IBD. To date, DNA methylation is amongst the best-studied of all epigenetic mechanisms and describes the enzymatic addition of a methyl group (CH3) to the fifth position of cytosine, forming 5-methylcytosine (5mC) [55]. DNA methylation plays a role in regulating gene expression; in particular, it is thought to target regulation sites and make them inaccessible in direct or indirect ways [56]. In mammals, cytosine methylation is not equally distributed across the genome but occurs mainly at CpG dinucleotides. The abbreviation CpG, standing for 5'-cytosine-phosphate-guanin-3', describes the linear sequence of a cytosine base followed by a guanine base, bound together by a phosphodiester bond. Overall, CpG dinucleotides are rare in the human genome but they are known to cluster together in so called CpG islands. CpG islands are often found in close proximity to the promoter region and the transcription start site of a gene and are mostly unmethylated [57,58].

Aberrant DNA methylation patterns have been associated with numerous pathologies, including autoimmune, metabolic, and neurological disorders, as well as cancer [59-63].

In support of the role played by epigenetic mechanisms, and DNA methylation in particular, in paediatric IBD, recent work has identified alterations in the DNA methylation profile of intestinal epithelial cells purified from children that are newly diagnosed with IBD, compared to those of control cells [64]. Moreover, disease specific changes in DNA methylation and transcription patterns of the intestinal epithelial cells have been described in patients with CD and UC. These changes appear to be stable over time and correlate with disease outcome parameters [65].

In conclusion, within a plausible model for disease pathogenesis in IBD, epigenetics may represent one of the major underlying mechanisms that mediate the effect of genetic predisposition, environmental triggers and the intestinal microbiome.

1.4 T-cell subsets and their role in IBD pathogenesis

T-cells play a central role in cell-mediated immunity. They are produced in the thymus where they mature from thymocytes. T-cells are distinguished from other lymphocytes by the presence of a T-cell receptor (TCR) on their surface.

Effector T-cells promote an active immediate response to a stimulus. The response involves helper T-cells, killer T-cells, and regulatory T-cells. At the opposite end of the spectrum, memory T-cells are longer lived to target future infections as necessary.

Memory CD8+ T-cells that circulate in the blood and are present in lymphoid organs embody features of both naïve and effector cells (Figure 1.4). It is still debated whether memory T-cells develop from effector cells through a process of dedifferentiation or directly from naive cells [66].

Previous studies show that when memory T-cells are generated after antigen exposure, the more activated T-cells become in response to an antigen (reflected in the "clonal burst" size), the more

memory T-cells are subsequently formed [67].

Helper T-cells (CD4+) assist other processes, including differentiation of B-cells into plasma cells and activation of cytotoxic T-cells and macrophages. Helper T-cells are activated through presentation of a peptide antigen by MCH class II molecules, expressed on the surface of antigen-presenting cells (APCs). Once activated, they secrete cytokines that mediate the active immune response.

Cytotoxic T-cells (CD8+) destroy virus-infected cells and tumor cells, and are also implicated in transplant rejection. These cells operate by binding to antigens presented by MCH class I molecules.

Memory T-cells include central memory T-cells (CD45+, CCR7+ and CD62L+), commonly found in the lymph-nodes and in the peripheral circulation, and effector memory T-cells (CD45+, CD44+, CCr7- and CD62L-) that lack of lymph node-homing receptors and are mainly found in the peripheral circulation and tissues.

Regulatory T-cells are crucial for the maintenance of immunological tolerance, by terminating the T-cell immune response toward the end of an immune reaction. They comprise two major classes, FOXP3+ and FOXP3-.

Natural killer T-cells link the adaptive immune response to the innate immune system through recognition of antigens presented by CD1d and activation of functions related to both helper T-cells and cytotoxic T-cells.

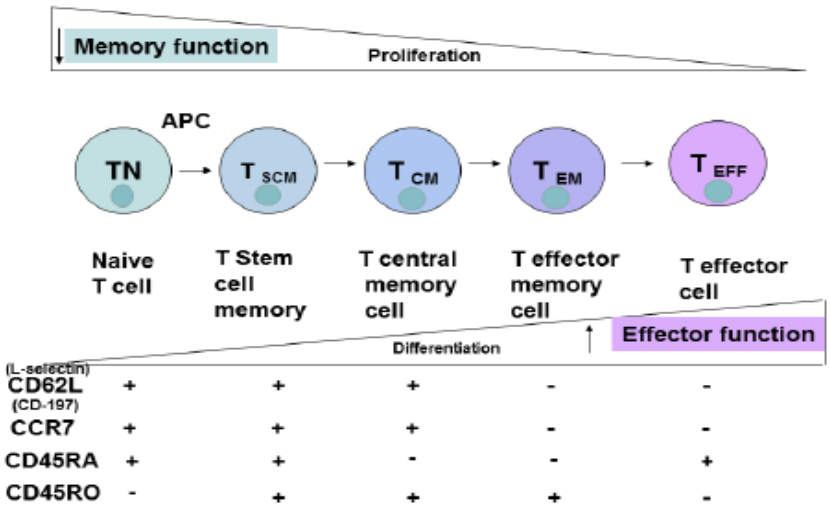

Figure 1.4 The differentiation of CD8+ T-cells and different CD8+ subsets. TN, naive T-cells; T SCM, stem cell memory T-cells; T CM, central memory T-cells; T EFF, effector T-cells; T EM, effector memory T-cells. (Taken from: Golubovskaya V, Wu L. Cancers 2016. [68])

Both CD4+ and CD8+ are known to play a role in the pathogenesis of IBD [69,70].

Immune responses in the intestine are regulated in a way that allows protective immunity against pathogens, while limiting responses to dietary antigens and commensal gut flora [71]. The gut-associated lymphoid tissue acts as a “mucosal firewall” by preventing systemic dissemination of pathogens. Dendritic cells drive regulatory T-cell differentiation in response to dietary antigens and commensal bacteria. Although this process can be beneficial during homeostasis, recent evidence from animal studies suggests that tolerance to commensal-derived antigens may be lost during pathogen-induced epithelial damage and subsequent transient exposure to commensals, causing deranged responses to commensals and promoting inflammatory conditions, such as IBD [71].

In addition to activated effector CD8+ T-cells being detectable in the mucosa of patients with IBD, several animal models [72,73] have identified in the destruction of intestinal epithelial cells by CD8+ T-cells the primary event leading to the loss of barrier function and exposure to microbial antigens. Based on this evidence, it has been speculated that CD8+ T-cells may play an early role in triggering IBD whilst CD4+ T-cells would play a secondary role in the disease pathogenesis. [67]

Recently, using transcriptional signatures from CD8+ T-cells separated from patients with autoimmune conditions including systemic lupus erythematosus (SLE), vasculitis (AAV) and IBD, researchers were able to separate patients into different prognostic groups [67,74]. These groups differed in gene expression within the IL-7 and TCR signaling pathways, including CD28 co-stimulation and IL-2 signaling. These pathways are implicated in T-cell activation and the subsequent development of antigen-specific T-cell memory. Moreover, IL-7 signaling facilitates the survival and differentiation of effector cells into long-lived antigen-specific memory cells (through Bcl2 family-mediated inhibition of the pro-apoptotic effects of Bim22) [67,74].

This data stands in support of a role for CD8+ T-cells in determining the disease course of IBD.

1.5 Clinical presentation and diagnostic work-up

The clinical presentation of childhood IBD is highly variable and symptoms can be subtle. However, there are a number of classical symptoms and, most importantly, some red flags that may indicate the presence of IBD in children and warrant further investigations.

Symptoms of CD commonly include chronic diarrhoea (i.e. longer than 6 weeks), abdominal pain and/or weight loss. Unexplained anaemia and growth failure in children are red flags and therefore should be investigated further. Similarly, blood and/or mucus in the stool may be seen in up to 40-50% of patients with CD and always requires further investigations [20]. Perianal fistulas are present in 10% of patients at the time of diagnosis, and may be the presenting sign of CD [20].

Extra-intestinal manifestations (EIMs) are seen in 10-20% of CD patients, and may even be present prior to the onset of gastrointestinal symptoms. Abnormalities of the musculoskeletal system, such as sacro-ileitis, ankylosing spondylitis, peripheral arthritis are the most frequent EIMs in CD.

Classical symptoms of UC are bloody diarrhoea, tenesmus and abdominal pain [75,76]. Nocturnal defaecation is also frequently reported. Systemic symptoms of malaise, anorexia, or fever are features of a severe presentation [22]. EIMs in UC include arthropathy, episcleritis and erythema nodosum and may accompany the presentation in about 10% of cases [20]. Another important EIM in patients with UC is primary sclerosing cholangitis (PSC). Hence, elevated liver enzymes combined with GI symptoms are highly indicative of UC and PSC [22].

As outlined in the ESPGHAN revised Porto criteria [2], diagnosing IBD in children and adolescents now requires a combination of clinical evaluation and endoscopic, histological, radiological, and/or biochemical investigations [2,34,35,76-81]. Upper and lower gastrointestinal endoscopies and histological examination are essential to assess the extent and activity of IBD [82].

1.6 Treatment

In the absence of a curative treatment, the overall aim of managing childhood IBD is to reduce symptoms, to optimise growth, and to maintain or improve quality of life, whilst minimising toxicity related to drugs over both the short and long term.

Treating active inflammation in IBD involves two phases, i.e. induction and maintenance of remission. Current treatments available encompass three main areas: nutrition, medical options, and surgery. Exclusive enteral nutrition (EEN) with polymeric formulas is used as induction treatment, but drugs for IBD are considered as either induction therapy or maintenance treatment, with some drugs being used for both. Surgery is required to either manage complications or as a last resort in case of treatment-resistant inflammation.

As reliable predictors of response to treatment are currently lacking in clinical practice, two therapeutic approaches (i.e. “step-up” versus “top-down”) are being used, mainly based on disease presentation at diagnosis. However, response to treatments still remains unpredictable, hence there is a need to escalate or de-escalate therapies according to the disease activity and behaviour of individual patients. A “step-up” therapeutic approach consists of escalating initially with corticosteroids, then with immunomodulators, and finally with biological therapies only if a treatment-refractory course evolves [74,75]. (Figure 1.5) An alternative “top-down” strategy (i.e. starting with a combination of biologics and immunosuppressants and “de-escalating” if possible) aims to achieve higher remission rates, restore “mucosal healing”, and decrease the rate of surgeries and hospitalizations in children with particularly severe disease onset by preventing mucosal and transmural damage to the intestinal wall [76-85].

Nowadays, an individualised approach according to the peculiarities of each patient’s disease behaviour remains the best way to optimise the treatment strategies available. In fact, although early aggressive therapy is supported by clinical trials, it needs to be balanced with safety concerns regarding the indiscriminate use of potent immunosuppressants [67]. Over-treating patients destined to develop an indolent disease course might expose them to rare but potentially life-threatening side effects of such drugs, including opportunistic infections [86], demyelination [87], and malignancy [88]. In addition, indiscriminate use of biologics upfront is extremely expensive [67].

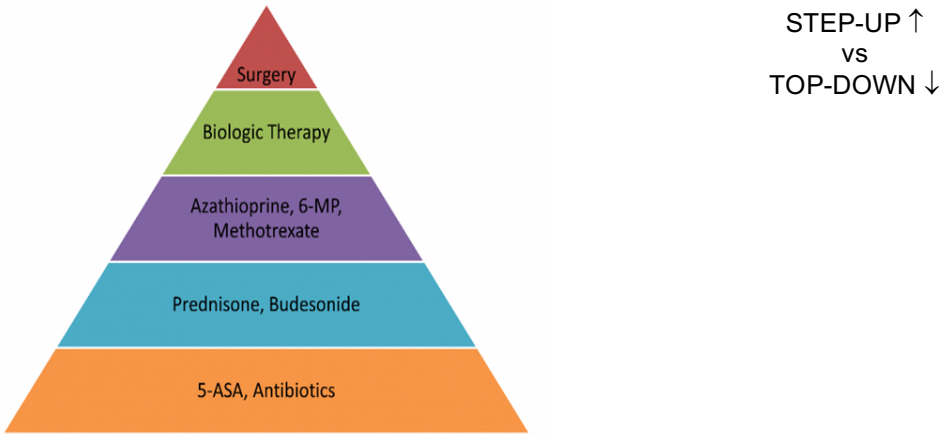

Figure 1.5 Treatment strategies for paediatric IBD. 5-ASA: 5-Aminosalicylates; 6-MP: 6-mercaptopurine. (Taken from: Aloi M, et al. Nat Rev Gastroenterol Hepatol 2014 [89])

With regards to paediatric CD, the most recent NICE guidelines suggest that a course of a conventional gluco-corticosteroid (e.g. oral prednisolone, i.v. methylprednisolone or hydrocortisone) should be offered as a first line treatment to induce remission in patients with a first presentation or a single inflammatory exacerbation of CD in a 12-month period [27].

EEN with polymeric formulas represents an equally effective alternative to conventional gluco-corticosteroids for the induction of remission in children for whom there is concern about growth or side effects [90,91]. EEN offers the advantage of improving the patient nutritional status as well as enabling the mucosa to heal at much the same rate as is achievable with corticosteroids [92-96].
5-aminosalicylates (5-ASA) are used for induction treatment of mild to moderate UC and for maintenance of UC at any disease severity [75], whereas the role of these medications is currently unsupported for children with CD [27]. Mesalazine and sulfasalazine are the 5-ASAs of choice.

The main drugs currently used for maintenance treatment of paediatric IBD are thiopurines (i.e. azathioprine or mercaptopurine), 5-ASAs and biologics. Additionally, methotrexate, cyclosporine and tacrolimus are alternative options when first line treatment fails.
Thiopurines are purine analogues used for the maintenance of disease remission in patients with CD and UC; they include the prodrug azathioprine (AZA) and the antimetabolite 6-mercaptopurine (6-MP) [97,98]. These drugs are steroid sparing agents and are able to block the rapid proliferation of T and B lymphocytes involved in inflammatory processes, which results in immunosuppression [98,99]. Thiopurines are also used effectively to maintain surgically-induced remission in CD [99]. The use of thiopurines is limited by an extensive spectrum of adverse events in up to almost half of patients, particularly within the first 12 months of treatment. Adverse effects include myelotoxicity, hepatotoxicity and pancreatitis [40,98,100].
Methotrexate (MTX), a dihydrofolate reductase inhibitor, has become one of the principal alternatives to thiopurines as a maintenance treatment [101,102] and is a first-line treatment option in patients who have concomitant inflammatory arthritis. Adverse events associated with MTX include flu-like symptoms, nausea and vomiting, transaminitis and, less frequently, myelosuppression, which may require an adjustment in dosage or drug withdrawal [103].
Biologics are a relatively new class of drugs [104-106]. The most frequently used for children are antibodies against TNF-alpha such as infliximab (IFX) or adalimumab (ADA). While IFX is licensed for use in children from 6 to 17 years of age, ADA is only approved for paediatric CD and is still off-label for paediatric UC [34,75,107].
One-year response and remission rates for IFX in luminal disease are reported as up to 90% and 55%-60%, respectively [108-110]. Repeated administration of IFX can lead to immunogenicity in some patients, with possible loss of efficacy and delayed-type hypersensitivity [111,112]. A low proportion of children with CD (10%-25%) are primary anti-TNF non-responders, i.e. they fail to respond after a six-weeks induction course. More commonly, however, the formation of antibodies against the drug over time can result in a secondary loss of response. Concomitant treatment with either thiopurines or MTX has been shown to hinder this process [111]. In anti-TNF antibody naive children, the one-year remission rate for ADA is 45%, and its efficacy has been documented in nearly two-thirds of patients for whom IFX was unsuccessful [113].

Anti-TNF agents are also used as a primary induction option for children with active perianal fistulising disease, in combination with targeted antibiotic and surgical intervention.

With regards to the use of biologics for maintenance of remission in children with UC, IFX (approved by the Food and Drug Administration for children ≥ 6 years of age with moderately-to-severely active UC) should be considered for treatment of cases with persistently active, or steroid-dependent UC, uncontrolled by 5-ASA and thiopurines. IFX should also be considered for steroid-refractory (whether oral or intravenous) disease [75,114].

1.6.1 Surgical treatment

The role of surgery in the management of paediatric IBD lies in treating complications as well as complementing the management of cases resistant to medical treatment.
Overall, approximately 50-80% of patients with CD will undergo surgery during the course of their disease [34]. The most common interventions include treatment of strictures causing symptoms of obstruction, or other complications such as fistula formation, perforation or failure of medical therapy. In patients with localised ileo-caecal CD, ileo-caecal resection is frequently performed as a useful surgical option to treat the isolated inflammation of this area.
For patients with severe, treatment-resistant UC, colectomy (and formation of ileostomy) is still a last resort [75]. Resecting the colon in patients with severe UC that is non-responsive to medical options represents a cure, as, by definition, UC only involves the large bowel. The main down side is the formation of an ileostomy which generally remains unreversed until adulthood. At this stage, ileo-anal pouch or ileal pouch-anal anastomosis are the preferred methods of choice for re-joint and reversal of ileostomy. Due to the major advances in the field, a laparoscopic surgical approach can be used safely in children with low complication rates and superior cosmetic results [75].

1.7 Natural history of paediatric IBD

The natural history of paediatric IBD is characteristically unpredictable, but data available so far shows that 25–33% of IBD patients with a non-complicated form of the disease transition to a stricturing or internal and perianal penetrating disease after 5 years, i.e. one third of patients, if undertreated, will transition from a non-complicated to a complicated disease state if followed up for a sufficient time [115 – 122].

In particular, a number of studies so far suggest a more severe disease phenotype and course in childhood onset IBD compared to adult patients. Vernier-Massouille G et al. described the complicated behaviour of CD in 29% of children at diagnosis and in 59% during the follow-up [123]. Intestinal surgery is required in as many as 80% of children with CD, with more than 10% of them having permanent stoma formation [115-117]. Post-surgical relapses occur in 50% of children with CD compared to 20-30% of adult patients after 5 years, with variability depending on disease location [124-127].

In UC, the cumulative rate of colectomy in children is 8% at 1 year, 15% at 3 years, and 20% at 5 years following diagnosis [128].

Whilst patients with CD have higher mortality rates with respect to the general population, this has not been observed for UC patients [128-131].

1.8 Disease prognostic biomarkers in IBD

The behaviour of IBD varies unpredictably among patients [67] and increasing evidence suggests that early, risk-stratified treatment (i.e. specific to those who will develop a severe disease phenotype) is likely to improve long-term disease outcomes [132,133].
The development of a reliable prognostic biomarker would enable the stratification of patients based on their predicted risk for a poor or benign prognosis, which would lead to personalised treatment. Patients destined to experience an aggressive form of the disease could receive appropriately robust intervention from the point of diagnosis, while those who will experience a more indolent disease course could be treated with more conservative therapeutic approaches with a lower risk of toxicity, as appropriate [67,134,135].

Although the biomarker concept is old, so far very few useful parameters have been identified in IBD [136-138]. Whilst a number of candidate biomarkers for IBD have been explored, ranging from genetic predictors (SNP-based risk scoring system) [45,115,139-141], and biochemical tests (in isolation or combination) [142-148], to endoscopic, histological [138,147] and clinical parameters [83,148-153], none have made it into routine clinical practice due to limitations in sensitivity, specificity or practical feasibility.

Recent paediatric literature has shown convincing results of a correlation between PUCAI score at 3 months over diagnosis and long-term outcomes (including risk for colectomy) in children with UC [148-150]. Although the use of this predictor is recommended in clinical practice, it is only applicable to UC and it is not accessible at diagnosis as it is based on response to treatment after 3 months. However, it might be of limited help to severe children in whom progression to severe pancolitis requiring colectomy could be already irreversible at that stage.
Faecal calprotectin is an example of a helpful tool for monitoring disease activity during the follow-up, as it enables the early prediction of relapses and prompt treatment escalation. However, it does not provide an overall prediction of disease severity and cannot be used to stratify patients based on risk at the time of diagnosis [154].

In summary, the main limitations in developing prognostic biomarkers so far have included failure to fulfil the classic traits of an ideal biomarker test (i.e. simple, accurate, easy to perform, minimally invasive, cheap, rapid and reproducible), low sensitivity, specificity and/or prognostic predictive values, lack of validation in independent cohorts, or inconsistent results when validation has been attempted. As a result, we are currently not in the position to advise children and parents at the point of diagnosis on disease outcomes, and hence are unable to propose a tailored, potentially more individualised treatment strategy. There is therefore a great need for prognostic biomarkers for the prediction of clinical outcomes and therapeutic effects in IBD.

1.8.1 CD8 T-cell gene expression signatures are promising prognostic biomarkers in adult IBD

Recent progress in the field of prognostic biomarkers in autoimmune diseases has been made by McKinney et al. [74] They identified a common CD8 T-cell transcriptional signature in two unrelated, autoimmune diseases: systemic lupus erythematosus (SLE) and ANCA-associated vasculitis (AAV). This signature predicted disease prognosis in both conditions [74].

Leading on from these findings, the group tested the potential value of CD8+ T-cell gene expression as a prognostic biomarker in adult onset IBD. Indeed, based on analyses of a large, prospectively recruited patient cohort, unsupervised clustering of IBD patient-derived CD8+ T-cell gene expression profiles separated patients into two distinct groups. Importantly, these groups differed significantly in their disease outcome as evaluated by the number of treatment escalations required [67]. Furthermore, the specific signature, i.e. set of genes that are differentially expressed between the two groups, was found to overlap with genes forming the prognostic signature in SLE and AAV (Figure 1.6 A-C). Together, these findings suggest the presence of a common CD8+ T-cell gene expression signature, which can be used to predict disease outcome in SLE, AAV and adult-onset IBD.

With the aim of identifying the potential underlying biological mechanisms at play, the group went on to demonstrate that CD8+ T-cell exhaustion strongly correlates with a better prognosis in these conditions. These findings were supported by demonstrating a major overlap of the disease prognostic CD8+ T-cell expression signatures with an “exhaustion signature” as well as the ability of the latter to divide patients according to the disease outcome. In addition, a more recent publication by McKinney et al. focused on the process of T-cell exhaustion during chronic infection, a mechanism that inhibits the immune response and facilitates viral persistence [155] (Figure 1.6 D-F).

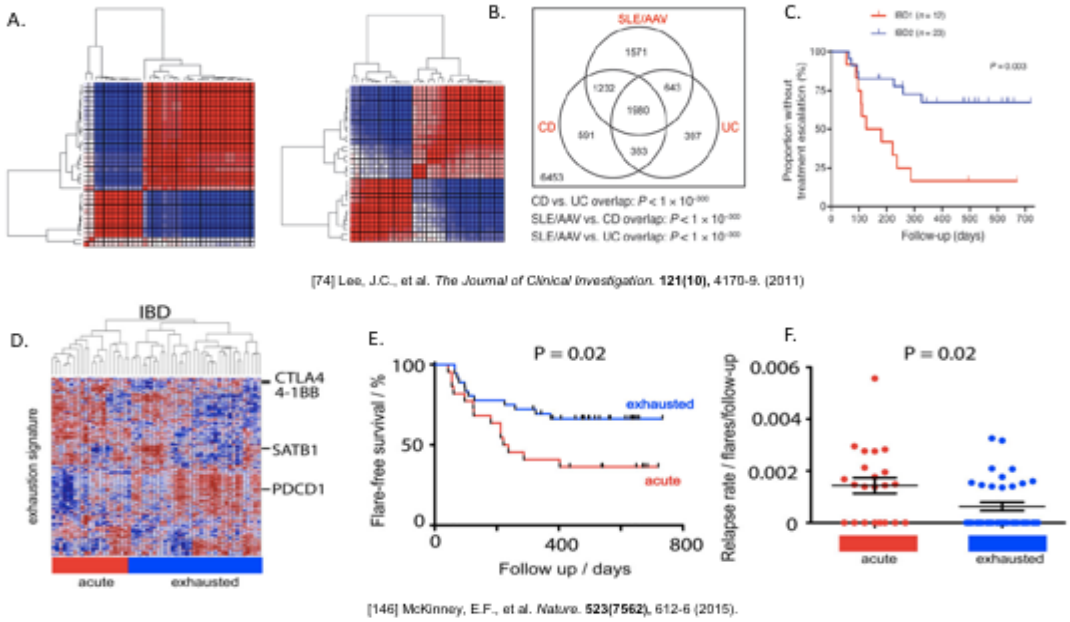

Figure 1.6 Summary of the main findings from studies on adult prognostic IBD signature and T-cell exhaustion signature (A., B. and C. are taken from Lee, J.C., et al. The Journal of Clinical Investigation 2011 [67]. D. E. and F. are taken from McKinney, E.F., et al. Nature 2015 [155]). A. shows CD8+ gene expression Consensus Clustering plots of adult CD and UC patients showing detection of subgroups IBD1 and IBD2. B. gives a Venn diagram illustrating the overlap between the gene signatures that distinguish the respective subgroups in CD, UC, and SLE/AAV. The statistical significance of each overlap was determined using a hypergeometric test. In C. survival analysis shows that the groups identified (IBD 1 and IBD2) have significantly different disease courses. In D., a heatmap shows hierarchical clustering of CD8+ T cell that are "exhausted" (blue) and "non-exhausted" (red) in IBD patient subgroups defined from the primary division of the cluster dendrogram. In E., Kaplan-Meier curves show censored flare-free survival for the adult IBD cohort. In F. scatterplots show normalised flare-rate against duration of follow-up for IBD patient subgroups.

1.9 Hypothesis and aims

We hypothesise that CD8+ T-cell gene expression can predict disease outcome in children that are newly diagnosed with IBD. Furthermore, we speculate that CD8+ T-cell DNA methylation may provide the epigenetic underpinning of prognostic gene expression signatures.

The specific aims of our study are:

- To apply the prognostic CD8+ T-cell signature and the T-cell exhaustion signature identified in adult patients to a cohort of children that are newly diagnosed with IBD and test their ability to differentiate patients based on the disease outcome;
- To investigate the existence of paediatric-specific prognostic CD8+ T-cell expression signatures;
- To investigate the use of CD8+ T-cell DNA methylation as an alternative prognostic biomarker, and/or elucidate a potential epigenetic signature that underlies variations in gene expression.

CHAPTER 2

Materials and Methods

2.1 Patient cohorts

This study was undertaken at Cambridge University Hospitals – NHS Foundation Trust in the Department of Paediatric Gastroenterology, Hepatology and Nutrition. 112 treatment-naïve, Caucasian patients aged between 5 and 16 were recruited prospectively at the point of IBD diagnosis between March 2013 and March 2016. Diagnosis was made according to current guidelines (ESPGHAN Porto criteria [2]) and included upper and lower gastrointestinal endoscopies and histological examination. A sample of peripheral blood for the purification of CD8 + T lymphocytes was taken on the day of diagnosis, i.e. before any treatments were started. Exclusion criteria included any patient with gastrointestinal and/or extra-intestinal diseases other than IBD, and any controls.

Patients were recruited for this project under an encompassing study (Genomics and Epigenetics in Paediatric Gastrointestinal and Immune Mediated Disease – GEPaedGI) which received ethics approval from the Central Cambridge Research Ethics Committee (REC 12/EE/0482) in November 2012 for the prospective enrolment of paediatric patients undergoing endoscopic investigation at Addenbrooke's Hospital, Cambridge, to support a clinical diagnosis. All investigations were carried out according to the Declaration of Helsinki and Good Clinical Practice Guidelines.

The final number of patients (samples) analysed was established through data pre-processing (bioinformatic analysis). Following the removal of samples that failed quality control, 107 samples remained and were included in the study (67 CD and 40 UC).

Table 2.1 illustrates the patient population demographics as well as the number of samples analysed at each step. Information on clinical outcomes including the number of treatment escalations, the use of biologics and the number of surgical interventions in the paediatric cohorts analysed is also included.

Paediatric population recruited (CD8+ T lymphocytes purified)	Gender	Diagnosis	Age at diagnosis (years)	Main clinical outcomes n (%)	Number of patients removed from the analysis
Initial population n=112	M 71 F 41	CD and IBD-U CD-like 71 UC and IBD-U UC-like 41	Average 12.4 ± SD 2.4 Range 5-16		
Unsupervised analysis n=107	M 67 F 40	CD and IBD-U CD-like 67 UC and IBD-U UC-like 40	Average 12.41 ± SD 2.44 Range 5-16	0 treat escal 25 (23%) 1 treat escal 34 (32%) 2 treat escal 20 (19%) 3 treat escal 20 (19%) 4 treat escal 8 (7%) Biologics 39 (36%) Surgery 6 (5.6%)	Outliers as per QC report: n=4 Incomplete clinical information as patient lost in follow-up: n=1
WGCNA analysis n=98	M 60 F 38	CD and IBD-U CD-like 60 UC and IBD-U UC-like 38	Average 12.33 ± SD 2.511 Range 5-15	0 treat escal 23 (24%) 1 treat escal 32 (33%) 2 treat escal 18 (18%) 3 treat escal 18 (18%) 4 treat escal 7 (7%) Biologics 30 (31%) Surgery 3 (3%)	Patients treated with biologics at time 0, i.e. within 8 weeks from diagnosis: n=9

Table 2.1. Population flow-chart, demographics and summary of the main disease outcomes. CD: Crohn's disease; SD: standard deviation; UC: ulcerative colitis; F: female; IBD-U: IBD unclassified; M: male; QC: quality control; treat escal: number of treatment escalations during follow-up; WGCNA: weighted gene co-expression network analysis.

2.2 Clinical information

All patients were followed for 1.5 years in our unit as part of their routine clinical care, and extensive clinical data including parameters at diagnosis (e.g. presence of diarrhoea, rectal bleeding, weight loss, EIMs, perianal disease, disease activity scores) and information on disease course and outcomes (e.g. number of treatment escalations, use of biologics, number of unplanned inpatient days, IBD related surgical intervention) was collected by the same researcher from the hospital patient electronic database (EPIC).

Appendix 1 on page 174 summarises the definitions, measurement units and normal values of each clinical item collected; Appendix 2 on page 165 shows the complete clinical database that was collected and used.

Appendices 3 (page 200) and 4 (page 205) show the IBD activity scores at diagnosis: Paediatric Crohn's Disease Activity Index (PCDAI) and Paediatric Ulcerative Colitis Activity Index (PUCAI) [34-35].

Appendix 5 on page 207 outlines the classification of IBD by disease location according to the Paris classification [13].

2.2.1 Severity score

In order to take into account that a severe disease course is reflected in a number of individual disease outcome measures, a specific disease severity score was developed by considering the key parameters that are strong indicators of disease outcome (Figure 2.1). This summary score was used as an additional outcome measure to correlate with CD8+ T-cell specific molecular signatures.

Crohn's disease

1. Number of treatment escalations:

0 - 1: 0 2: 1 >= 3: 2

2. Biologics:

No: 0 Yes: 2

3. Surgery (intestinal resection / diversion ileostomy):

No: 0 Yes: 2

4. Perianal disease

Absent: 0
Medical management (Antibiotics/Seton/IFX): 1
Surgical management (Fistulotomy/Fistulectomy): 2

5. Unplanned/urgent inpatient days:

0 – 2: 0 3 - 4: 1 >= 5: 2

Total: 0-1: Mild 2-4: Moderate 5-10: Severe

Ulcerative colitis

1. Number of treatment escalations:

0 - 1: 0 2: 1 >= 3: 2

2. Biologics:

No: 0 Yes: 2

3. Surgery (colectomy):

No: 0 Yes: 2

4. Response to steroids at 3 months:

Yes: 0 No: 2

5. Unplanned/urgent inpatient days:

0 – 2: 0 3 - 4: 1 >= 5: 2

Total: 0-1: Mild 2-4: Moderate 5-10: Severe

Figure 2.1 Severity scores for CD and UC used to provide an overall estimate of disease course severity and to identify predicting modules (signatures) through WGCNA analysis. IFX: Infliximab.

2.3 Collection of blood samples and purification of CD8 + T-cells

Blood samples were obtained at diagnosis from all patients during the endoscopic procedure while under general anaesthetic (Table 2.2). Whole blood samples were collected in Falcon tubes with 4% sodium citrate. Samples were immediately sent to the lab for processing as per cell separation protocol [156] (Appendix 3 on page 200).

Age of the patient	**Volume of blood (ml)**	**Volume of 4% sodium citrate (1ml/10ml of blood)**
5-10 years	10	1
10-16 years	25	2.5

Table 2.2 Volume of blood collected according to patient age.

Samples were diluted in a 1:2 ratio with MACS rinsing buffer. Peripheral blood mononuclear cells (PBMCs) and neutrophils were isolated by centrifugation over Ficoll (Histopaque 1077) (density gradient separation). Following the removal of the plasma, the PBMC interface was transferred to a fresh Falcon tube and after several wash and centrifugation steps, CD8+ and CD8- T lymphocytes were separated through anti CD8 microbeads and magnetic sorting (auto-MACS). CD8+ T lymphocyte samples were stored at -80°C until required for further processing.
See Appendix 3 on page 200 for further details on the CD8+ T-cell separation protocol.

2.4 Purity assessment via Fluorescence Activated Cell Sorting (FACS)

Flow cytometry was performed on selected samples following CD8+ T cell isolation using BD Fortessa to determine the level of purity. The CD3-PE and CD8-APC antibodies were used (BD Pharmingen), along with the Zombie Aqua Fixable Viability Kit (Biolegend).
A total of 8 randomly selected samples were subjected to flow cytometry analysis, and the average cell purity for CD8+ T-cells was 84% (Table 2.3).
Figure 2.2 demonstrates the process of flow cytometry in one example patient sample through a series of plots. In A., analysis was conducted on the PBMC sample (pre-purification protocol) to visualise the data and set gates, with each dot on the plot representing a cell. In B. and C., the same gates were applied to the positive and negative fractions of T-cells, respectively. The plots were further gated to analyse single cells and avoid doublets and debris etc. Cells were also stained with Aqua Zombie to distinguish between the live and dead cells. The final image within Figures A. B. and C. displays the live single cells only and the gate surrounds those samples that are dual stained for CD3 and CD8+ T-cells.

For this particular sample, out of a total of 10,000 events, the CD8+ T-cell sample purity came out as 93.3% within the gated region of all dual stained (CD3 and CD8) live single cells, or 82.1% when taking into account the total cell population. The series of plots in Figure C. for the negative fraction (CD8-) confirms that the CD8+ T-cells have been eluted in the positive fraction, as very few appear in the negative plots.

Together, this data confirms the successful isolation of CD8+ T-cells and a level of purity that was in the region of that reported in previous work published on adult IBD patients (Lee et al, 2011 [67]).

Sample number	% cell purity (CD8+ T-cells)
1	75.7
2	86.3
3	89.3
4	90.9
5	93.8
6	80.5
7	80.7
8	72.5
Average cell purity	**84%**

Table 2.3 Percentage of cell purity for CD8+ T cells across 8 samples subjected to flow cytometry.

A.

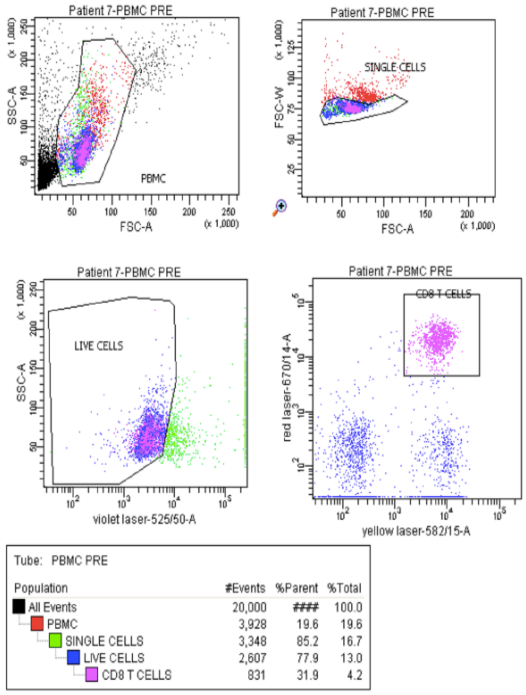

B.

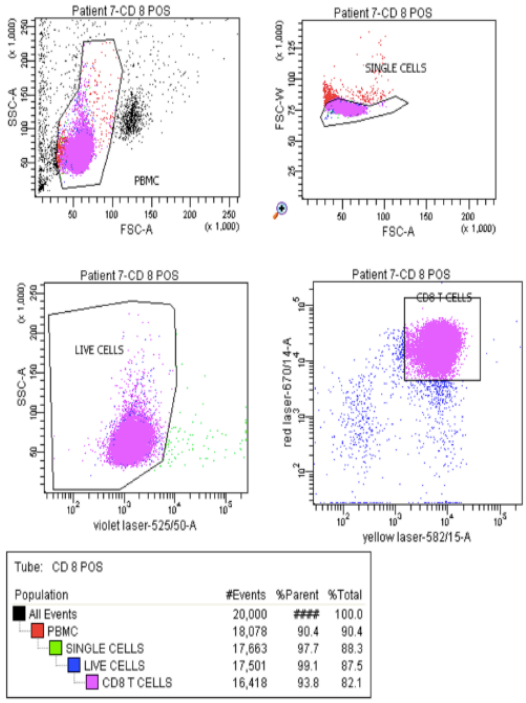

C.

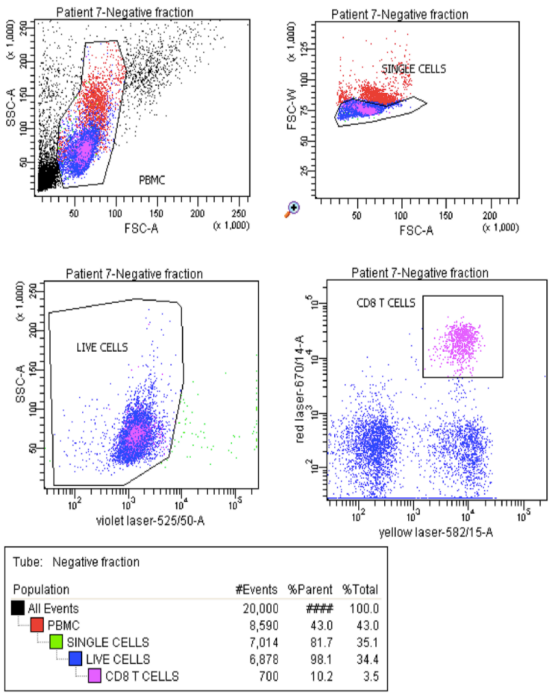

Figure 2.2 Flow cytometry (FACS analysis) for a single patient sample. A. shows the plots for PBMC (pre-purification protocol). B. and C. demonstrate the analysis of the positive and negative CD8 fractions respectively.

2.5 RNA and DNA Extraction

DNA and RNA were extracted simultaneously from the CD8+ samples using AllPrep DNA/RNA MiniKit (Qiagen, UK). Quantification and purity of RNA and DNA was evaluated using a Nanodrop 1000 spectrophotometer (Thermo Scientific, UK) and a Qubit. A ratio absorbance at 260nm/280nm of 1.8 for DNA was considered to be pure.
The RNA yield was in the region of 1-4 µg and hence was sufficient for genome-wide downstream analysis.

2.6 DNA bisulfite-conversion

Prior to genome-wide DNA methylation profiling, DNA samples were bisulfite-converted using Zymo DNA methylation Gold kit (Zymo Research).
DNA bisulfite-conversion consists in treating DNA with sodium bisulfite, so that unmethylated cytosine is converted to uracil by deamination, whereas methylated cytosine remains unchanged. Uracil is then amplified as thymidine. One limitation of this technic is that 5' hydroxymethylation cannot be distinguished from 5' methylation.
The conversion reagent supplied was added to the DNA samples (500 ng). Subsequently, the samples were heated following 4 main steps as per manufacturer's protocol (98^C for 10 min; 53^C for 30 min; 53^C for 6 min; 37^C for 30 min; steps 3 and 4 were repeated 8 times). Following, the samples were cooled down and stored at 4^C. Finally, the converted DNA was purified from the mix as per kit protocol, it was diluted in water and stored at -20^C.

2.7 Microarray analysis

Microarray analysis in this study was used to generate genome-wide transcriptional and methylation profiles.

Gene expression was analysed using Affymetrix Human Gene ST 2.0 Array (Affymetrix UK Ltd, High Wycombe, UK), which covers 53,617 probes.

Genome-wide DNA methylation was profiled using bisulfite-converted DNA on the EPIC BeadChip platforms (Illumina, Cambridge, UK). EPIC methylation array provides a quantitative measure for DNA methylation at > 850,000 single CpG sites across the genome.

2.7.1 Preparation of samples for microarray analysis

As a first preparation step for gene expression microarray analysis, RNA samples were bioanalysed using Agilent 2100 Bioanalyser System. The kit contains RNA chips with an interconnected set of microchannels that is used for separation of nucleic acid fragments based on their size as they are driven through it electrophoretically.

Next, the samples were prepared for hybridization onto Affymetrix Human Gene ST 2.0 microarrays by using the Ambion WT Expression Kit, according to the manufacturer's instructions.

In brief, first-strand and second-strand of cDNA were synthetized. Antisense cRNA was then produced by in-vitro transcription of the second strand cDNA template using T7RNA polymerase.

Subsequently, the cRNA was then stabilized by purification aimed to remove the enzymes, salts, inorganic phosphates and unincorporated nucleotides. Sense-strand cDNA was then synthesized by reverse transcription of cRNA, using random primers, followed by hydrolysis using RNase H which degrades the cRNA template leaving single-stranded cDNA.

Finally, the second-strand cDNA was purified to prepare for fragmentation and labeling.

2.8 Bioinformatic analysis

Bioinformatic analyses were performed by importing raw data into the statistical software "R", followed by data analysis using BioConductor packages.

Patients were initially analysed altogether (i.e. all IBD, n=107) and subsequently grouped by type of IBD (i.e. CD (n=67) and UC (n=40)).

The following sub-sections provide information on the methods used for bioinformatic data analysis in this project.

2.8.1 Data pre-processing: normalisation, quality control and batch correction

Quantile normalisation was performed using BioConductor package “affy” (“rma” function). Package “arrayQualityMetrics” was then applied to assess the quality of the normalised gene expression dataset, to identify outliers and proceed to their removal prior to subsequent data analysis.
As the presence of a batch effect was noted, batch correction was performed through the “Combat” function (“sva” package). An adjustment for gender and type of diagnosis (i.e. CD vs UC) was also performed alongside batch correction, by adding these variables as co-variates.

2.8.2 Gene filter

The “genefilter” package was used to subset 50% of the probes (genes) with more variation in gene expression (var.cut-off: 0.5) from the microarray expression dataset.

A selection of 20% of the probes (genes) with more variation in methylation (var.cut-off: 0.8) was used for the array methylation dataset.

2.8.3 Hierarchical Clustering

This methodology (BioConductor function “hclust”) was used to determine whether the data was organised in clusters, i.e. whether a substructure could be detected. In the context of this study, clusters are groups of samples with similar gene expression profiles. The main limitation of this method is that it doesn’t provide with a measure of the strength of the clustering (i.e. there is no p-value associated to the clusters detected).

2.8.4 Consensus Clustering

Consensus Clustering is a clustering method that indicates whether stable and reproducible clusters (i.e. groups) are present across a dataset [157]. This analysis was performed through BioConductor package “ConsensusClusterPlus”.

This method clusters fractions of the data and provides a consensus output, indicating whether stable/reproducible subgroups are present. *K* indicates the specified cluster counts, i.e. the number and membership of possible clusters within a dataset.

The consensus matrix is summarized in several graphical displays that enable a user to decide upon a reasonable cluster number and membership (one example on Fig. 3.1, page 60). The graphics provided are heatmaps of the consensus matrices for the selected *k* (e.g. 2, 3, 4, 5, 6 etc.). The consensus matrices have items values range from 0 (never clustered together) to 1 (always clustered together) marked by white to dark blue.

The consensus CDF plot shows the cumulative distribution functions of the consensus matrix for each *k*. This allows a user to determine at what number of clusters, *k*, the CDF reaches an approximate maximum, thus consensus and cluster confidence is at a maximum at this *k* (one example on Fig. 3.1, page 60).

The Delta area graphic shows the relative change in area under the CDF curve comparing *k* and *k*-1 (one example on Fig. 3.1, page 60). This plot allows a user to determine the relative increase in consensus and determine k at which there is no appreciable increase.

Although superior to hierarchical clustering in detecting the best clustering option, Consensus Clustering also does not provide with a p-value expressing the strength of the clustering detected. Hence, we also resorted to the SigClust method described below in order to assess the significance of the clusters identified.

2.8.5 SigClust Clustering

This method tests the reliability of the clusters identified through the above methods, by using the 2-means (k = 2) clustering index as a statistic. It assesses the significance of clustering by simulation from a single null Gaussian distribution. Null Gaussian parameters are estimated from the data [158].

The null hypothesis of SigClust is that the data are from a single Gaussian distribution. The SigClust method uses a test statistic called the cluster index (CI) which is defined to be the sum of within-class sums of squares about the mean divided by the total sum of squares about the overall mean.

SigClust is superior to the alternative clustering methods described above as it assesses the significance of a given clustering by calculating an appropriate p-value.

2.8.6 Differential Gene Expression Analysis and Annotation

Differential gene expression analysis (DGEA) was used to identify genes that were differentially expressed between groups of patients identified through Consensus Clustering. The Bioconductor package “Limma” was used. The threshold for the Bonferroni Correction was set at a p-value of 0.05. Annotation of differentially expressed genes was performed through packages “Annotate” and “hugene20sttranscriptcluster”.

2.8.7 Gene Set Enrichment Analysis

In our experiment, mRNA expression profiles were generated for thousands of genes from a collection of samples, which were then categorised into two groups, based on unsupervised clustering (Consensus Clustering).
Gene Set Enrichment Analysis (GSEA) was used to detect whether significant differentially expressed genes between groups identified through Consensus Clustering were coordinately found within specific cellular pathways, which could elucidate aspects of the underlying biology.

2.8.8 Weighted Gene Co-expression Network Analysis (WGCNA)

This analysis investigates correlations between gene expression profiles and clinical information, including disease outcomes [159,160]. BioConductor package “WGCNA” was used.
Clinical information was collected as a “.csv” file, as shown in Appendix 2 on page 176.
The general concept of WGCNA is the clustering of data points into modules to reduce the dimensions of the dataset. In the context of this study, modules are groups of genes with similar gene expression or similar methylation profile. Using modules relieves the necessity of multiple testing as the number of tests performed is not based on the size of the dataset, but rather on the number of modules and the clinical parameters.
By using WGCNA, the data is clustered in modules that are then matched with clinical variables (as opposed to identifying clusters of samples/patients and comparing these groups for specific clinical outcomes with survival analysis).
Significant correlations (positive or negative) between modules and clinical outcomes, allow for the identification of potential prognostic signatures of interest for those specific outcomes.

2.8.9 Survival Analysis

Censored Kaplan-Meier survival curves for events including treatment escalations, use of biologics and surgery were created using the function “survfit” from CRAN package “survival”, based on a tabulation of the number at risk and the number of events as recorded in our clinical database.

The significance of any split observed in the Kaplan Meier plots was checked through the “coxph” function, which uses a Cox proportional hazards regression model. The function “summary.coxph” returns a summary of a fitted coxph model, displaying p-values based on a likelihood ratio, Wald test and score (logrank) test.

CHAPTER 3

Testing the predictive value of an adult prognostic CD8+ T-cell and T-cell exhaustion signature on a paediatric patient cohort

3.1 Introduction

Prognostic CD8 T-cell transcriptional signatures have been identified in adult autoimmune diseases including systemic lupus erythematosus (SLE), ANCA-associated vasculitis (AAV) and IBD by researchers from the Cambridge Department of Medicine [74]. In particular, they identified a specific gene expression signature in CD8+ T-cells isolated from adult patients with IBD, which is able to cluster them in subgroups with different disease course and outcomes [67]. In addition, a more recent publication from their research group focused on the process of T-cell exhaustion during chronic infection, a mechanism that associates with poor clearance of chronic viral infection, but conversely predicts better prognosis in multiple autoimmune diseases [155].
In the first part of this thesis, we aimed to test whether the CD8 signature and the T-cell exhaustion signature identified as prognostic in previous studies on adult patients with IBD (Lee JC et al. [67] and McKinney E et al. [155]) would also be able to distinguish paediatric IBD patients based on their disease severity.

Our first goal was therefore to test the prognostic power of signatures available from previous studies in adult patients with IBD, on a prospective paediatric cohort, for the first time.

3.2 Materials and methods

Two alternative and complementary methods were used to address the question above: unsupervised clustering analysis and WGCNA.

In the first instance, annotated gene lists corresponding to the adult prognostic signatures were used to filter out the matching probes from the paediatric dataset. BioConductor function “subset” was applied and subsetting was based on gene “entrezID”. This provided a submatrix of the paediatric data, only including probes related to the adult signatures of interest, and their expression levels across the paediatric cohort.

Unsupervised clustering analysis (Consensus Clustering) allowed identification of reliable subgroups of patients, based on the gene expression profiles of this selection of probes across the dataset.

Survival analysis (Kaplan-Meier) was then performed to compare the groups above for main disease prognostic outcomes including number of treatment escalations, treatment with biologics and surgical intervention.

As a second step, WGCNA was performed to identify modules (i.e. groups of gene with similar gene expression levels) correlating with disease outcomes of interest.

The adult study [67] was published in 2011 and findings were mainly based on unsupervised clustering analysis and GSEA. WGCNA was not applied to the data in that study. We resorted to WGCNA in our paediatric study as an improved methodology compared to clustering analysis.

In order to compare the paediatric and the adult data, we first ran WGCNA in the adult dataset to identify the modules corresponding to the adult prognostic signature, i.e. modules correlating to prognostic groups 1 (severe) and 2 (mild) based on number of treatment escalations.

We then applied these modules to the paediatric data to test whether they would still show a correlation with disease outcomes in the paediatric cohort. More specifically, probes in the modules corresponding to disease severity in the adult population were first subset from the paediatric data. Subsequently, WGCNA was run for this selection of the paediatric data and correlations between modules and specific outcomes (number of treatment escalations, use of biologics, surgical intervention and severity score) were investigated.

Children who were treated with biologics right at diagnosis (e.g. because of perianal disease) were removed from WGCNA; in fact, outcomes like “treatment with biologics” and “number of treatment escalations” would not have been comparable with the majority of children who received a strict step-up treatment (i.e. escalation to biologics only after failing conventional immune-suppressants).

Therefore, as shown in Table 2.1 (page 44), the number of patients included in the WGCNA analysis was 98 (60 CD and 38 UC).

The same protocol was used to analyse all of the paediatric samples together (i.e. paediatric IBD cohort) as well as subgroups by type of IBD diagnosis (i.e. paediatric CD cohort and paediatric UC cohort).

3.3 RESULTS

3.3.1 Testing the adult CD8 prognostic signature on paediatric IBD: unsupervised analysis

In the first instance, we tested whether the adult prognostic signature identified in the study by Lee JC at al. [67] could also be applied to the paediatric data and whether it would identify groups of children with different disease course and severity.

First, we filtered out of the paediatric data the probes corresponding to the adult prognostic signature, and ran Consensus Clustering analysis. Clusters based on gene expression profiles of this selection of the paediatric data (i.e. adult prognostic signature applied to the paediatric IBD cohort (n=107)) were identified as shown in Figure 3.1.

At this stage, we focused on whether the groups identified through Consensus Clustering (Figure 3.1C *k*5: group 1 (n=95) vs groups 2+3+4+5 (n=12), renamed as group 2) would differ in respect to their disease course and outcomes.

Survival analysis did not identify a significant split between the groups in terms of treatment escalations, use of biologics and surgical intervention during a follow-up of 1.5 years (Kaplan Meier curves on Figure 3.2).

In summary, applying the adult signature to the paediatric data did not generate any significant split in clinical outcomes.

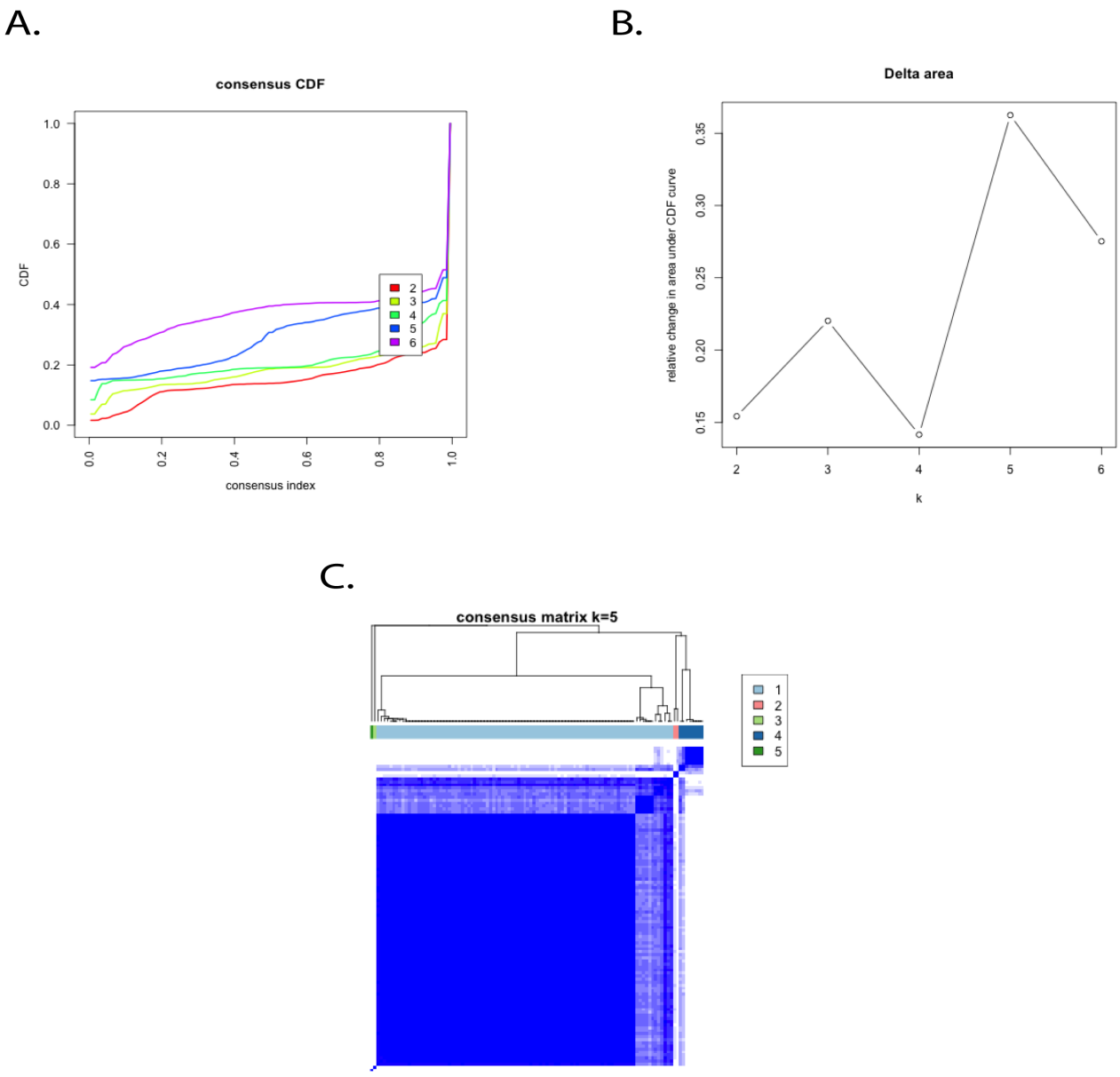

Figure 3.1 Consensus Clustering plots of a selection of the paediatric data (paediatric IBD cohort, n=107) based on the CD8 prognostic signature identified in adult IBD [67]. In A. Consensus Cumulative Distribution Function (CDF) shows at what number of clusters (k) consensus and cluster confidence reach a maximum. In B. Delta area plot shows the relative change in area under the CDF curve, i.e. at which k there is no further appreciable increase. K5 is identified as the strongest clustering split. In C. clusters are shown as dendrogram (top), colour bar, and gene expression heatmap.

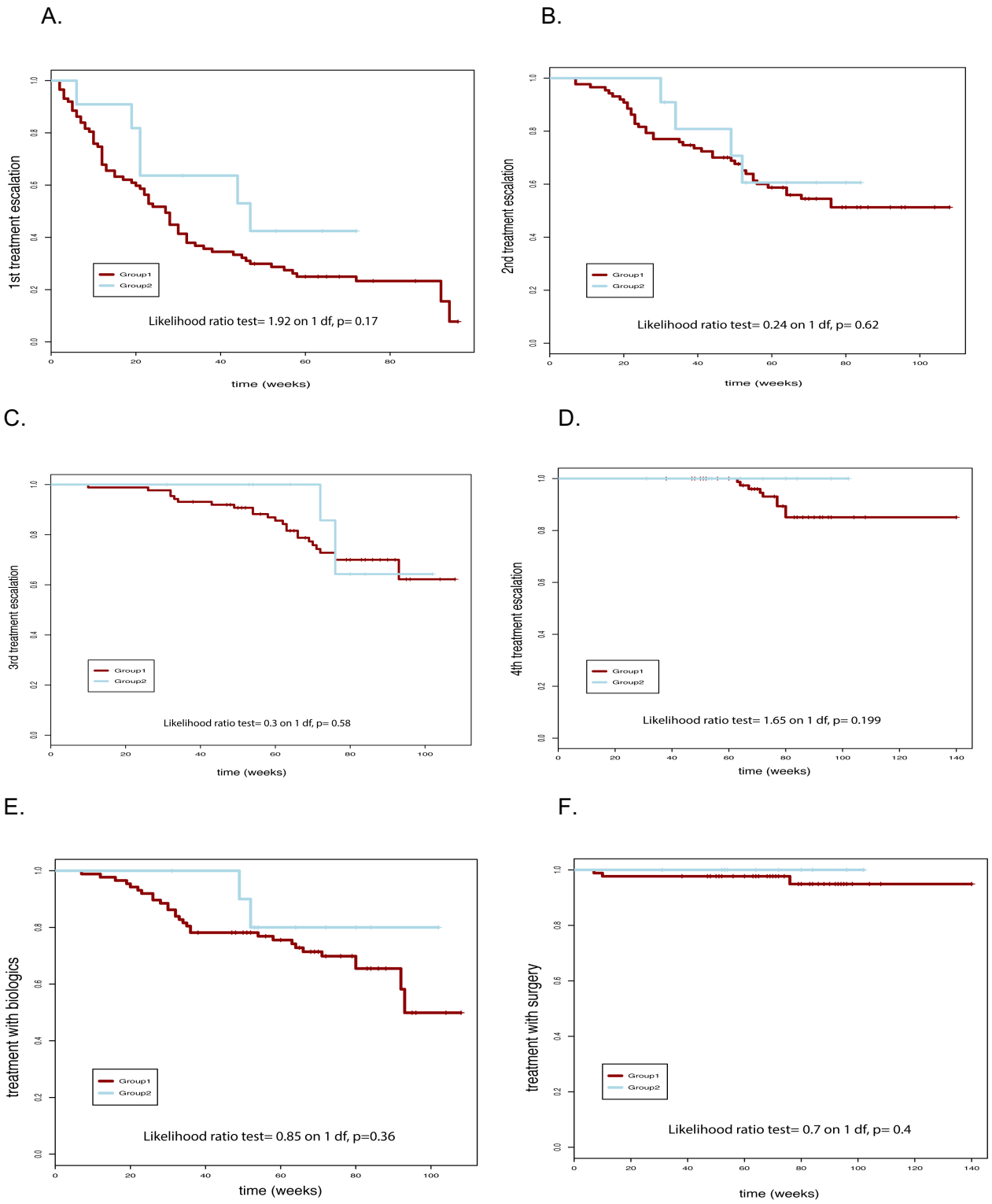

Figure 3.2. Kaplan Meier curves for the paediatric IBD cohort (n=107) comparing group 1 (n=95) and group 2 (n=12) identified through Consensus Clustering limited to genes in the adult CD8 prognostic signature (Lee JC et al. [67]) (Figure 3.1C). Patients in the two groups are compared for the following outcomes: A) first treatment escalation; B) second treatment escalation; C) third treatment escalation; D) fourth treatment escalation; E) use of biologics; F) surgical intervention.

3.3.2 Testing the adult CD8 prognostic signature on paediatric IBD: WGCNA

In order to address whether the adult CD8 prognostic signature would identify groups of children with different disease outcome, we first ran WGCNA on the adult data [67] and identified modules that correlated strongly with disease severity in the adult cohort, i.e. adult group IBD1 (severe) vs adult group IBD2 (mild) based on number of treatment escalations (More details on this step are provided in the Materials and Methods part on page 53).

Module-trait relationships from WGCNA analysis of the adult data is shown in Figure 3.3, where a selection of modules strongly correlated with the clinical variable “Group” (i.e. adult prognostic groups IBD1 (severe) vs IBD2 (mild)) is highlighted.

At this stage, the top modules identified above were applied to the paediatric data. Probes included in these modules were filtered out of the paediatric dataset and modules were matched against clinical outcomes including use of biologics, surgical intervention, number of relapses, number of unplanned inpatient days and severity score.

As shown in Figure 3.4 (top positively correlated modules in the adult dataset), and in Figure 3.5 (top negatively correlated modules in the adult dataset), there was no significant correlation (i.e. correlation index < 0.3) between modules and clinical outcomes in the paediatric dataset.

Together, these results suggest that the prognostic CD8+ T-cell gene expression signatures derived from an adult cohort of IBD patients are unable to differentiate children suffering from IBD at the point of diagnosis when applied to their CD8+ T-cells.

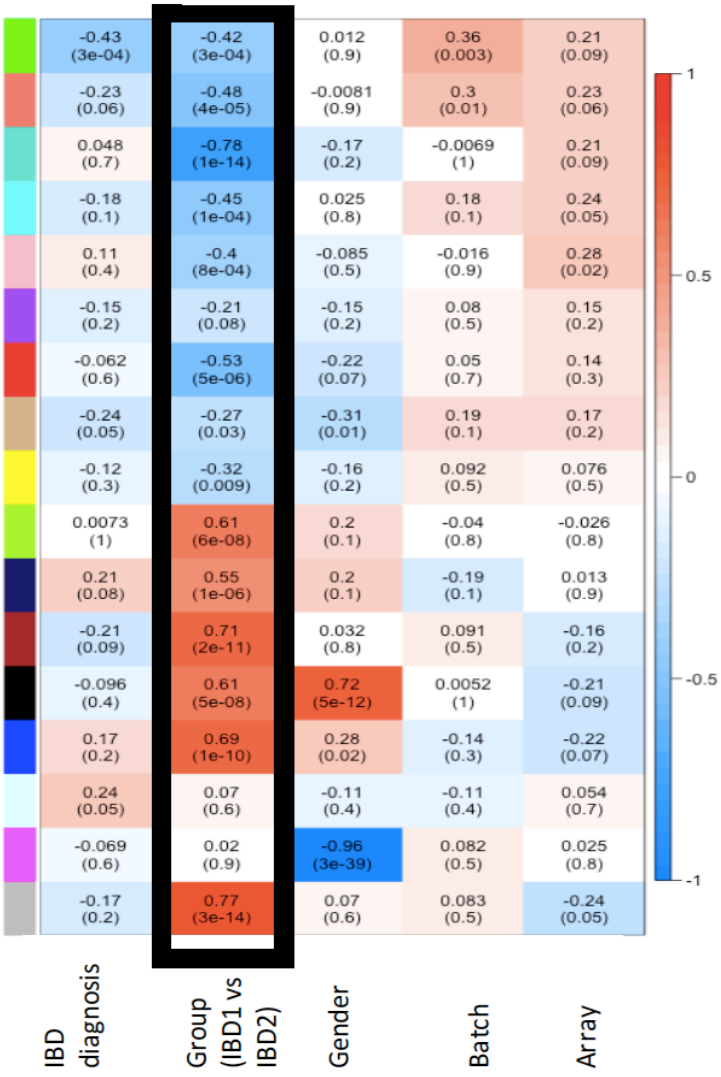

Figure 3.3 WGCNA. Module-trait relationships in the adult dataset (Lee JC et al. [67]) (n=67) showing modules (colour bars on the y axis) and clinical variables (x axis) including "Group" (i.e. different prognostic groups IBD1 (severe) vs IBD2 (mild) based on number of treatment escalations during the follow-up). The figures in the plot refer to correlation index and p-value (in brackets). A selection of the modules highlighted correlates significantly with "Group" either directly (in red) or inversely (in blue).

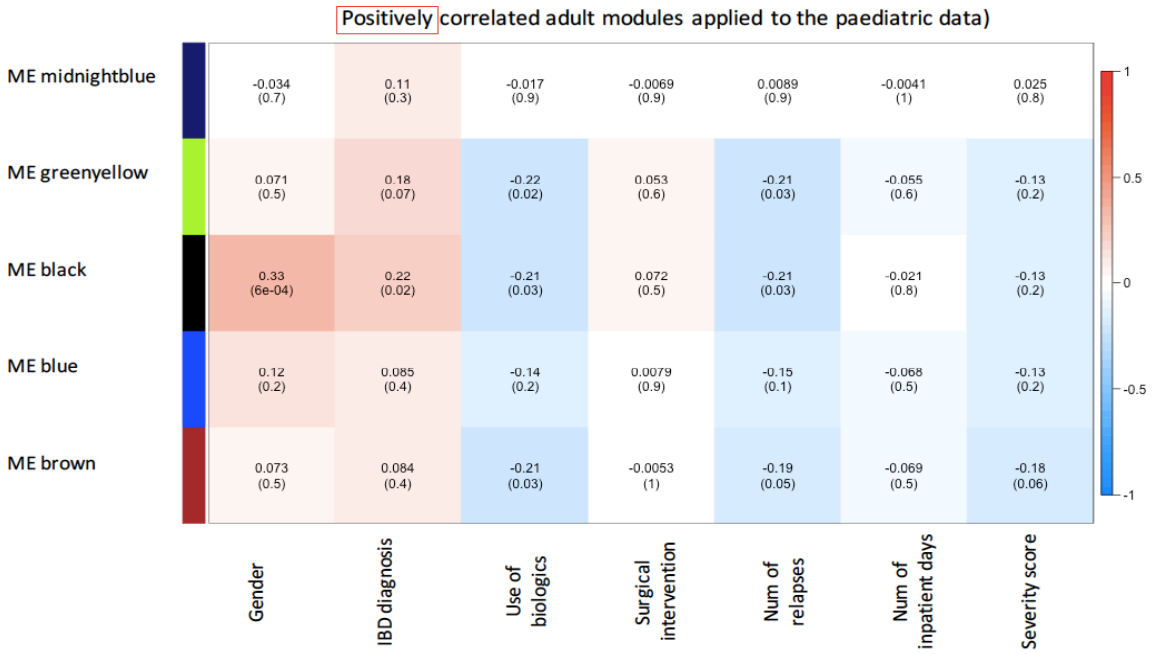

Figure 3.4 WGCNA. Module-trait relationships in the paediatric dataset (paediatric IBD cohort, n=98). Significant prognostic signatures from the adult study [67] (i.e. top modules directly correlated to the outcome "number of treatment escalations") were applied to the paediatric dataset and plotted against clinical outcomes. The plot shows modules (colour bars on the y axis) and clinical variables (x axis) including number of relapses, use of biologics, surgical intervention and severity score. The figures in the plot refer to correlation index and p-value (in brackets).

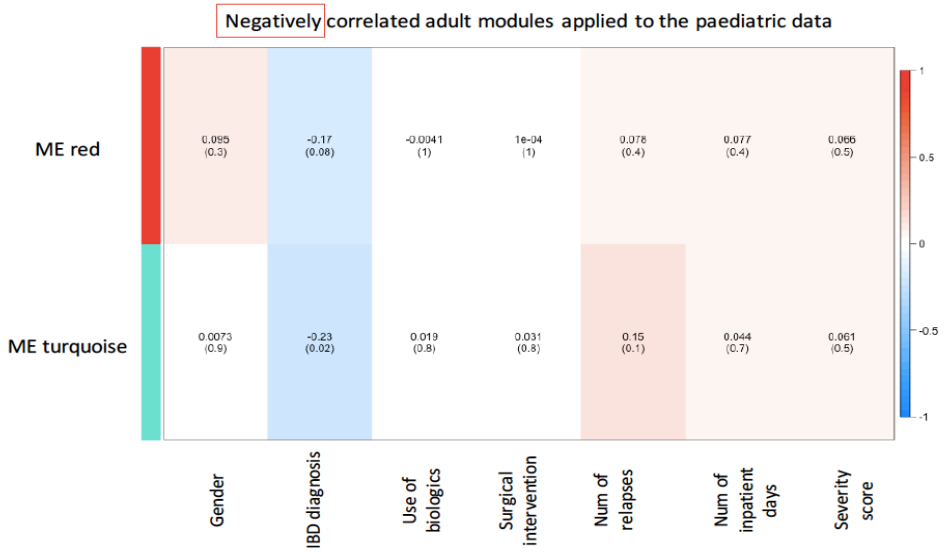

Figure 3.5 WGCNA. Module-trait relationships in the paediatric dataset (paediatric IBD cohort, n=98). Significant prognostic signatures from the adult study [67] (i.e. top modules inversely correlated with the outcome "number of treatment escalations") were applied to the paediatric dataset and plotted against clinical outcomes. The plot shows modules (colour bars on the y axis) and clinical variables (x axis) including number of relapses, use of biologics, surgical intervention and severity score. The figures in the plot refer to correlation index and p-value (in brackets).

3.3.3 Testing the T-cell exhaustion signature on the paediatric IBD cohort

We investigated whether the T-cell exhaustion signature, identified in adults as predictive towards a severe course of autoimmune diseases (including IBD) [155], would also play a role in paediatric IBD and whether it may serve as a prognostic biomarker.

Genes (probes) related to the T-cell exhaustion signature were filtered out from the paediatric IBD dataset (n=107) in order to look for presence of clusters based on the gene expression profiles in this selection (Figure 3.6). The heatmap on figure 3.6 identifies two groups of patients (dendrogram on top), although no clear difference was detected in their gene expression profiles.

We performed survival analysis to test whether the groups identified by applying the T-cell exhaustion signature to the paediatric data (Figure 3.6) would differ in respect to their disease course and outcomes (Kaplan Meier curves shown in Figure 3.7). The survival analysis did not identify any significant split between these groups with regard to treatment escalations, use of biologics and surgical intervention (Figure 3.7).

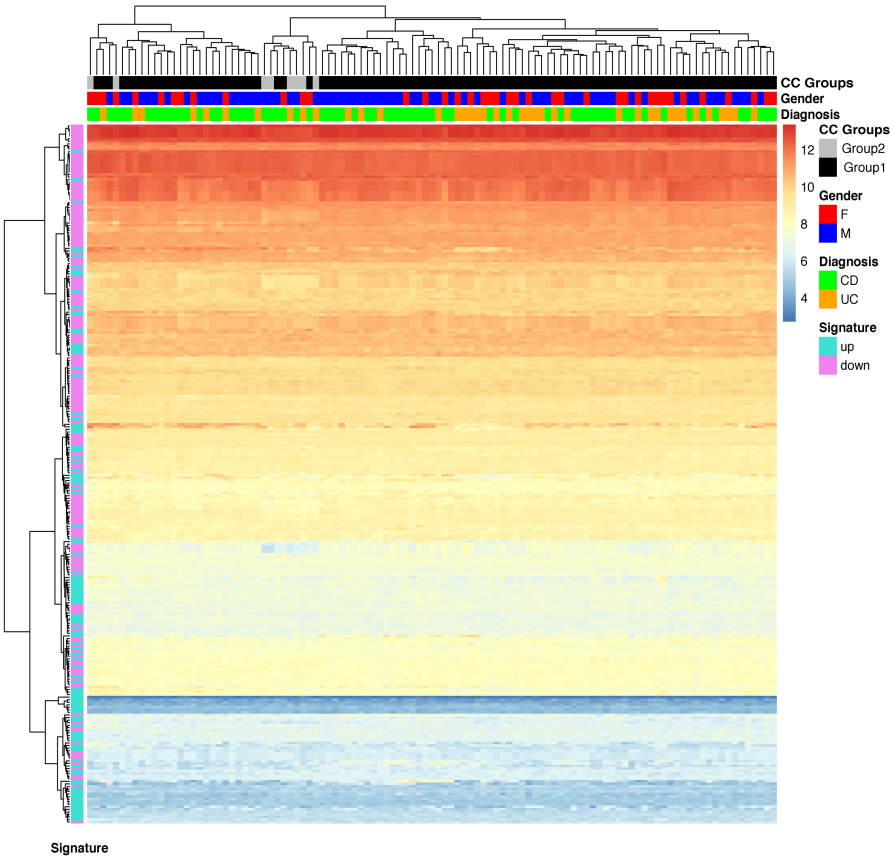

Figure 3.6 Heatmap showing gene expression profiles of the paediatric IBD cohort (n=107) for a selection of probes included in the T-cell exhaustion signature identified in adult autoimmune diseases [155]. On the y axis, the exhaustion signature is represented as a dendrogram (left) and it is colour coded for up-regulated and down-regulated exhaustion genes as a list. On the x axes the paediatric patients (paediatric IBD cohort, n=107) are shown as a dendrogram tree (top). Colour bars on the top of the chart display gender and type of diagnosis (i.e. CD vs UC) for each patient, as well as the unsupervised Consensus Clustering groups.

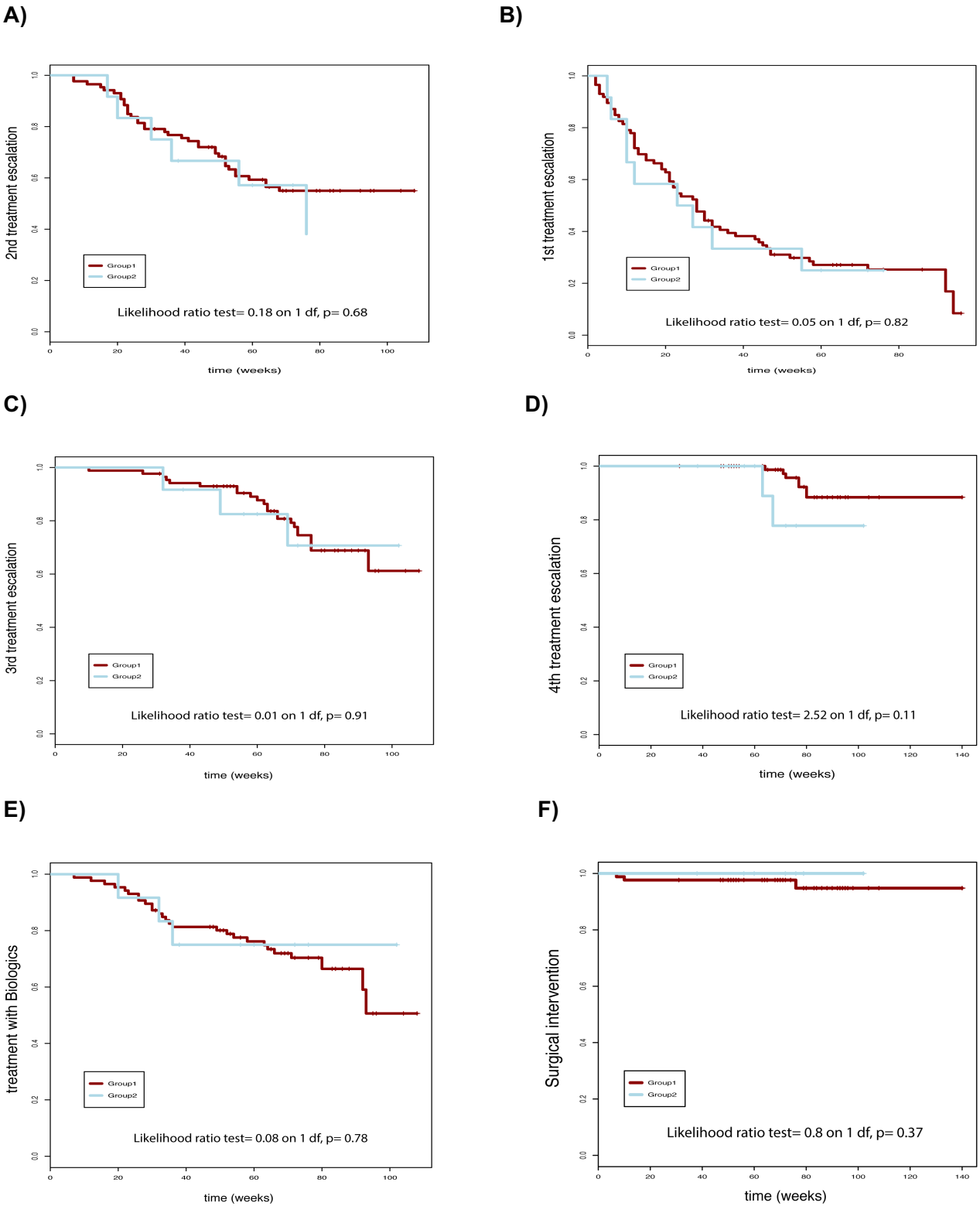

Figure 3.7 Kaplan Meier curves for the paediatric IBD cohort (n=107) comparing group 1 (n=80) and group 2 (n=27) identified in Figure 3.6. Patients in the two groups are compared for the following outcomes: A) first treatment escalation; B) second treatment escalation; C) third treatment escalation; D) fourth treatment escalation; E) use of biologics; F) surgical intervention.

At this stage, we moved on to split our paediatric cohort (n=107) by type of diagnosis, in order to analyse CD (n=67) and UC (n=40) separately, in consideration of the fact that clinical outcomes and indications to treatments including use of biologics and surgical intervention may differ according to the specific type of IBD. Nevertheless, separate analyses of CD and UC paediatric cohorts produced similar findings. No split in disease outcomes including number of treatment escalations, use of biologics and surgery was observed by applying the adult CD8 prognostic signature [67] or the T-cell exhaustion signature [155]. (Figure 3.8).

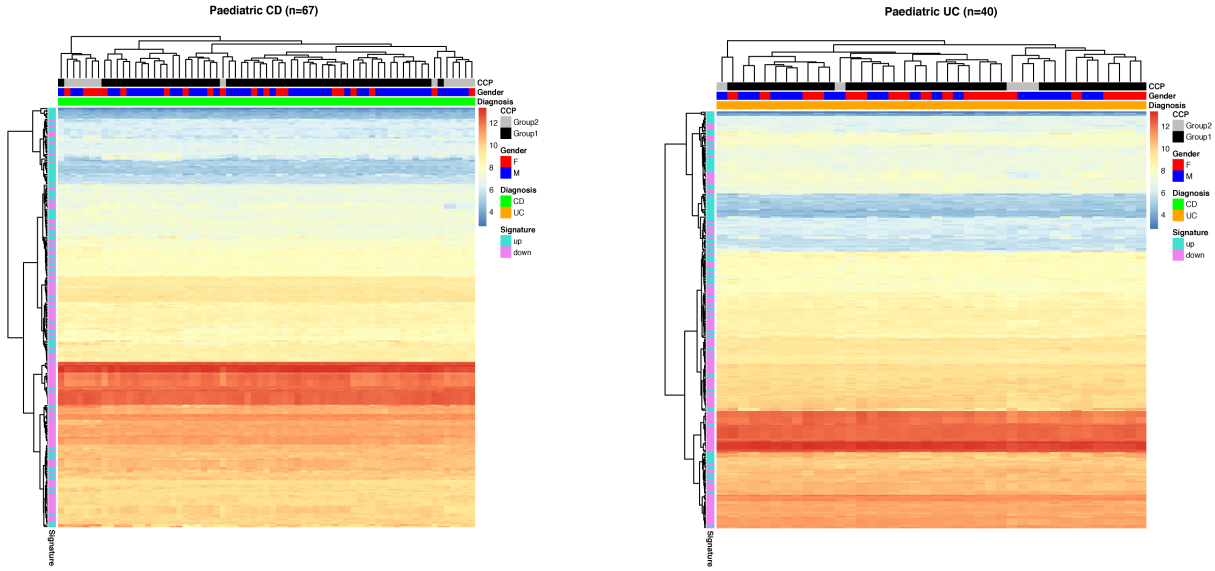

Figure 3.8 Heatmaps showing gene expression profiles of the paediatric CD (n=67) and UC (n=40) cohorts for a selection of probes included in the T-cell exhaustion signature identified in adult autoimmune diseases [155]. On the y axis, the exhaustion signature is represented as a dendrogram (left) and it is colour coded for up-regulated and down-regulated exhaustion genes as a list. On the x axes the paediatric patients are shown as a dendrogram tree (top). Colour bars on the top of the chart display gender and type of diagnosis for each patient, as well as the unsupervised Consensus Clustering groups.

3.3.4 Distinct differences in disease behaviour of children diagnosed with IBD compared to adults.

In light of our findings so far, we speculated whether the inability of an adult derived expression signature to predict disease outcome in children could be related to differences in phenotype between adult and paediatric onset IBD. We therefore compared the two cohorts based on overlapping clinical outcome parameters that were available for both patient groups (i.e. number of treatment escalations).

Indeed, as shown in Figure 3.9 (and reported in Table 2.1, on page 44), in the paediatric cohort the number of treatment escalations was significantly higher than in the adult population, suggesting that children suffer an overall worse disease outcome and hence could display a “severe” CD8+ expression signature.

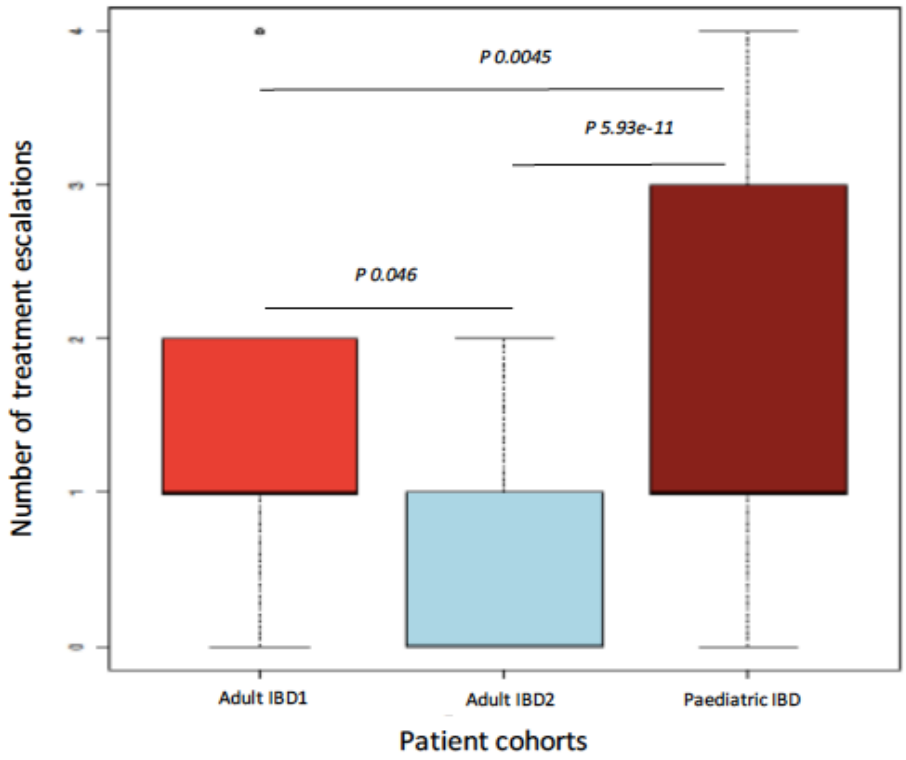

Figure 3.9 Comparison of clinical outcome “number of treatment escalations” between the paediatric cohort (box plot on the right) and the adult data available from the study by Lee JC et al. [67]; Ad_IBD1: Adult poor prognosis group (n=25), Ad_IBD2: Adult good prognosis group (n=42); Paed_IBD: Paediatric cohort altogether (n=107).

3.4 Discussion

In this chapter, we show that the adult CD8 and T-cell exhaustion signatures identified as predictive for disease severity in adult IBD patients do not generate a similar split when applied to our paediatric IBD cohort.

The use of two complementary approaches (i.e. unsupervised analysis and WGCNA) showing no significant differences in outcome between the groups identified, and no correlation between modules and specific outcomes respectively, negates any prognostic power of these adult signatures in our paediatric cohort.

The analysis was conducted on the joint paediatric IBD cohort as well as on the paediatric CD and UC cohorts separately, within an attempt of removing any confounders related to different indications to treatments and disease outcomes in the two types of IBD. Nevertheless, results were consistently negative across the three datasets analysed. This may suggest that in paediatric onset IBD, T-cells are not exhausted, therefore paediatric patients are predisposed to a more severe disease phenotype and course compared to adults, as they would lack of the protective role of T-cell exhaustion.
This would also explain the absence of a significant split in clinical outcomes between the groups identified, as all of the children would fall into the “severe prognosis group”.
The comparison between children and adults in terms of number of treatment escalations during the follow-up shown in Figure 3.9 would also stand in support of this hypothesis.

At this stage, in the absence of a prognostic role of adult CD8 and T-cell exhaustion signatures in our paediatric cohorts, we went on to address the question of whether “paediatric specific” CD8 signatures further able to differentiate patients according to disease outcome exist.

CHAPTER 4

Identification of paediatric CD8+ T-cell expression derived prognostic signatures

4.1 Introduction

As demonstrated in previous chapters, applying a prognostic T-cell expression signature derived from an adult IBD patient cohort to our paediatric data, did not yield any significant separation of patients according to disease outcome. Furthermore, T-cell exhaustion did not seem to differ in CD8+ T-cells derived from paediatric IBD patients, leading us to speculate whether a paediatric specific disease prognostic expression profile could be identified.
Hence, we next went on to identify such a signature by analysing the paediatric cohort in isolation using the same analyses as previously described (i.e. unsupervised clustering methods and WGCNA).

4.2 Materials and methods

Samples were first analysed altogether (paediatric IBD cohort, n=107), and then split by type of IBD diagnosis (CD (n=67) and UC (n=40)).
Normalisation, removal of outliers and batch correction were performed in the joint IBD dataset (n=107). Samples were then split by type of IBD diagnosis (i.e. CD and UC).

4.2.1 Unsupervised clustering analysis

Unsupervised clustering analysis included Hierarchical Clustering and Consensus Clustering.
Hierarchical Clustering (BioConductor function “hclust”) was used to test whether datasets had a substructure, i.e. whether clusters and subclusters could be identified, based on the patients’ gene expression profiles.
Consensus Clustering was utilised as a more accurate clustering methodology to identify presence of stable groups across the dataset, and to choose the strongest clustering option. Top clustering option is shown by the Consensus Distribution Function (CDF) plot; it consists in the recommended number of clusters amongst various output options displayed and indicated with letter “k” followed by progressive numbering. Prior to running Consensus Clustering, the data was filtered by using the R package “genefilter” and half of the genes (var. cutoff: 0.5) with more variation in gene expression across this dataset were selected. The strength of clusters across the data was also tested by using R package “SigClust”, a method that measures the reliability of clusters by using the 2-means (k = 2) clustering index as a statistic (Figure 4.1).

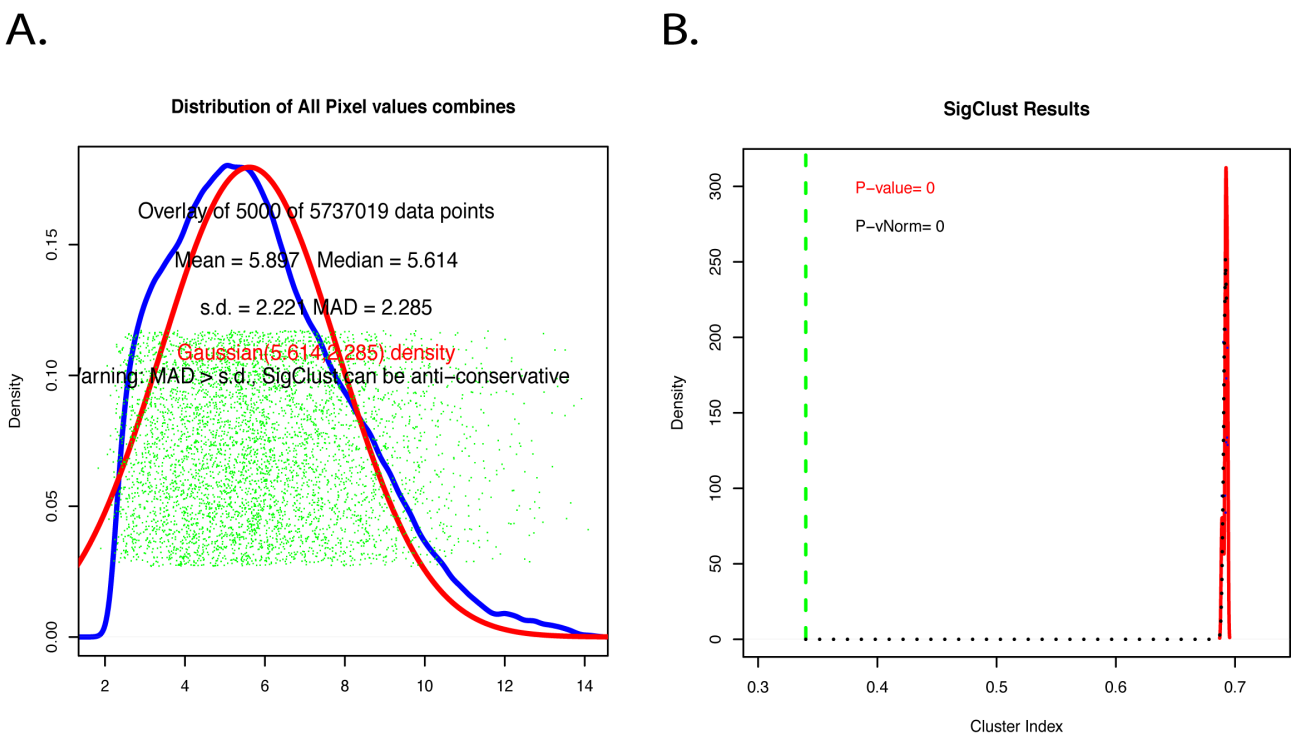

Figure 4.1 SigClust analysis of CD8+ T-cell gene expression data from the paediatric IBD cohort (n=107). In A., SigClust analysis assesses the significance of clustering by simulation from a single null Gaussian distribution. The null hypothesis of SigClust is that the data is from a single Gaussian distribution. In B., the SigClust method uses a test statistic called the cluster index (CI) which is defined to be the within-class sums of squares about the mean divided by the total sum of squares about the overall mean.

When significant differences in disease outcomes were observed between groups identified through Consensus Clustering, GSEA was also performed to compare the groups identified and to detect whether they would differ in molecular pathways of biological relevance.

4.2.2 WGCNA

WGCNA was performed on 98 IBD patients (i.e. 60 CD and 38 UC) due to the removal of those treated with biologics from the time of diagnosis. In fact, in terms of disease course and clinical outcomes these patients would not be comparable with the remainder of the children receiving a strict step-up treatment approach.

As a first step, WGCNA aligns the gene expression data with clinical information collected on a ".csv" spreadsheet (Figure 4.2; the ".csv" file used is shown in table format in Appendix 2, on page 176).

The next step of WGCNA consists in the choice of a soft thresholding power [159,160] based on the criterion of scale-free topology (Figure 4.3).

This number represents the stage where the network (based on gene expression similarity in this context) stabilises, and corresponds to the point where the curves for scale independence and mean connectivity reach a plateau.

At this stage, it is possible to compute and display the number of modules identified in each dataset. We set up minimal module size at 20 probes/module. An example plot of module detection in the joint IBD cohort (n=98), based on clustering dendrogram of genes and on their dissimilarity according to topological overlap, is shown in Figure 4.4. Moreover, Table 4.1 shows the corresponding list of modules identified and their size.

Final step of WGCNA is testing the correlation between modules and measured clinical traits. The summary profile (eigengene) for each module is used for correlation with clinical variables imported from the ".csv" file (and aligned with the data in the initial step of WGCNA). Correlation index and p-value are provided for each match between modules and clinical variables, which in this context allowed the identification of modules (signatures) more significantly correlated with disease outcomes.

In order to test further the prognostic role of the relevant modules (signatures) identified, probes in these modules of interest were subset from the paediatric dataset. Consensus Clustering was then run on this selection and the patient groups identified were compared for the specific outcomes through survival analysis. In case of a significant split, GSEA was also performed to detect whether the groups identified would differ in molecular pathways of biological relevance.

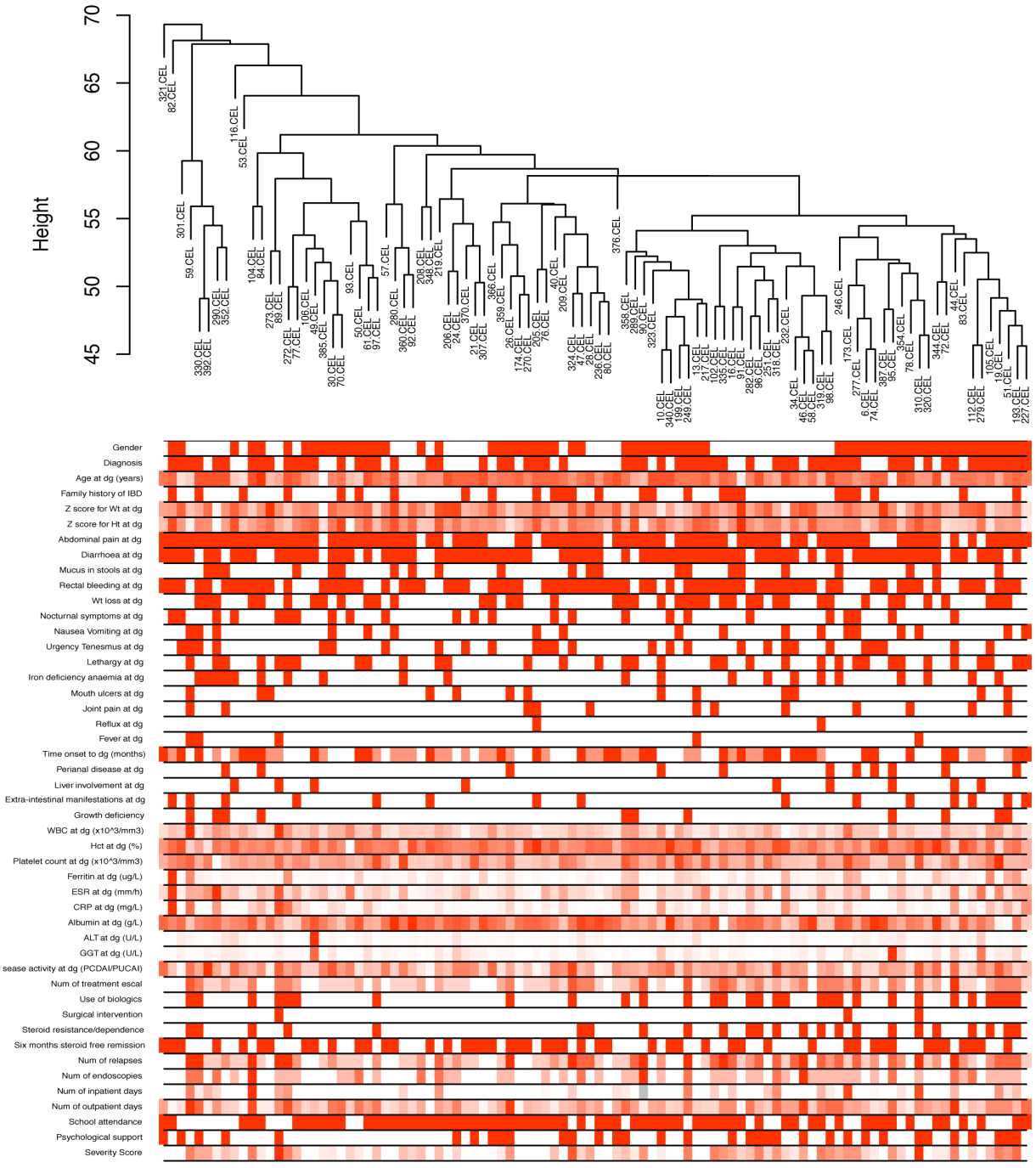

Figure 4.2 WGCNA analysis of the paediatric IBD cohort (n=98). Sample dendrogram and trait heatmap. The dendrogram on top displays the samples in this cohort based on hierarchical clustering of their CD8 gene expression data. The heatmap below aligns all clinical information available for each patient / sample presented as colour coded for each variable. For dichotomous variables (e.g. presence of symptoms): white = no, red = yes; for continuous variables (e.g. blood test results): white = minimum, red = maximum, shades of red for values in between.

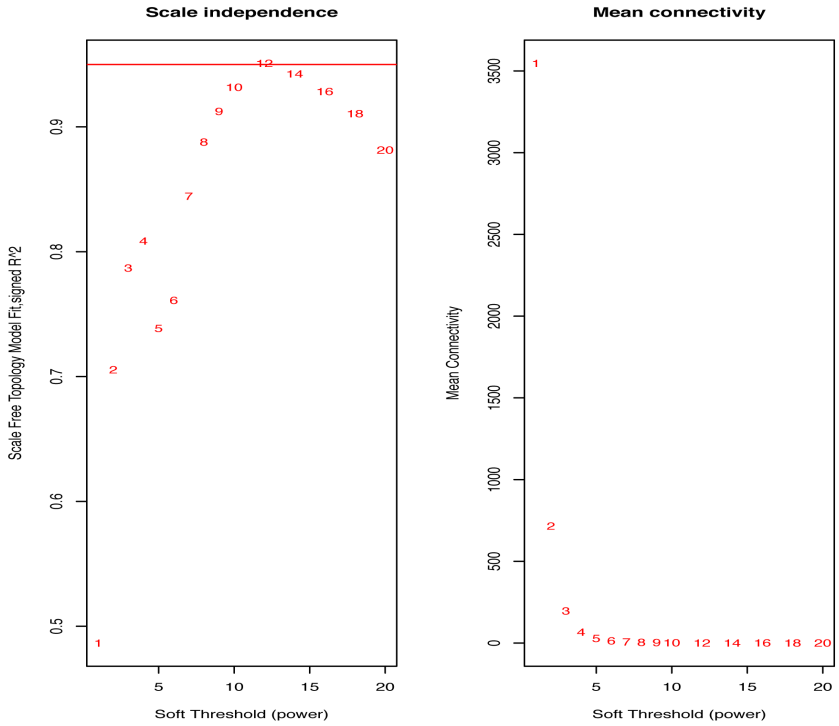

Figure 4.3 WGCNA. Analysis of network topology in the paediatric IBD cohort (n=98) for various soft-thresholding powers. The left panel shows the scale-free topology index (y axis) as a function of the soft-thresholding power (x axis). The right panel displays the mean connectivity (degree, y axis) as a function of the soft-thresholding power (x axis). Soft thresholding power chosen: 12.

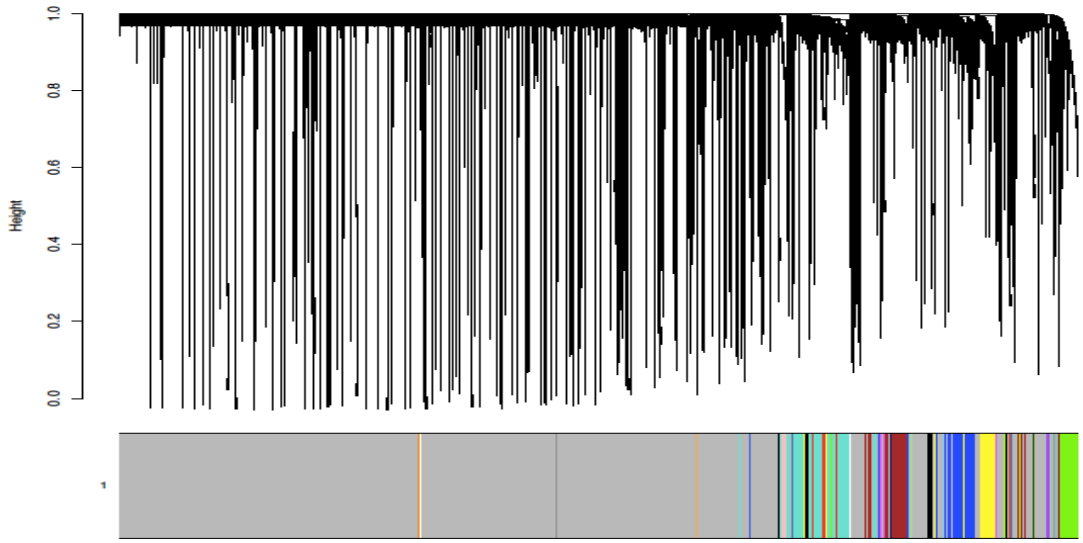

Figure 4.4 Clustering dendrogram of genes, with dissimilarity based on topological overlap, together with assigned module colours (paediatric IBD cohort, n=98).

Module Number	Genes in each module	Module Number	Genes in each module
0	24396	**12**	71
1	837	**13**	71
2	664	**14**	52
3	588	**15**	47
4	583	**16**	44
5	502	**17**	41
6	411	**18**	34
7	249	**19**	34
8	175	**20**	30
9	169	**21**	30
10	118	**22**	29
11	96	**23**	27

Table 4.1 WGCNA of the paediatric IBD cohort (n=98). Module numbers and their size. The label 0 is reserved for genes outside of all modules, so it is not a module per se.

4.3 RESULTS

4.3.1 Analysis of CD8+ T-cell gene expression profiles from the combined paediatric IBD cohort

In the first instance, we performed unsupervised clustering analyses on the combined paediatric IBD cohort (i.e. samples from children with CD and UC).
We started with Hierarchical Clustering to investigate whether the CD8+ gene expression data in this cohort had a substructure, i.e. whether clusters of samples with similar gene expression levels could be detected. As shown in Figure 4.5 A, the data clustered into two main groups, with an approximate size of 2/3 and 1/3 respectively. Each group was clustered into further subgroups.

We then performed Consensus Clustering as an alternative clustering methodology to identify presence of reliable stable clusters within the dataset. The consensus output identified three more solid groups of patients across this dataset. Figure 4.5 D shows the Consensus Clustering plot for k=3, which provides the strongest clustering: the three groups differ in size, with a larger group including approximately 90% of the patients and two smaller groups accounting in total for 10% of the patients.

As a further step, we addressed the question of whether the groups identified through Consensus Clustering (Figure 4.5 D: group 1 (n=99) vs groups 2+3 (n=8), renamed as group 2) would differ in respect to their disease course and outcomes, i.e. whether groups identified in this cohort based on the paediatric CD8 gene expression profiles would be different in their disease outcomes.
Survival analysis did not identify significant differences between these groups in terms of use of biologics, treatment escalations and surgical intervention (Kaplan Meier curves on Figure 4.6).
Although children in group 2 were milder in their disease course, the difference in the groups' size affected the power of the survival analysis which didn't reach significance except for the outcome "first treatment escalation" (Figure 4.6 A).

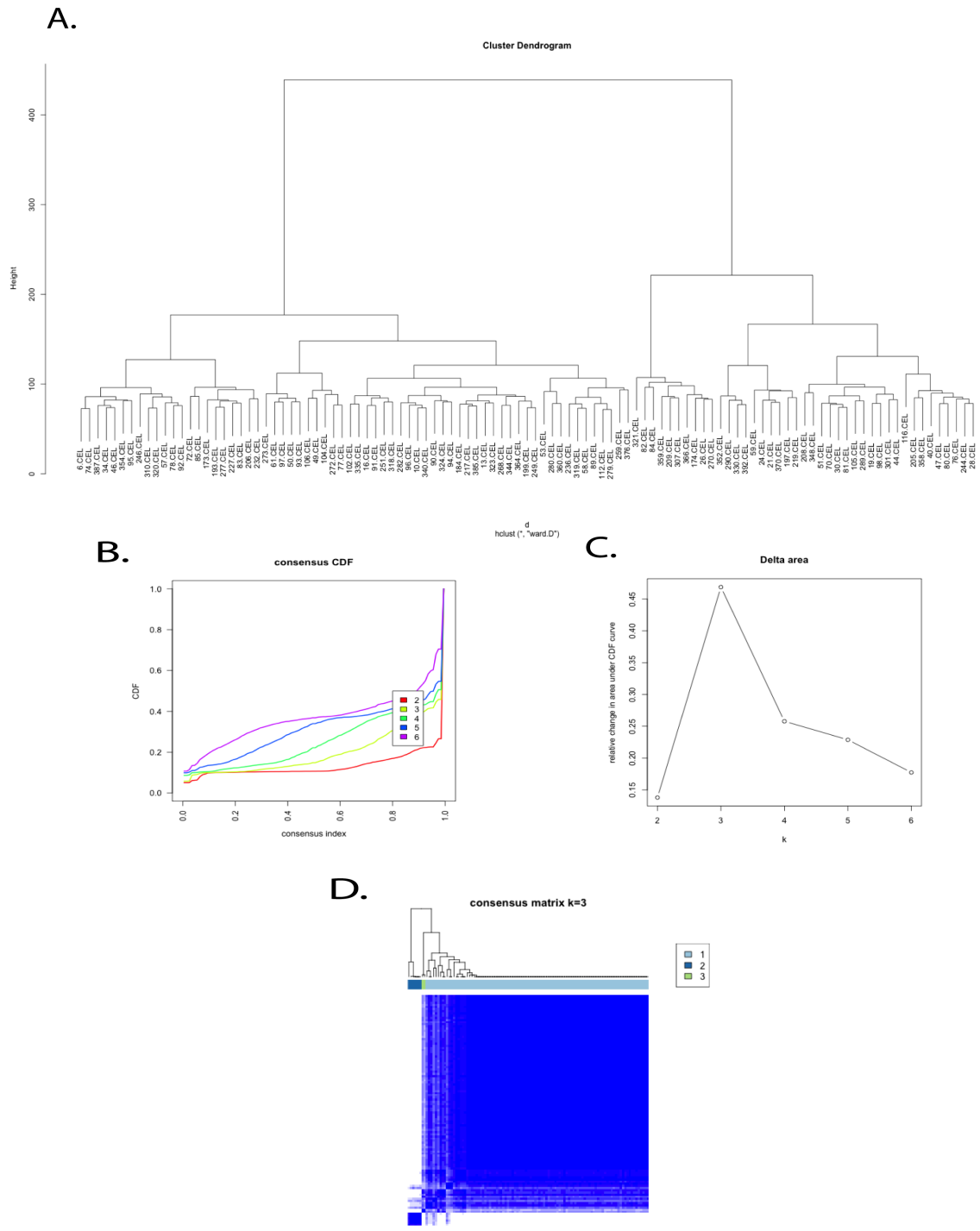

Figure 4.5. In A. Hierarchical Clustering of the CD8 gene expression data in the paediatric IBD cohort (n=107). In B. CDF: Consensus Cumulative Distribution Function showing at what number of clusters, k, consensus and cluster confidence reach a maximum. In C. Delta area plot showing the relative change in area under the CDF curve, with no further appreciable increase at k=3. k3 is identified as the strongest clustering option. In D. Consensus Clustering plot (for k=3) of gene expression data from the paediatric IBD cohort (n=107): clusters are shown as dendrogram (top), colour bar, and gene expression heatmap.

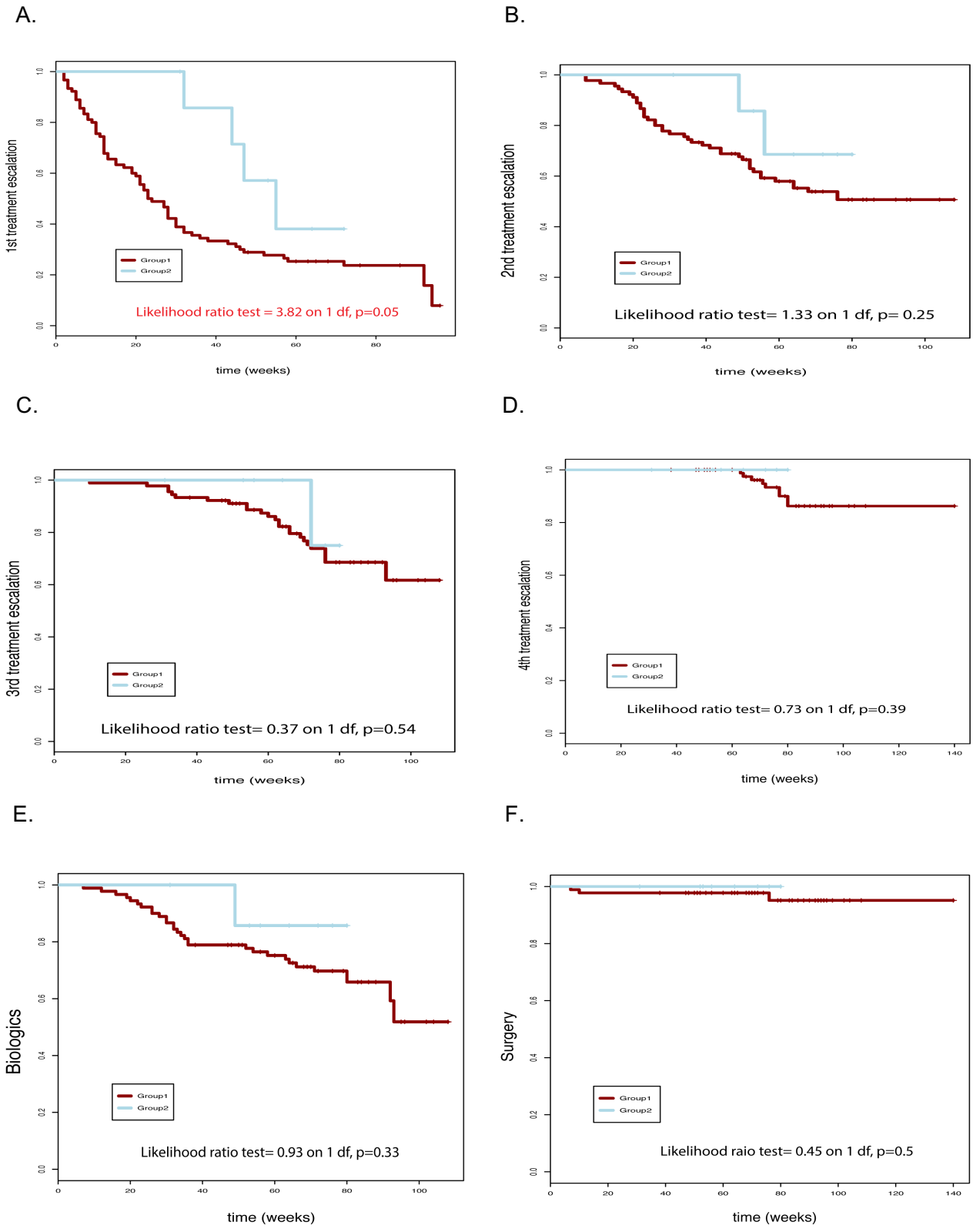

Figure 4.6 Kaplan Meier curves for the paediatric IBD cohort (n=107) comparing group 1 (n=99) and group 2 (n=8) identified through Consensus Clustering (Figure 4.5 D). Patients in the two groups are compared for the following outcomes: A) first treatment escalation; B) second treatment escalation; C) third treatment escalation; D) fourth treatment escalation; E) use of biologics; F) surgical intervention.

Next, in order to address the same question, i.e. whether a paediatric CD8 signature to be able to predict disease severity exists, we also performed WGCNA of CD8+ T-cell gene expression profiles from the combined paediatric IBD cohort. More specifically, WGCNA aimed to explore whether the gene expression data would be organised in groups of genes with similar expression (modules) and whether any of these modules would correlate with specific disease outcomes reflecting severity of disease course. The ultimate aim of WGCNA was to detect specific signatures for clinical variables reflecting disease severity (i.e. outcomes).

First, as shown in Table 4.1 on page 78, 22 modules were detected in this cohort.
As a next step, correlations between modules and measured clinical traits were tested. Figure 4.7 displays correlations between each module and all clinical variables recorded, while in Figure 4.8 only the modules of relevance to disease outcomes are shown.
As recapped in Table 4.2., module lightyellow [5] and module pink [11] showed the strongest correlation with disease outcomes, though correlation indexes only ranged between ± 0.18 and ± 0.24. Module light yellow was correlated with several clinical outcomes, i.e. number of relapses, number of treatment escalations and use of biologics.

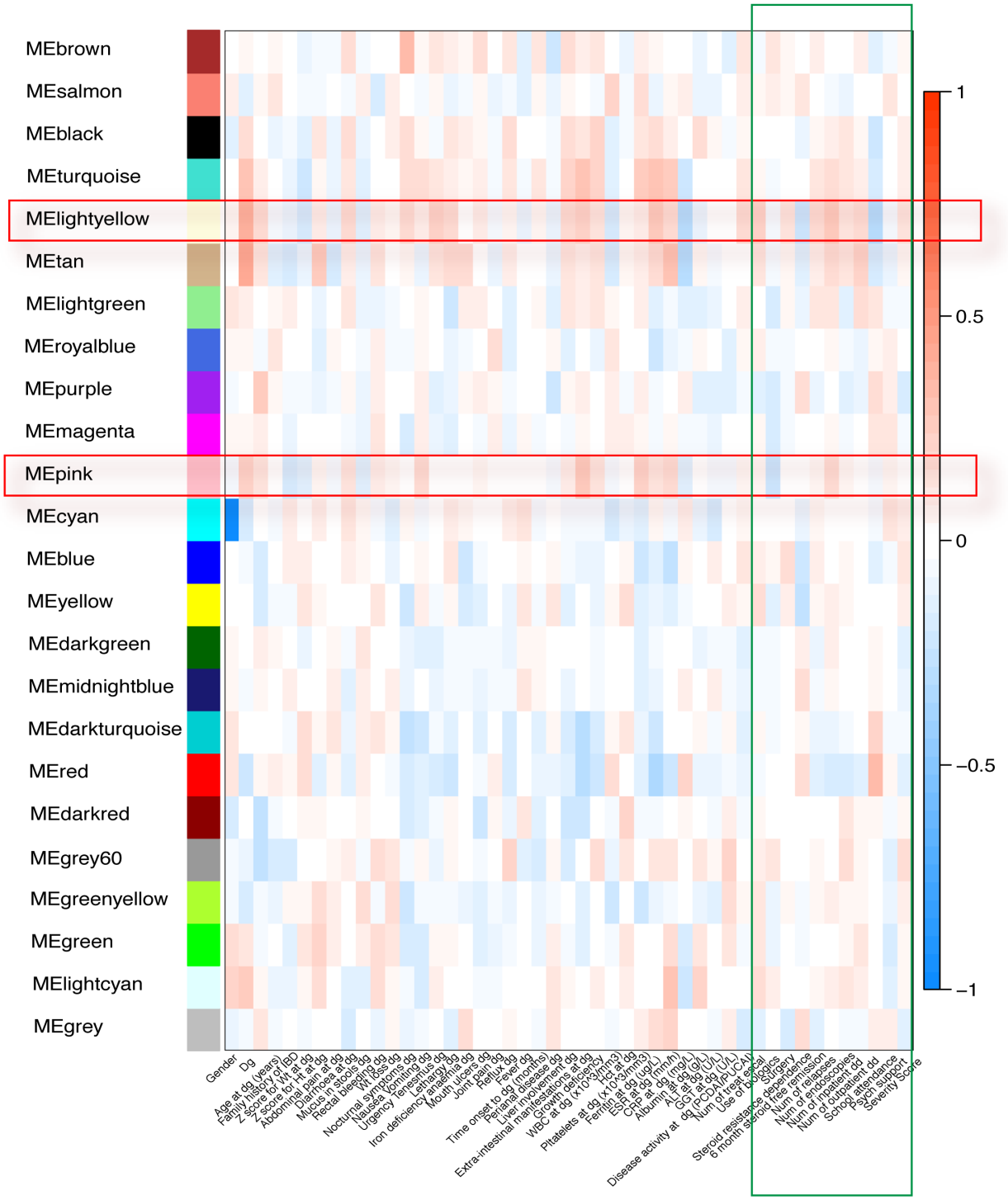

Figure 4.7 WGCNA. Module-trait associations. Paediatric IBD cohort (n=98). Each row corresponds to a module eigengene, column to a trait. Each cell contains the corresponding correlation index and p-value (colour-coded, numbers not displayed in this plot, but available separately). The table is colour-coded by correlation according to the colour legend (i.e. 1 = highest direct correlation, red; -1 = highest inverse correlation, blue). Red frames highlight modules that correlate with outcomes more than they do with clinical parameters at diagnosis. The green frame highlights clinical outcome measures (e.g. number of treatment escalations, surgery, use of biologics etc.)

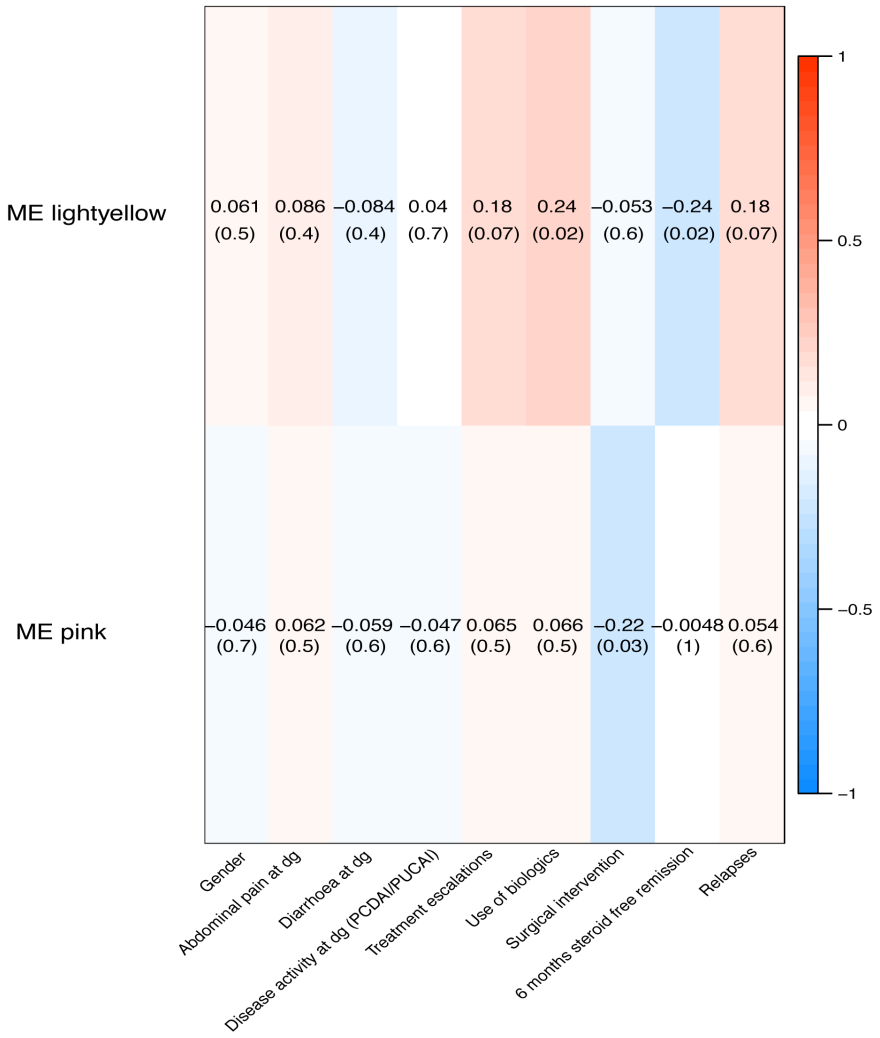

Figure 4.8 WGCNA. Module-trait associations. Paediatric IBD cohort (n=98). Selection of modules correlated with clinical outcomes from Figure 4.7. On the x axis are variables related to the disease at diagnosis (e.g. gender, abdominal pain at diagnosis, diarrhoea and disease activity score at diagnosis (e.g. PCDAI, PUCAI)) followed by variables describing disease outcomes (e.g. use of biologics, surgery). On the y axis, selected modules are listed (indicated by colour names). The plot shows how these modules correlate more strongly (directly or inversely) with disease outcomes than they do with parameters describing disease at diagnosis.

CLINICAL OUTCOMES	CORRELATION INDEX	P-VALUE
BIOLOGICS		
ME lightyellow [5]	0.24	0.02
TREATMENT ESCALATIONS		
ME lightyellow [5]	0.18	0.07
6 MONTHS STEROID FREE REMISSION		
ME lightyellow [5]	- 0.24	0.02
ME blue [13]	- 0.21	0.03
ME yellow [14]	- 0.24	0.02
ME midnightblue [16]	0.2	0.05
RELAPSES		
ME lightyellow [5]	0.18	0.07
SURGERY		
ME pink [11]	- 0.22	0.03

Table 4.2 WGCNA. Paediatric IBD cohort (n=98). Main modules correlating with disease outcomes.

Finally, in order to test the prognostic power of the modules (signatures) identified, we subset their corresponding probes from this dataset (i.e. paediatric IBD cohort, n=98) and performed Consensus Clustering of this selection. We then compared the groups identified for the specific outcomes correlated with those modules.

We first tested module light yellow (34 probes), correlated with number of relapses, treatment escalations and use of biologics. Groups based on this module were identified through Consensus Clustering, as shown in Figure 4.9 C (*k*3: group 1 (n=67) vs groups 2+3 (n=31), renamed as group 2). The survival analysis performed to compare these groups for clinical outcomes (Figure 4.10) did not show significant differences.

We then tested module pink (175 probes), correlated with surgical intervention. Groups identified through Consensus Clustering (Figure 4.11 C *k*3: group 1 (n=85) vs groups 2+3 (n=13), renamed as group 2) did not show a significant split on the Kaplan Meier analysis for surgical intervention. Nevertheless, whilst none of the patients in group 2 had surgery, 3 patients in group 1 required surgical intervention.

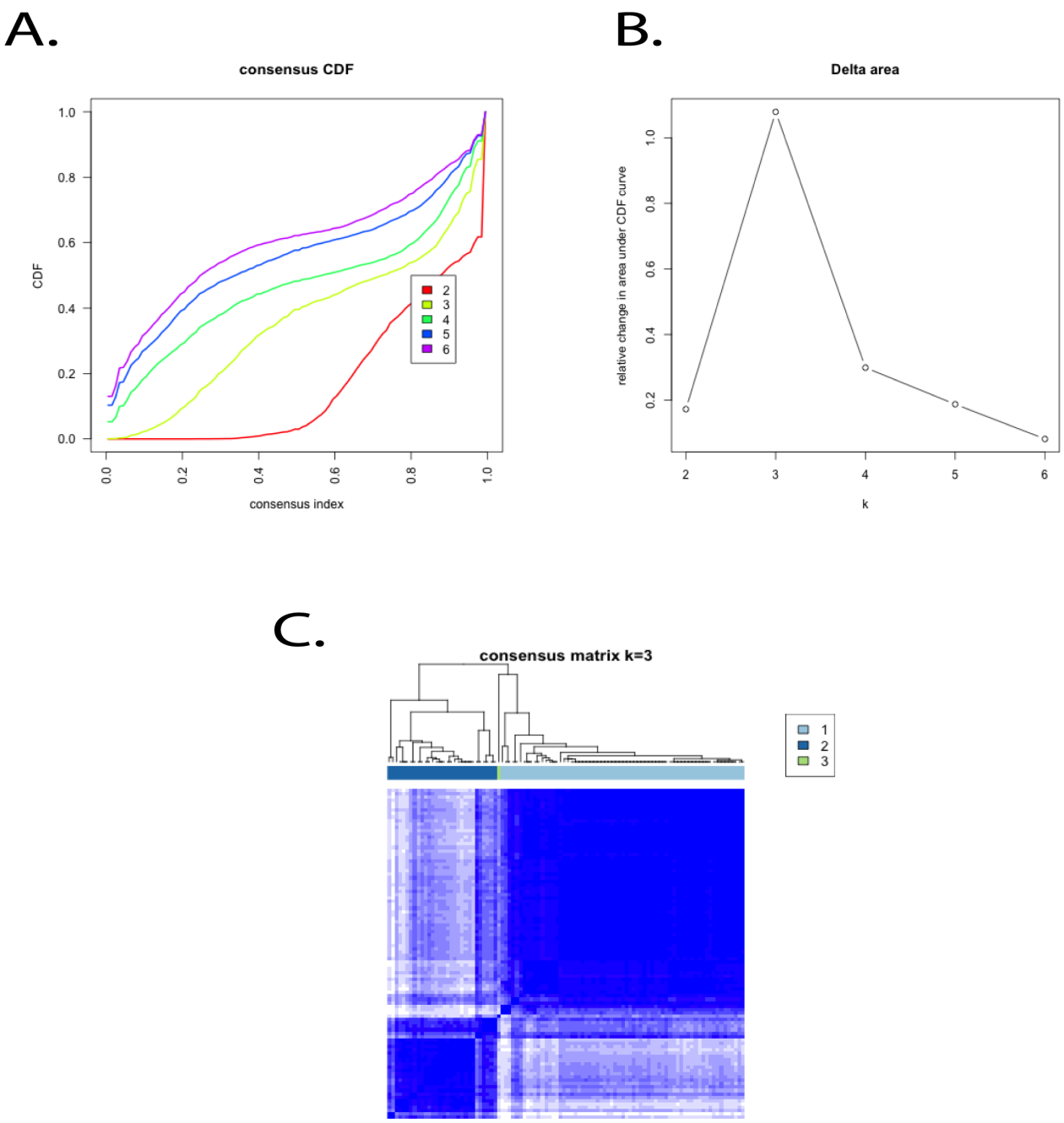

Figure 4.9 Consensus Clustering of a selection of probes included in the WGCNA module light yellow (34 probes), correlated with "number of relapses", "number of treatment escalations" and "use of biologics". In A. CDF: Consensus Cumulative Distribution Function showing at what number of clusters, k, the consensus and cluster confidence reach a maximum. In B. Delta area plot showing the relative change in area under the CDF curve, with no further appreciable increase at k=3. k3 is identified as the strongest clustering option. In C. Consensus Clustering plot for k=3.

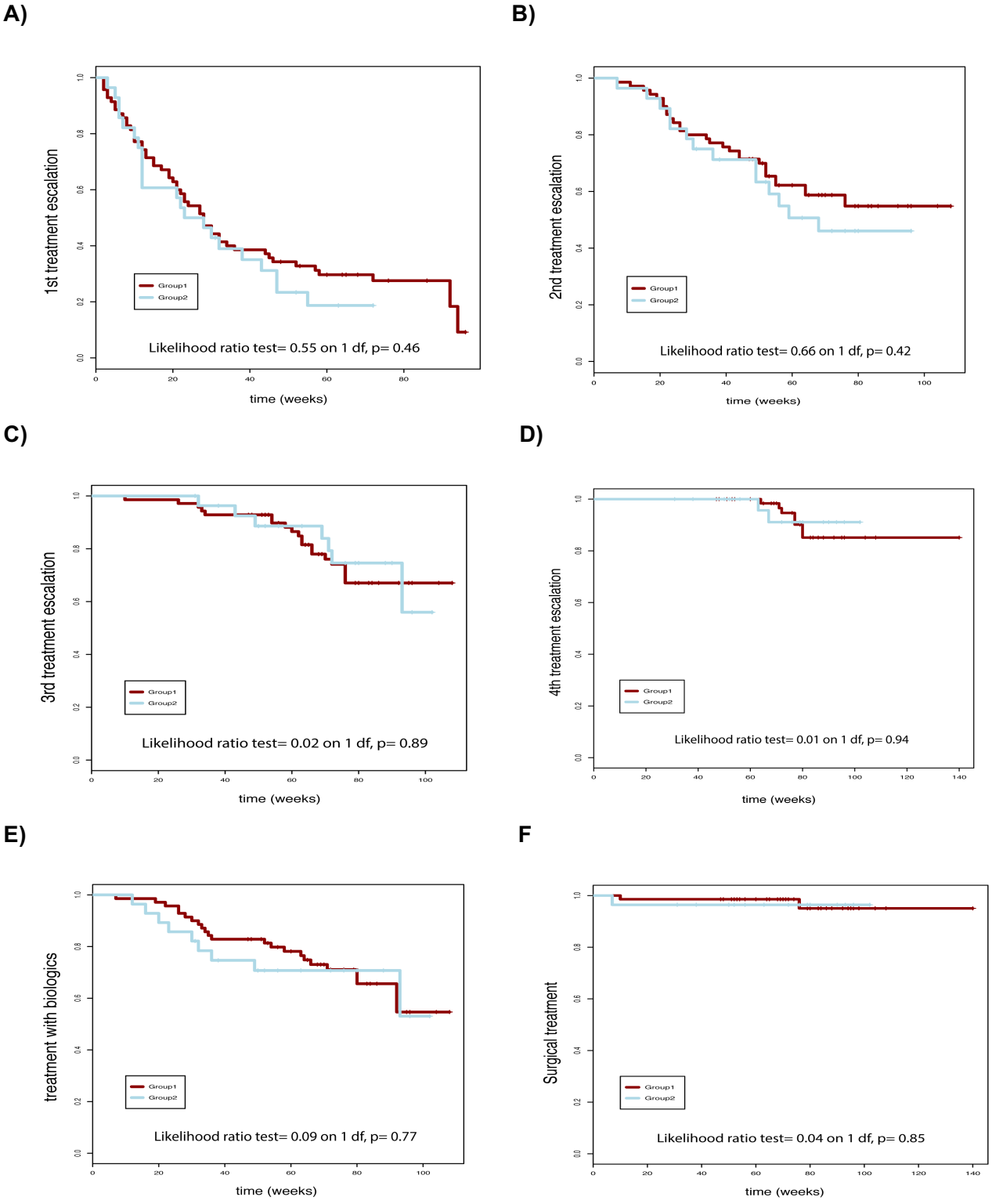

Figure 4.10 Kaplan Meier curves comparing the groups identified in 4.9 C (group 1: n=67 and group 2 (i.e. 2+3): n=31) for the following outcomes: A) first treatment escalation; B) second treatment escalation; C) third treatment escalation; D) fourth treatment escalation; E) use of biologics; F) surgical intervention.

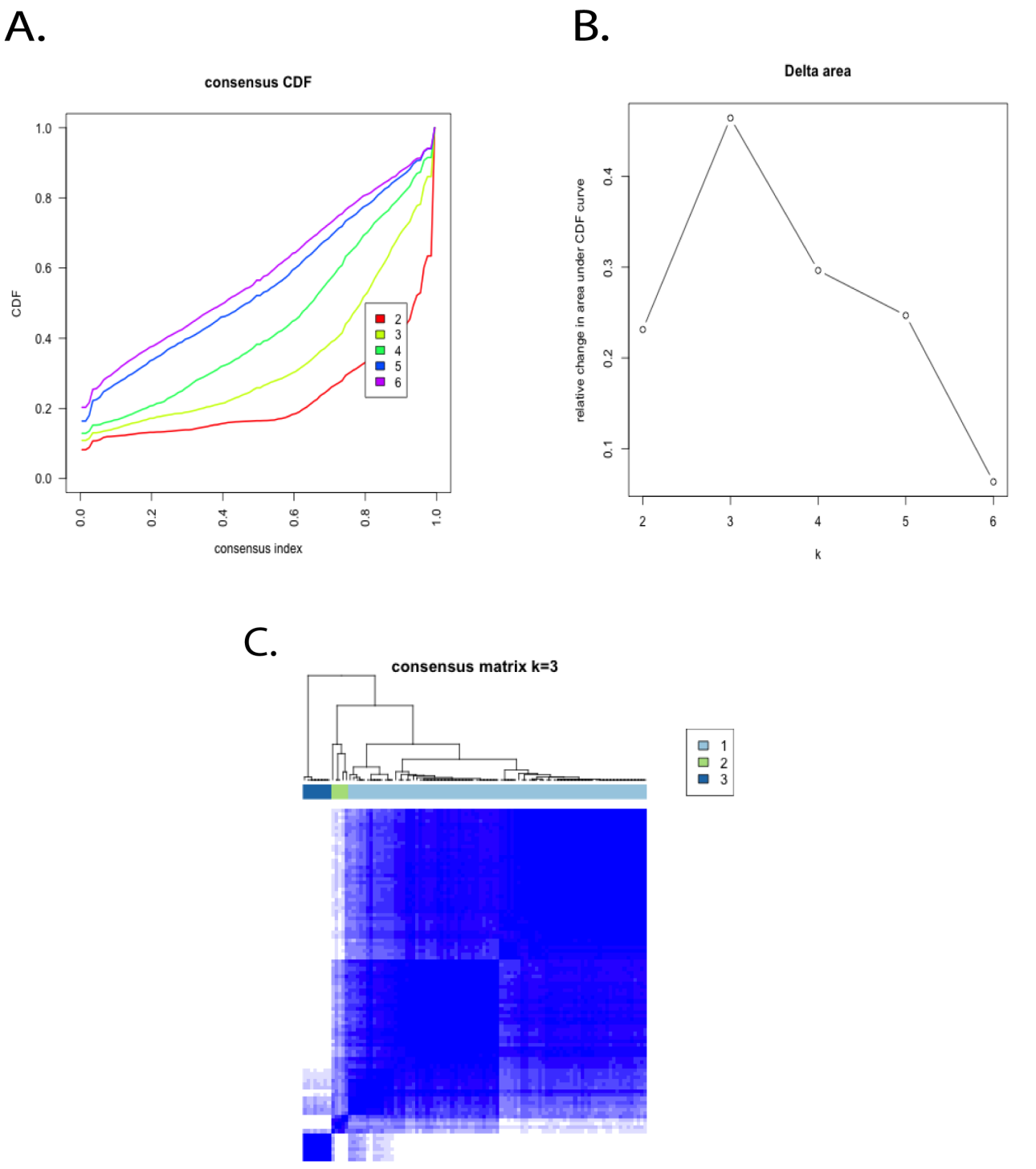

Figure 4.11 Consensus Clustering of a selection of probes included in the WGCNA module pink (175 probes), correlated to "surgical intervention". In A. Consensus Cumulative Distribution Function (CDF) showing at what number of clusters, k, the consensus and cluster confidence reach a maximum. In B. Delta area plot showing the relative change in area under the CDF curve, with no further appreciable increase at k=3. k3 is identified as the strongest clustering option. In C. Consensus Clustering plot for k=3.

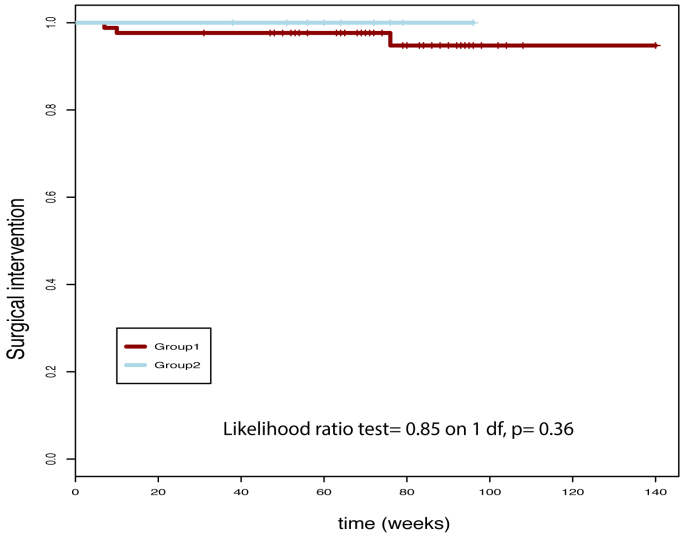

Figure 4.12 Kaplan Meier curves comparing the groups identified in 4.11 C (group1: n=85 and group2 (i.e. 2+3): n=13) for the event "surgical intervention".

In summary, in the joint paediatric IBD cohort we could not identify strong correlations between gene expression profiles (i.e. signatures, modules) and prognostic outcomes, neither by using unsupervised clustering analyses nor by applying WGCNA.

4.3.2 Analysis of CD8+ T-cell gene expression profiles from the paediatric CD cohort

In this section, we applied the same methods utilised above (i.e. unsupervised clustering analyses and WGCNA) to analyse our paediatric CD cohort separately (n=67) and identify whether signatures specific to paediatric CD able to differentiate children for their disease severity exist.
First, we performed Hierarchical Clustering to investigate whether the CD8+ gene expression data in this cohort had a substructure. Similarly to what identified in the combined IBD cohort, this dataset also clustered into two main groups, with an approximate size of 3/4 and 1/4 respectively (Figure 4.13 A). Each group was clustered into further subgroups.
Consensus Clustering analysis identified three more solid groups of patients throughout the dataset. Figure 4.13 C shows the top Consensus Clustering plot, where *k*=3 provides the strongest clustering: one bigger and two smaller clusters were identified, with an approximate size of 3/4 and 1/4 for group 1 and for groups 2+3, respectively.

Next, we tested whether the groups identified through Consensus Clustering (Figure 4.13 D *k*3: group 1 (n=54) vs groups 2+3 (n=13), renamed as group 2) would split for disease outcomes, i.e. whether groups identified in this cohort based on CD8 gene expression profiles would differ in terms of disease severity over time. Survival analysis identified a significant difference between the groups in respect to treatment with biologics, as well as differences (though not reaching significance) in number of treatment escalations (Kaplan Meier curves on Figure 4.14). In particular, group 2 included milder patients who never had a fourth treatment escalation and only one child in this group was treated with biologics, as opposed to 60% of the children in group 1.
As previously shown for the paediatric IBD dataset, the difference in size between group 1 and 2 affected the power of the survival analysis performed (Figure 4.14).

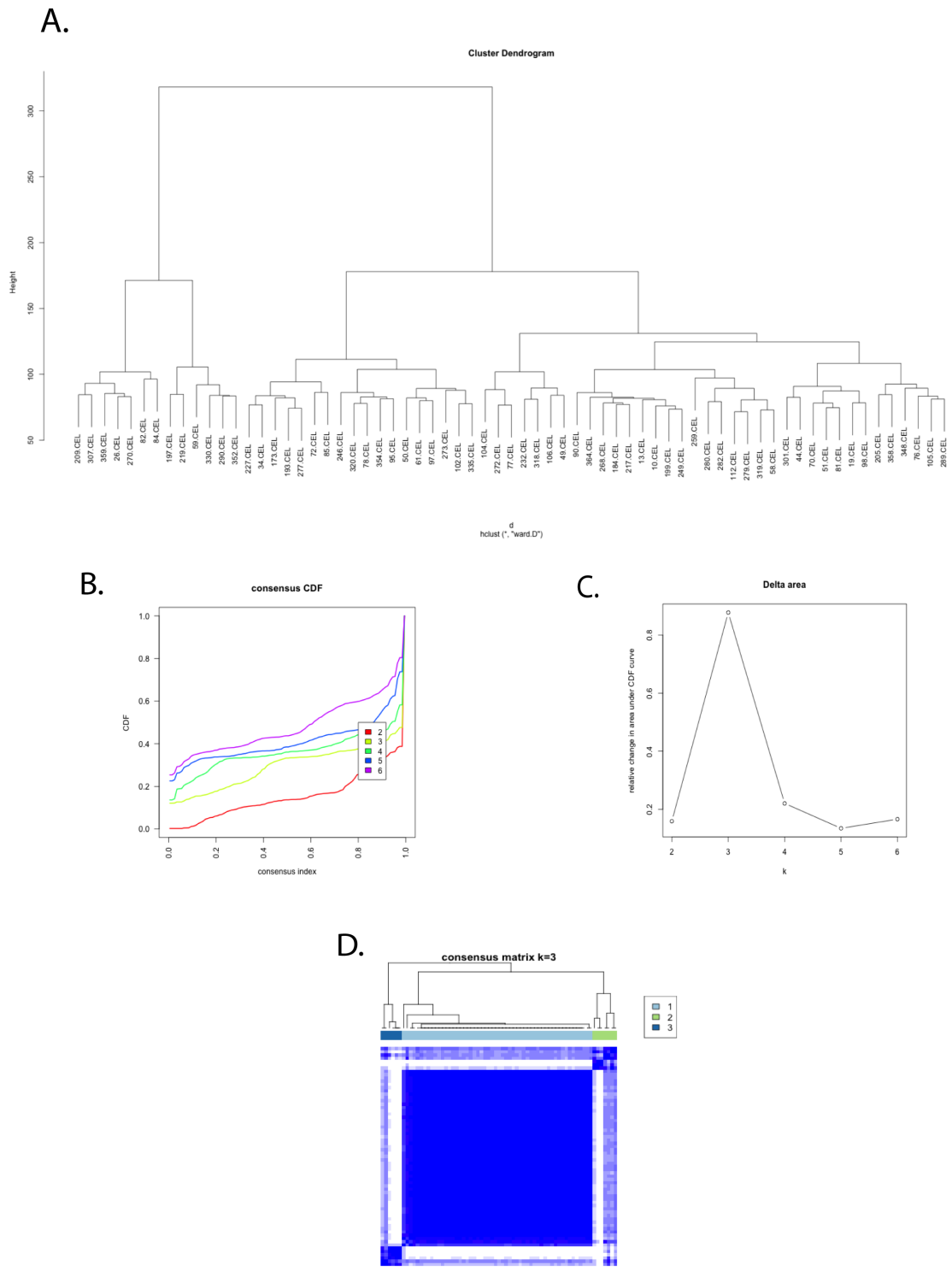

Figure 4.13. In A. Hierarchical Clustering of the CD8 gene expression data in the paediatric CD cohort (n=67). In B. CDF: Consensus Cumulative Distribution Function showing at what number of clusters, k, the consensus and cluster confidence reach a maximum. In C. Delta area plot showing the relative change in area under the CDF curve, with no further appreciable increase at k=3. k3 is identified as the strongest clustering option. In D. Consensus Clustering plot (for k=3) of the gene expression data from the paediatric CD cohort (n=67).

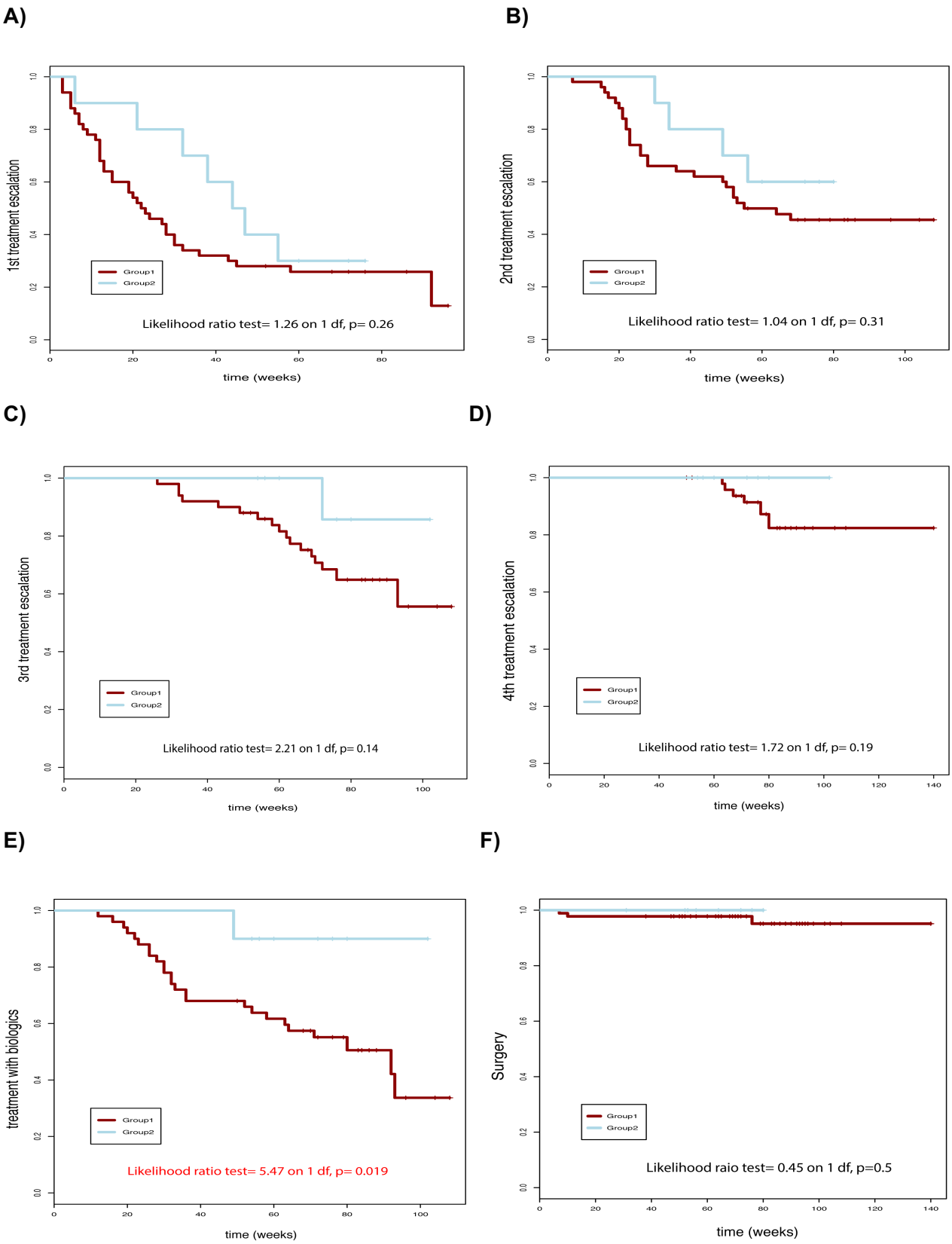

Figure 4.14 Kaplan Meier curves for the paediatric CD cohort (n=67) comparing group 1 (n=54) and group 2 (n=13) identified through Consensus Clustering (Figure 4.13 D). Patients in the two groups are compared for the following outcomes: A) first treatment escalation; B) second treatment escalation; C) third treatment escalation; D) fourth treatment escalation; E) use of biologics; F) surgical intervention.

We went on to perform differential gene expression analysis (DGEA) in order to investigate significant differentially expressed genes between the groups of patients identified through Consensus Clustering (*k*3). As summarised in Figure 4.15, 12461 differentially expressed genes were identified in this cohort between Consensus Clustering group 1 (n=54) and group 2 (n=13); 6342 of these were annotatable.
We also performed GSEA to detect whether genes differentially expressed between groups 1 and 2 identified through Consensus Clustering were organized in molecular pathways of biological relevance.

4562 gene sets had positive enrichment score (i.e. they correlated with group 1); 68 were significantly enriched at nominal p-value < 1% and 397 were significantly enriched at nominal p-value < 5%. None of them was significant at FDR < 25%. Genes in the core enrichment included IL6 receptor, IL12 receptor, IL18 receptor, IFN induced proteins, chemokine receptor 2, chemokine ligands, TNF-alpha induced proteins, toll-like receptors.
310 gene sets had negative enrichment score (i.e. they correlated with group 2); of these, only 2 were significantly enriched at nominal p-value < 5%, and none at nominal p-value < 1%. None was significant at FDR < 25%. Genes in the core enrichment included IL15 receptor, IL22 receptor, IL25, TNF ligands, IFN alpha and chemokine ligands.

A.

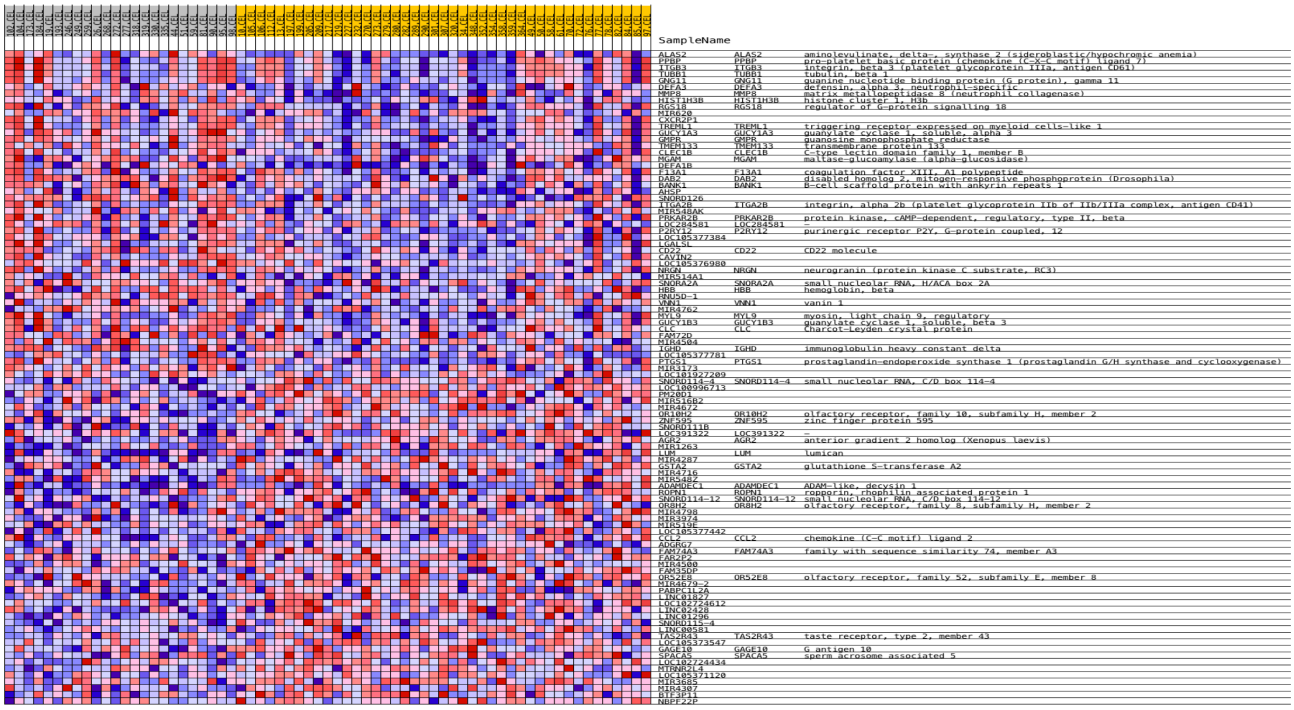

B.

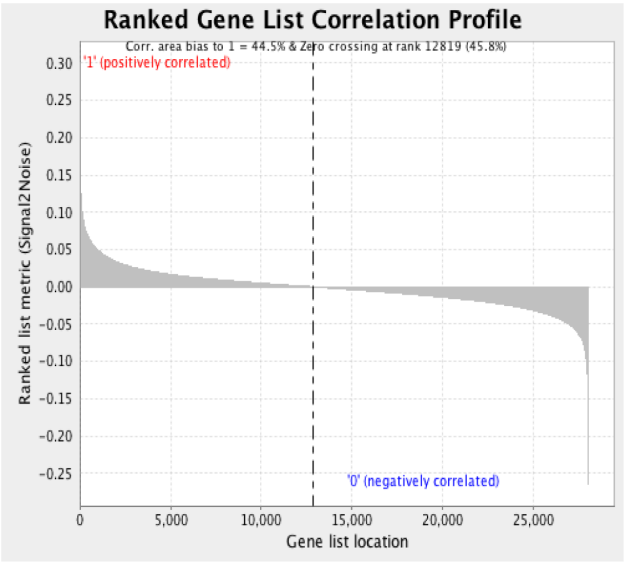

C.

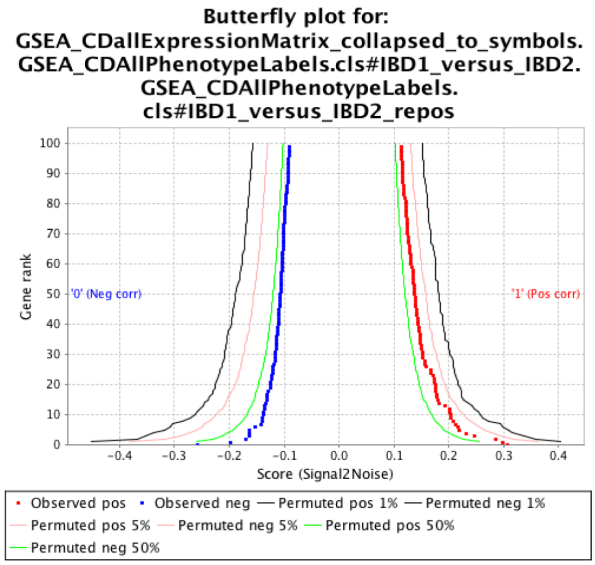

Figure 4.15 Main GSEA findings from the paediatric CD cohort (n=67). Groups as identified through Consensus Clustering. In A. Heatmap of the top 50 features for each phenotype (Consensus Clustering groups 1 vs 2). In B. Plot showing correlation between the ranked genes and the groups 1 and 2. In C. Butterfly plot showing the top 100 positive and negative correlations between gene rank and the ranking metric score (i.e. first and last 100 genes in the ranked list). Observed correlation and permuted (1%, 5%, 50%) positive and negative correlations are shown for the top genes. This plot describes the extent to which dataset permutations change the correlation between gene rank and the ranking metric score.

At this stage, in order to address the same question, i.e. whether a paediatric CD8 signature able to predict disease severity in this cohort exists, we also performed WGCNA. WGCNA was run on 60 paediatric CD samples, as patients with perianal disease who were treated with biologics from the time of diagnosis were removed from this step.

The 27 modules identified in this cohort were tested for correlations with measured clinical traits, as shown in Figure 4.16. In Figure 4.17 only the modules of relevance to disease outcomes are shown. As recapped in Table 4.3, the positive and negative correlation indexes for the top modules ranged between +0.25 and +0.33, and between –0.28 and -0.37, respectively. Module orange was correlated with several clinical outcomes, including number of relapses, number of treatment escalations and severity score.

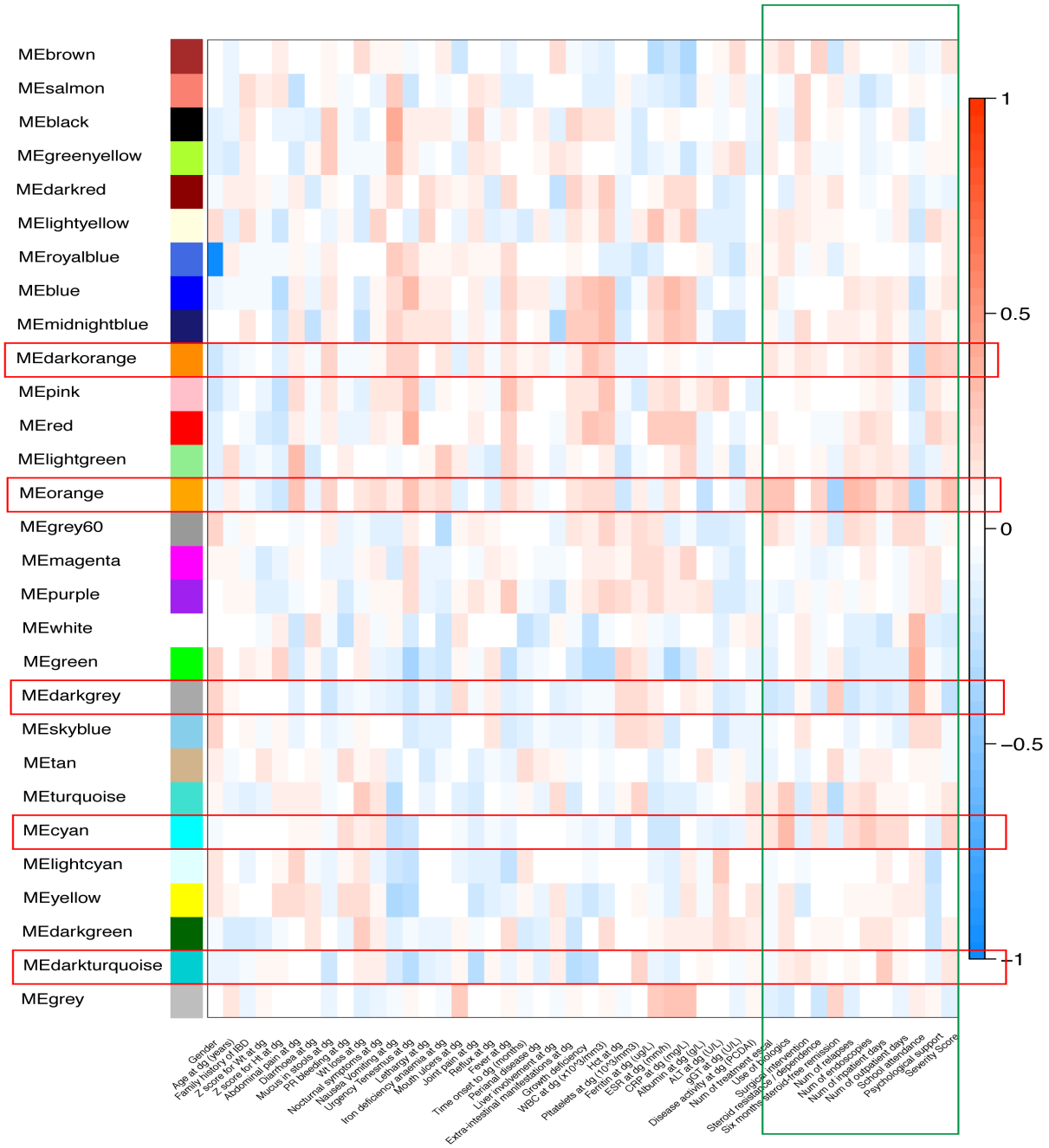

Figure 4.16 WGCNA. Paediatric CD cohort (n=60). Module-trait associations. Each row corresponds to a module eigengene, column to a trait. Each cell contains the corresponding correlation index and p-value (colour-coded, numbers not displayed on this plot). The table is colour-coded by correlation according to the colour legend (i.e. 1 = highest direct correlation, -1 = highest inverse correlation). Red frames highlight modules that correlate with outcomes more than they do with clinical parameters at diagnosis. The green frame highlights clinical outcome measures (i.e. number of treatment escalations, surgery, use of biologics, severity score).

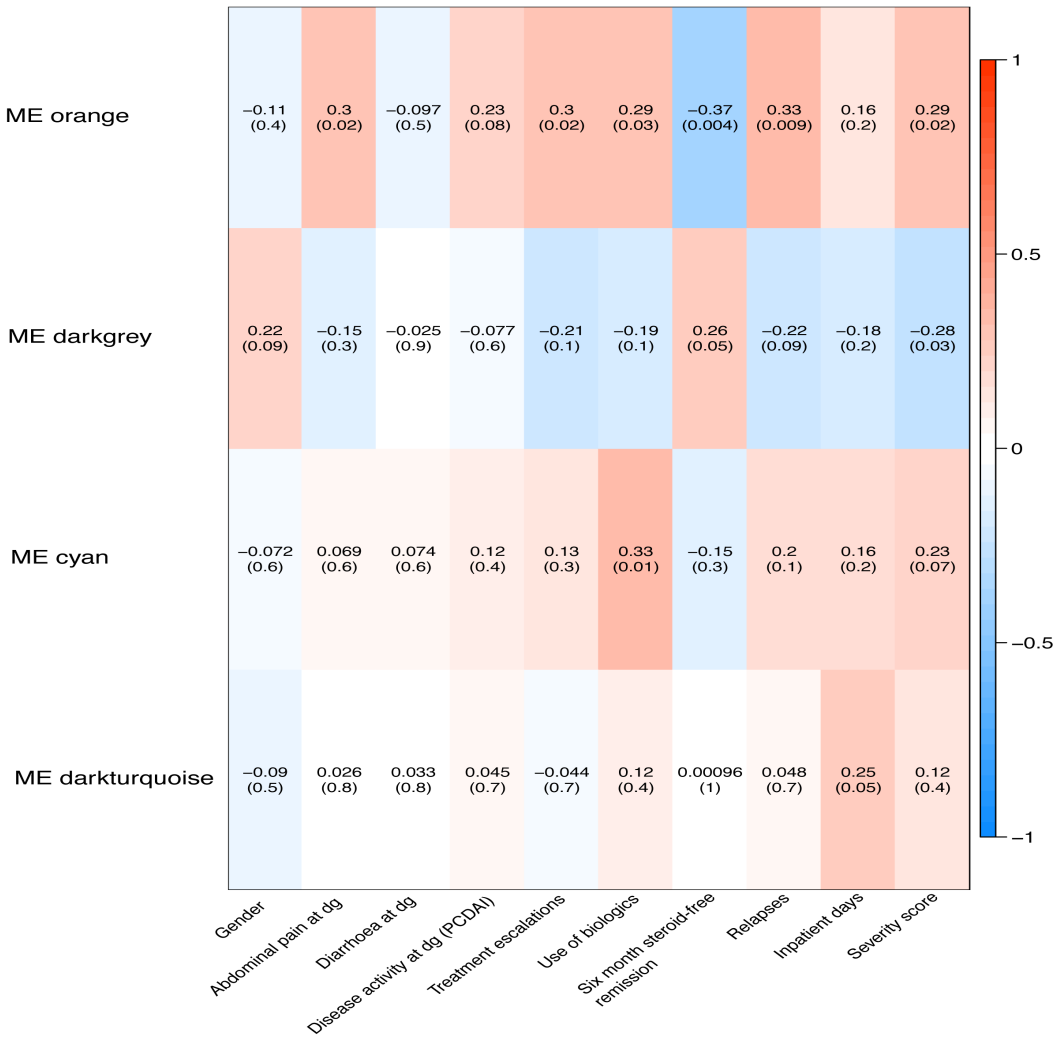

Figure 4.17 Selection of modules correlated with clinical outcomes from Figure 4.16. On the x axis are variables related to the disease at diagnosis (i.e. gender, abdominal pain at diagnosis, diarrhoea and disease activity score at diagnosis (i.e. PCDAI)) followed by variables describing disease outcomes (including use of biologics, surgery, steroid resistance, severity score). On the y axis, selected modules are listed (indicated by numbers and colour names). The plot shows how these modules correlate more strongly (directly or inversely) with disease outcomes than they do with parameters describing disease at diagnosis.

CLINICAL OUTCOMES	CORRELATION INDEX	P-VALUE
BIOLOGICS		
ME orange [14]	0.29	0.03
ME cyan [24]	0.33	0.01
TREATMENT ESCALATIONS		
ME orange [14]	0.3	0.02
6 MONTHS STEROID FREE REMISSION		
ME orange [14]	- 0.37	0.004
RELAPSES		
ME orange [14]	0.33	0.009
INPATIENT DAYS		
ME darkturquoise [28]	0.25	0.05
SEVERITY SCORE		
ME orange [14]	0.29	0.02
ME darkgrey [20]	-0.28	0.03

Table 4.3 WGCNA. Paediatric CD cohort (n=60). Main modules correlating with disease outcomes.

In order to test the prognostic role of these modules further, we filtered out of this dataset the probes corresponding to modules of interest for specific outcomes. We then performed Consensus Clustering of this selection to test whether the groups of patients identified would differ in respect to those outcomes.

First, we tested module orange (29 probes), correlated to number of relapses, treatment escalations and severity score. Groups based on this module were identified through Consensus Clustering, as shown in Figure 4.18 C (*k*3: group 1 (n=52) vs groups 2+3 (n=8), renamed as group 2). The survival analysis performed to compare these groups for clinical outcomes (Figure 4.19) showed significant differences in first and second treatment escalations. Children in group 2 were overall milder than group 1, with only one patient in group 2 receiving biologics as opposed to 60% of those in group 1.

We then tested modules orange and cyan (111 probes), correlated to treatment with biologics. Groups identified through Consensus Clustering (Figure 4.20 C *k*2: group 1 (n=44) vs groups 2 (n=16)) did not differ significantly in respect to use of biologics (Kaplan Meier curve in Figure 4.21).

Finally, we looked at the signature in module dark turquoise (34 probes) correlated to the clinical outcome “unplanned inpatient days”. As shown in Figure 4.23, survival analysis of the groups identified through Consensus Clustering (Figure 4.22 C, *k*3: group 1 (n=36) vs groups 2+3 (n=24), renamed as group 2) showed significant splits between the groups for number of treatment escalations and use of biologics.

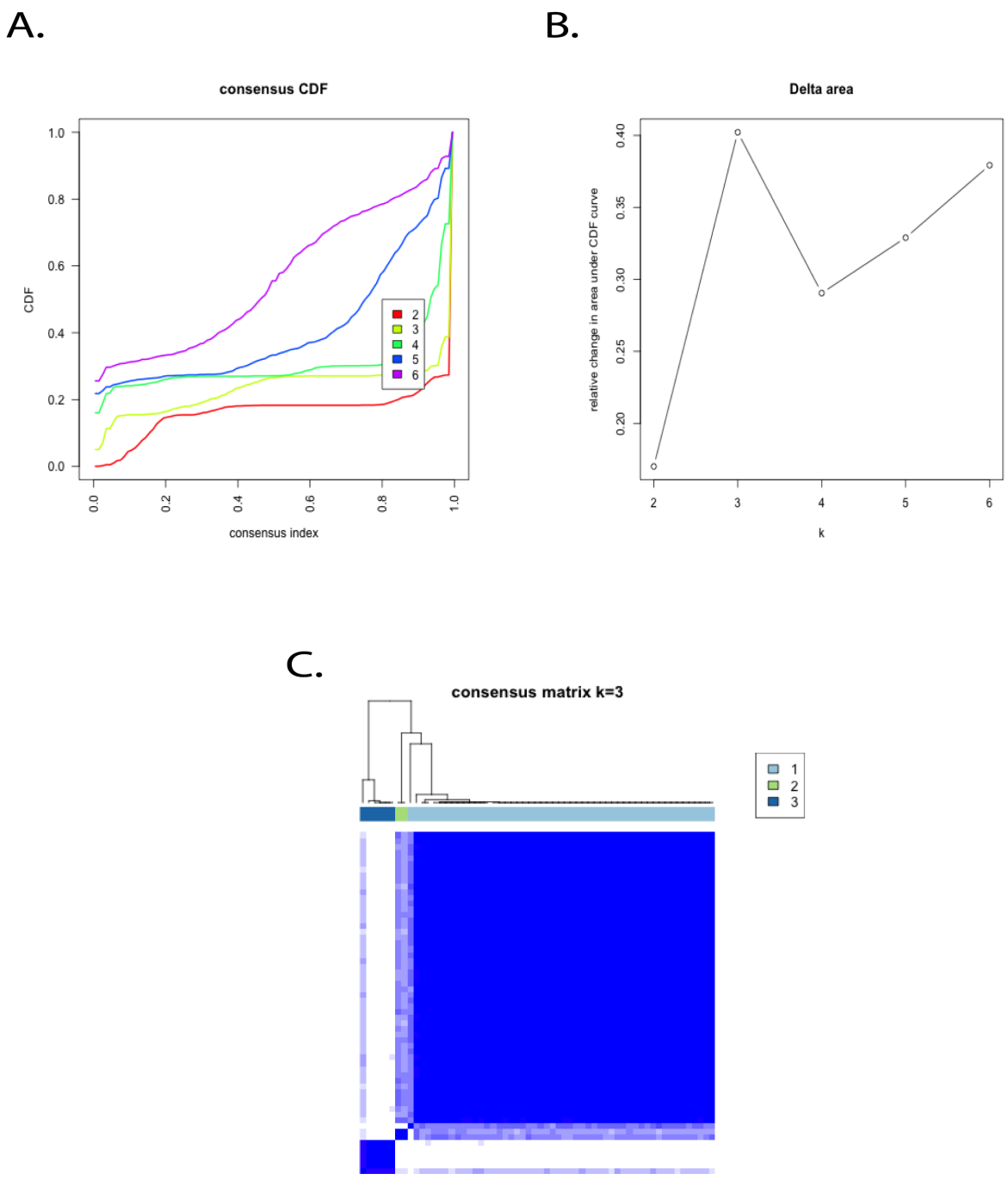

Figure 4.18 Consensus Clustering of a selection of probes included in the WGCNA module orange (29 probes), correlated to "number of relapses", "number of treatment escalations" and "severity score". In A. CDF: Consensus Cumulative Distribution Function, showing at what number of clusters, k, the consensus and cluster confidence reach a maximum. In B. Delta area plot, showing the relative change in area under the CDF curve, with no further increase appreciable at k=3. k3 is identified as the strongest clustering option. In C. Consensus Clustering plot for k=3.

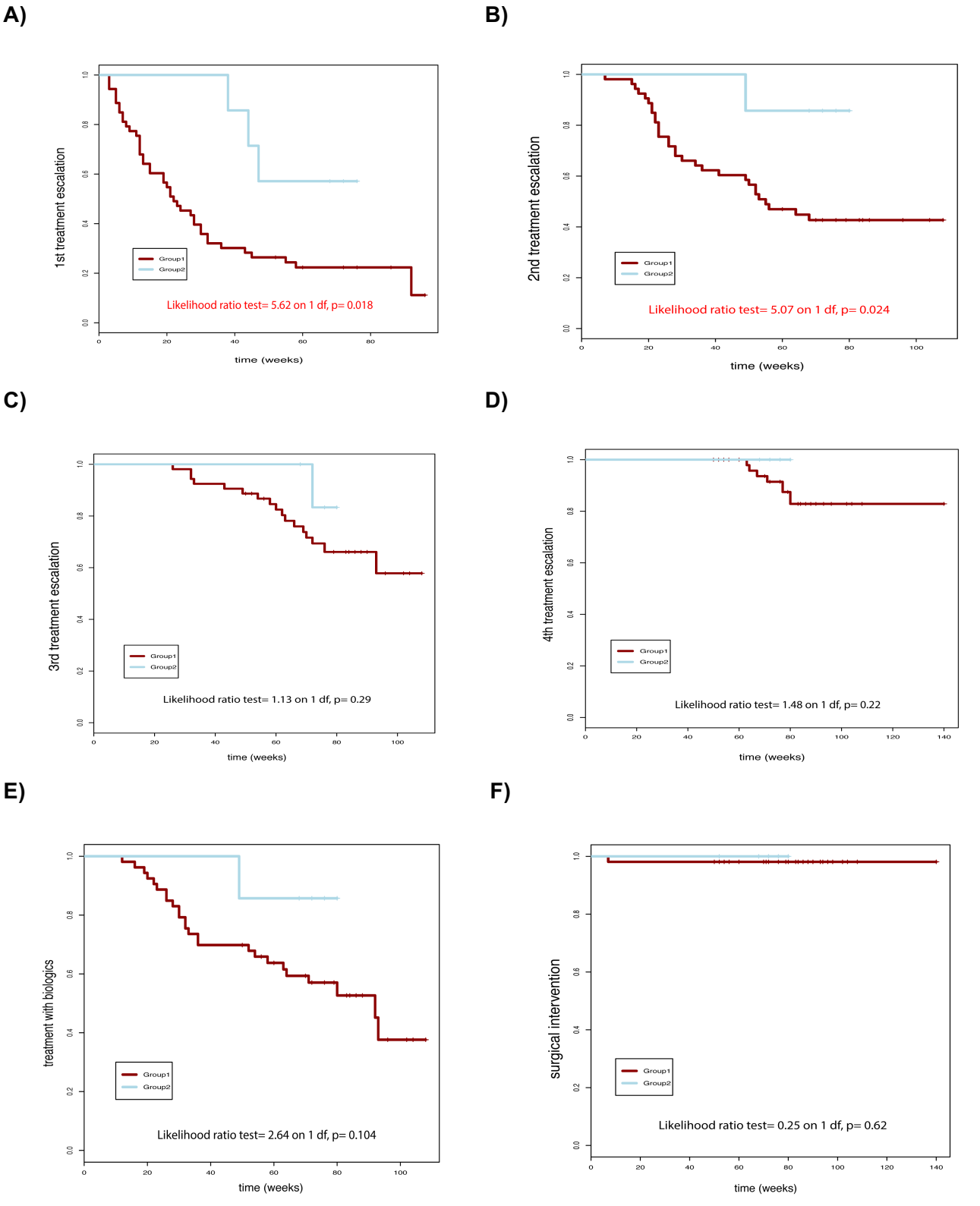

Figure 4.19 Kaplan Meier curves comparing the groups identified in 4.18 C (group 1: n=52 vs group 2 (i.e. 2+3): n=8) for the following outcomes: A) first treatment escalation; B) second treatment escalation; C) third treatment escalation; D) fourth treatment escalation; E) use of biologics; F) surgical intervention.

A.

B.

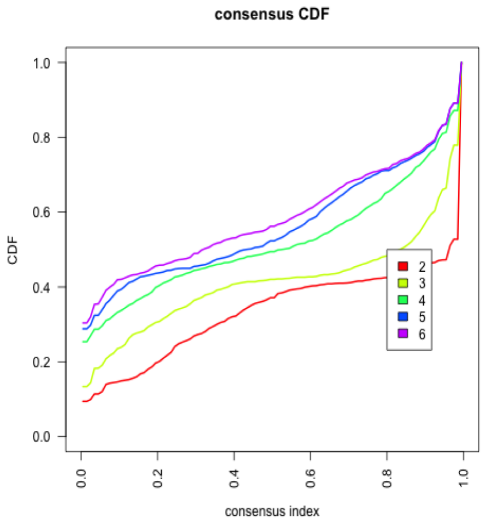

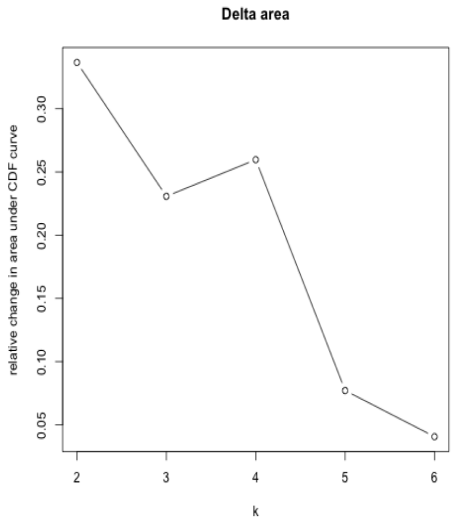

C.

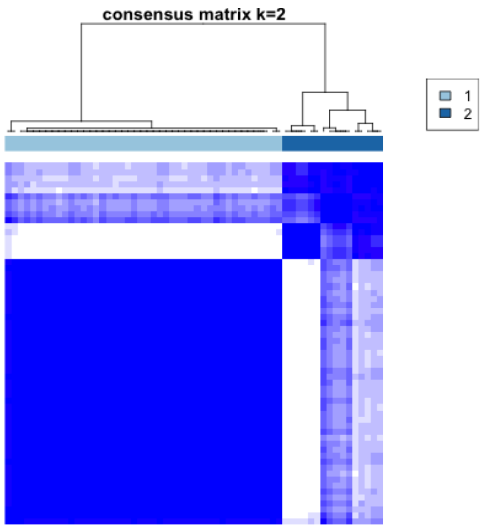

Figure 4.20 Consensus Clustering of a selection of probes included in the WGCNA modules orange and cyan (111 probes), correlated to "use of biologics". In A. CDF: Consensus Cumulative Distribution Function, showing at what number of clusters, k, the consensus and cluster confidence reach a maximum. In B. Delta area plot, showing the relative change in area under the CDF curve, with no further appreciable increase at k=2. k2 is identified as the strongest clustering option. In C. Consensus Clustering plot for k=3.

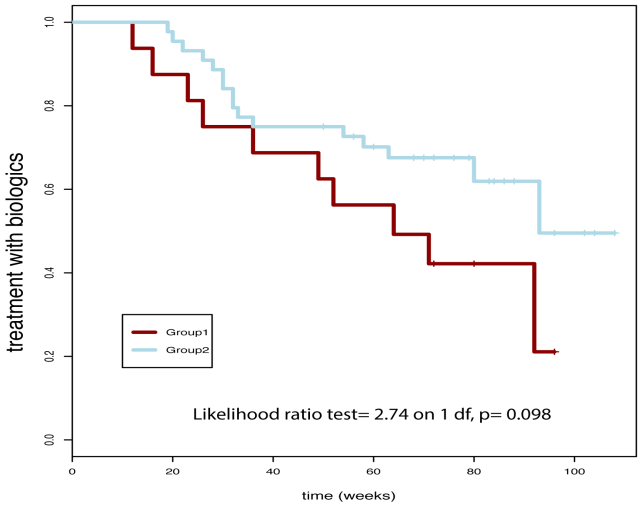

Figure 4.21 Kaplan Meier curves comparing the groups identified in 4.20 C (group 1: n=44 vs groups 2: n=16) for the outcome "use of biologics".

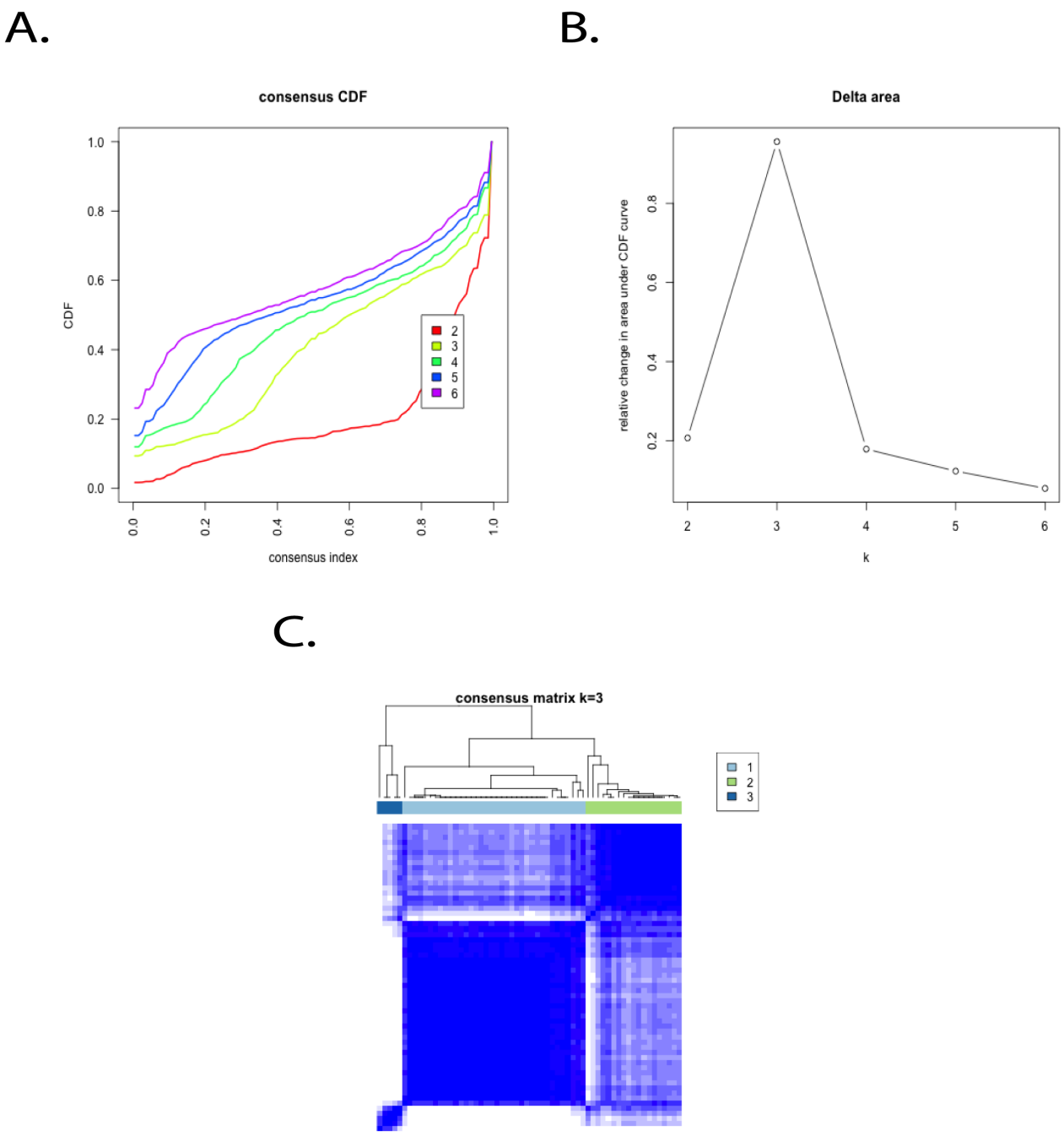

Figure 4.22 Consensus Clustering of a selection of probes included in the WGCNA module dark turquoise (34 probes), correlated to "unplanned inpatient days". In A. CDF: Consensus Cumulative Distribution Function, showing at what number of clusters, k, the consensus and cluster confidence reach a maximum. In B. Delta area plot showing the relative change in area under the CDF curve, with no further appreciable increase at k=3. k3 is identified as the strongest clustering option. In C. Consensus Clustering plot for k3.

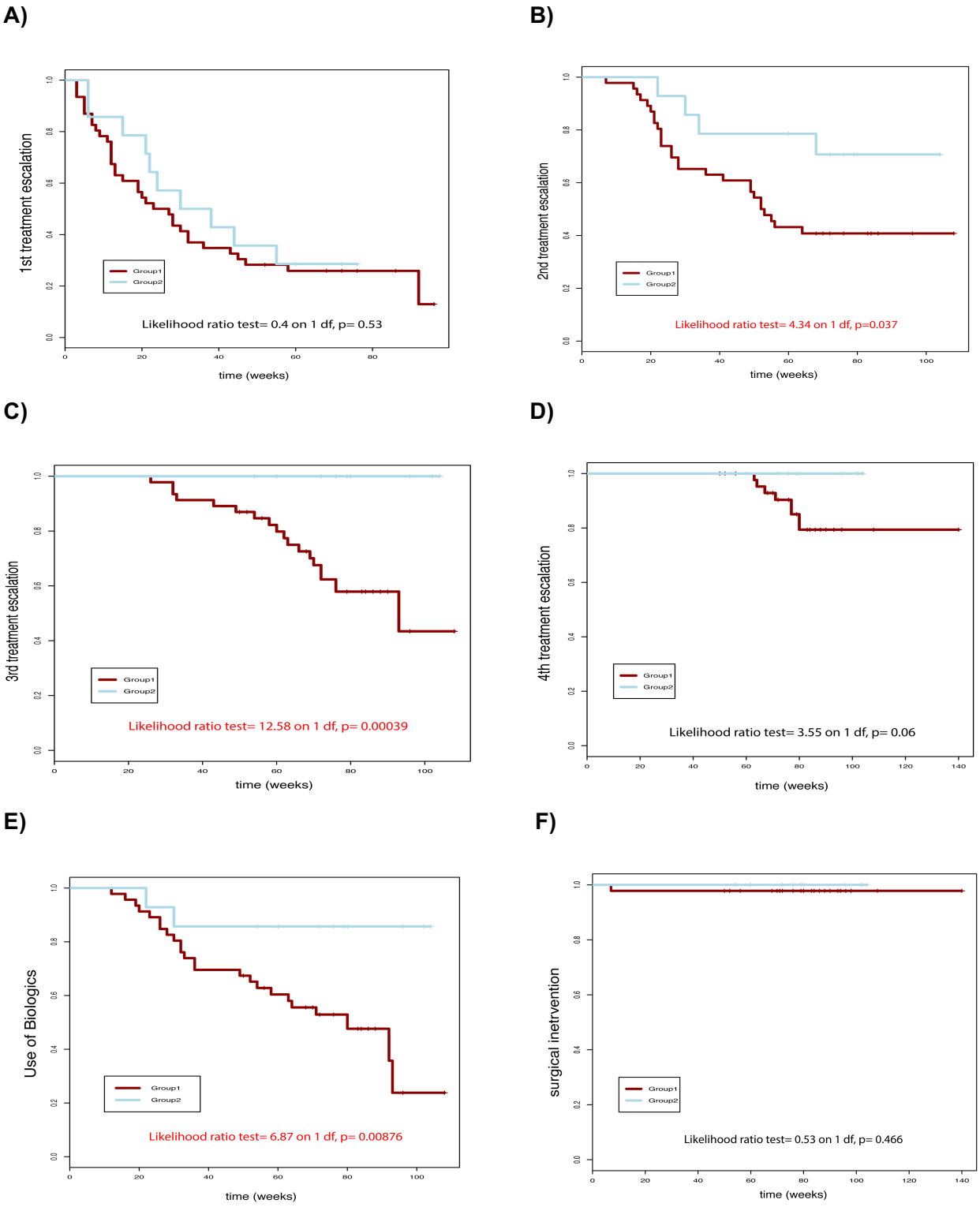

Figure 4.23 Kaplan Meier curves comparing the groups identified in 4.22 C (group 1: n=36 vs group 2 (i.e. 2+3): n=24) for the following outcomes: A) first treatment escalation; B) second treatment escalation; C) third treatment escalation; D) fourth treatment escalation; E) use of biologics; F) surgical intervention.

Given the significant differences in outcomes identified between the Consensus Clustering groups related to module dark turquoise, we also performed GSEA in order to detect whether such groups would differ in molecular pathways of biological relevance.

As summarised in Figure 4.24, 2647 gene sets had positive enrichment score (i.e. they showed enrichment at the top of the ranked list and correlated with group 1); 6 of these were significantly enriched at nominal p-value < 1% and 23 were significantly enriched at nominal p-value < 5%. None of them was significant at FDR < 25%.
Genes in core enrichment included NKT recognition sequences, GABA receptors, chemokine ligands, TNF receptors, TNF receptor associated factors, TNF and IFN induced proteins, IL15 and toll-like receptor 3.
2225 gene sets had negative enrichment score (i.e. they showed enrichment at the bottom of the ranked list and correlated with group 2); of these, 8 were significantly enriched at nominal p-value < 1% and 42 were significantly enriched at nominal p-value < 5%. None was significant at FDR < 25%.
Genes in core enrichment included TNF receptors, IFN alpha, chemokine receptors, GABA receptors, VIP receptor 1.

A.

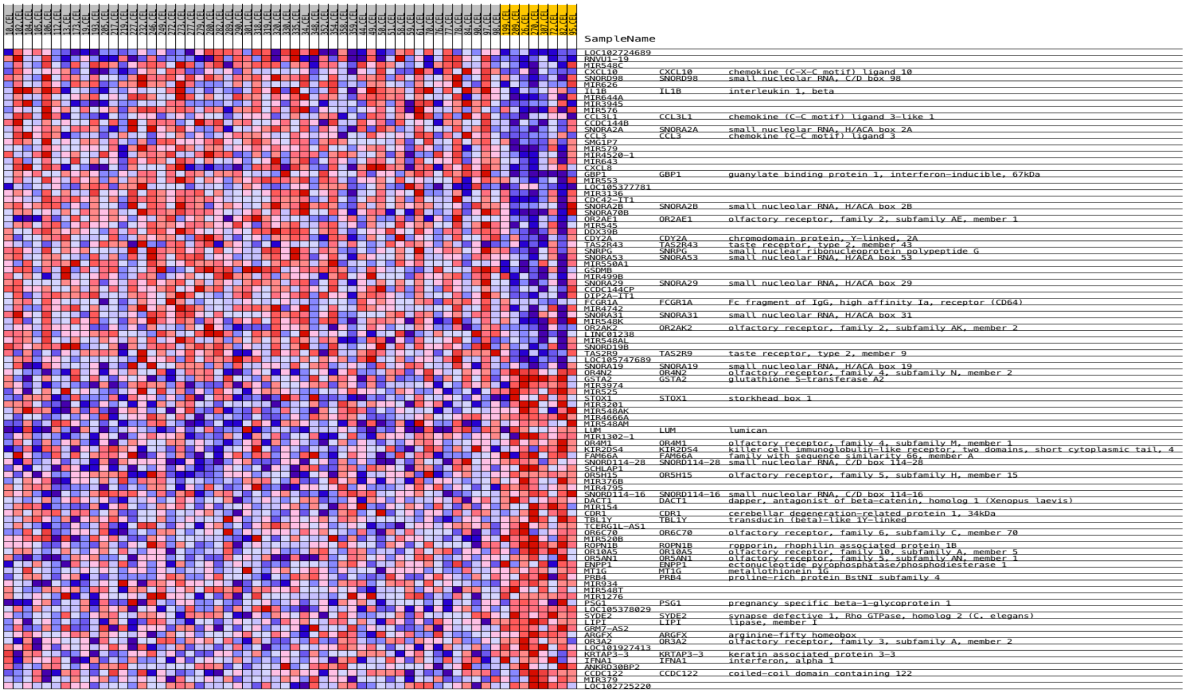

B.

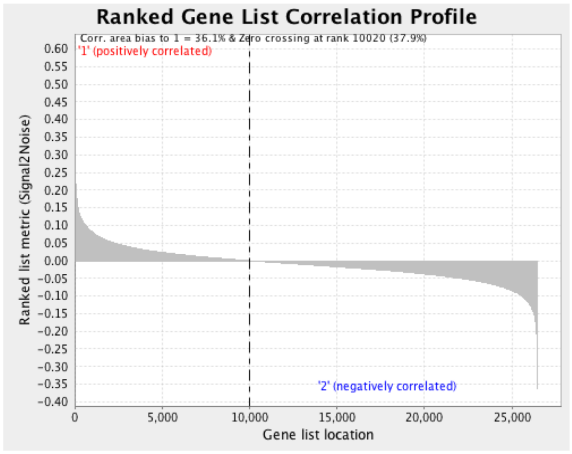

C.

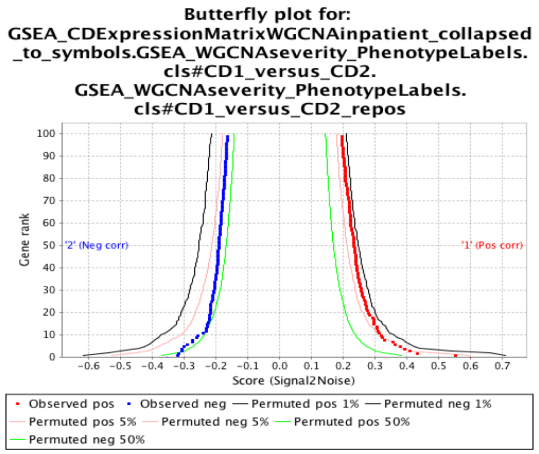

Figure 4.24 Main GSEA findings from the paediatric CD cohort (n=60). Groups as identified through Consensus Clustering (module dark turquoise correlated to "number of unplanned inpatient days"). In A. Heatmap of the top 50 features for each phenotype (Consensus Clustering groups 1 vs 2). In B. Plot showing correlation between the ranked genes and the groups 1 and 2. In C. Butterfly plot showing the top 100 positive and negative correlation between gene rank and the ranking metric score (i.e. first and last 100 genes in the ranked list). Observed correlation and permuted (1%, 5%, 50%) positive and negative correlations are shown for the top genes. This plot describes the extent to which dataset permutations change the correlation between gene rank and the ranking metric score.

In summary, the paediatric signatures identified from WGCNA of the paediatric CD cohort (i.e. module orange correlated with “number of relapses”, “number of treatment escalations” and “severity score”, and module dark turquoise correlated with “number of unplanned inpatient days”) did identify groups of children with significant differences in disease outcomes (Kaplan Meier curves from the survival analysis), although with correlation indexes within a range of only 0.25-0.37.

4.3.3 Analysis of CD8+ T-cell gene expression profiles from the paediatric UC cohort

In this section, we briefly summarise the main results obtained by applying the same analyses shown above (i.e. unsupervised clustering analyses and WGCNA) to our cohort of children with UC (n=40). First, we performed Hierarchical Clustering which demonstrated the presence of a substructure, with two groups including 1/3 and 2/3 of the patients approximately (Figure 4.25 A).
Consensus Clustering of this dataset identified five more solid groups of patients throughout the gene expression data as shown in Figure 4.25 B and C, where k=5 provides the strongest clustering. As previously observed in the paediatric CD cohort, the clusters of patients identified in this dataset also differ in size, with one group including 90% of patients, and the remaining 10% of them clustering out.

As a next step, we tested whether the groups identified through Consensus Clustering (Figure 4.25 D, k5: group 2 (n=35, renamed as group 1) vs groups 1+3+4+5 (n=5, renamed as group 2)) would differ in respect to their disease course and outcomes, i.e. whether groups identified in this cohort based on their CD8 gene expression profiles would have different disease severity over time.
Survival analysis identified differences, although not reaching significance, between these two groups in respect to number of treatment escalations, use of biologics and surgical intervention (Kaplan Meier curves on Figure 4.26). In particular, group 2 in the survival analysis (i.e. Consensus Clustering groups 1,3,4,5 combined) included milder patients who never had more than two treatment escalations, and who were never treated with biologics, as opposed to 20% of the children in group 1. Also, children in group 2 never had surgical intervention as opposed to 2 children in group 1 who required colectomy.

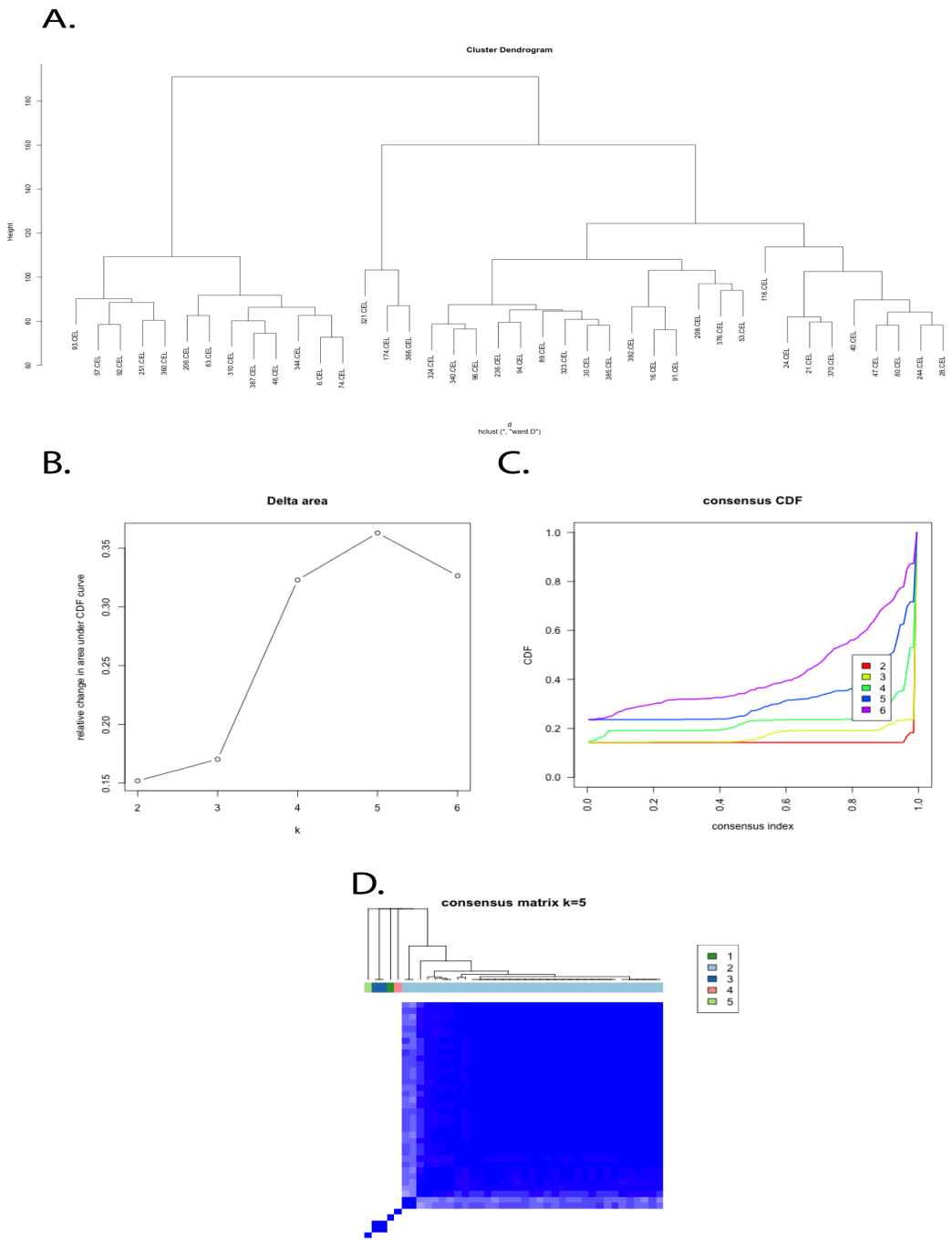

Figure 4.25. In A. Hierarchical Clustering of the CD8 gene expression data in the paediatric UC cohort (n=40). In B. CDF: Consensus Cumulative Distribution Function showing at what number of clusters, k, the consensus and cluster confidence reach a maximum. In C. Delta area plot showing the relative change in area under the CDF curve, with no further appreciable increase at k=5. k5 is identified as the strongest clustering option. In D. Consensus Clustering plot (for k=5) of gene expression data from the paediatric UC cohort (n=40).

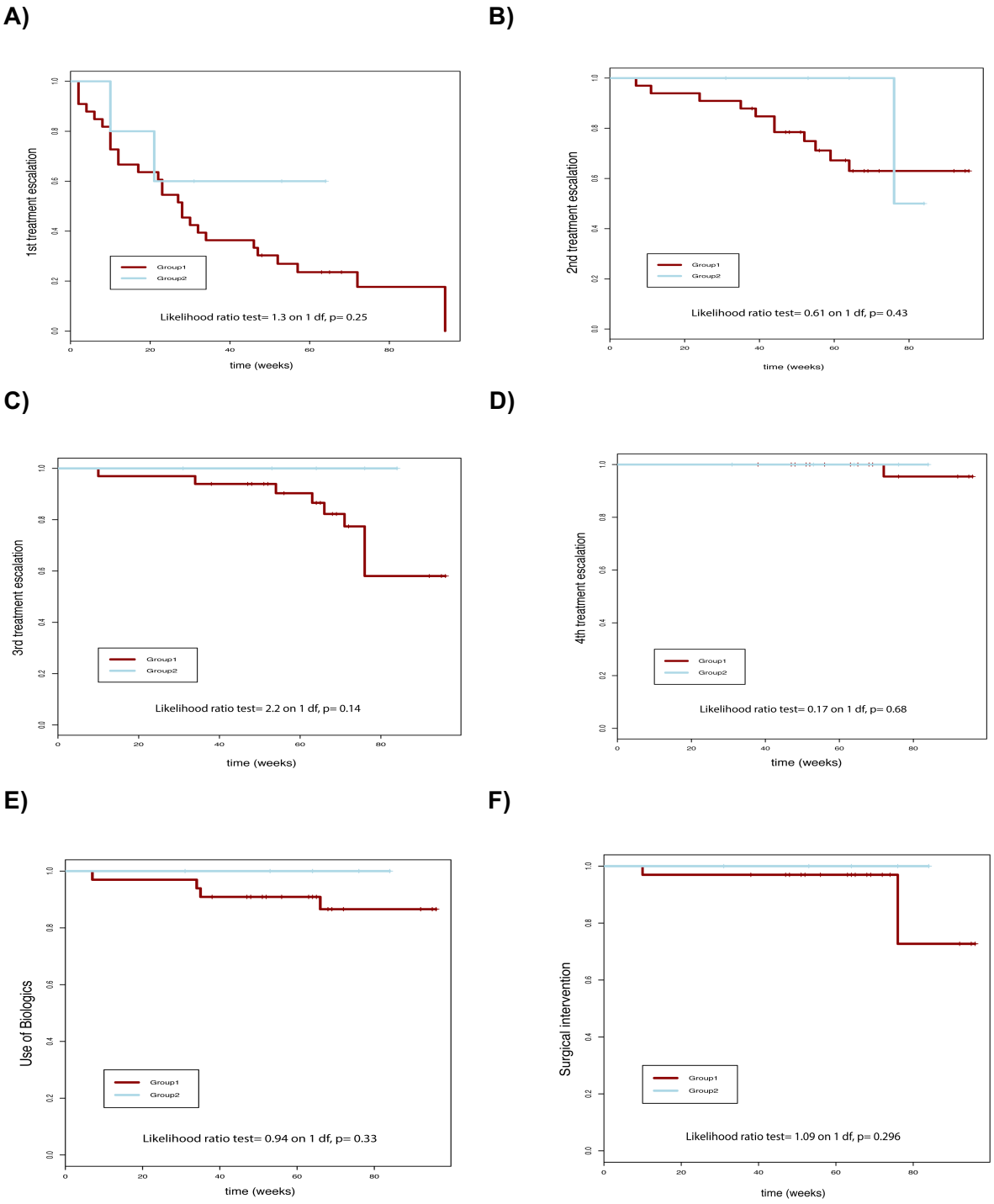

Figure 4.26 Kaplan Meier curves for the paediatric UC cohort (n=40) comparing group 1 (n=35) and group 2 (n=5) identified through Consensus Clustering (Figure 4.25 D). Patients in the two groups are compared for the following outcomes: A) first treatment escalation; B) second treatment escalation; C) third treatment escalation; D) fourth treatment escalation; E) use of biologics; F) surgical intervention.

At this stage, we went on to perform differential gene expression analysis (DGEA) using R package "limma" in order to investigate significantly differentially expressed genes between the groups of patients identified through Consensus Clustering (*k*5). In this cohort, 3549 differentially expressed genes were identified between Consensus Clustering group 1 (n=35) and group 2 (n=5); 1312 of these were annotatable. We also performed GSEA to detect whether genes differentially expressed between groups 1 and 2 identified through Consensus Clustering were organised into molecular pathways of biological relevance. As summarised in Figure 4.27, 4290 gene sets had positive enrichment score (i.e. they showed enrichment at the top of the ranked list and correlated with group 1); 111 of these were significantly enriched at nominal p-value < 1% and 603 were significantly enriched at nominal p-value < 5%. 1165 were significant at FDR < 25%. Genes in core enrichment included chemokine ligands, VIP receptor 1, IL2, IL22 receptor, IL25 and GABA receptor.

582 gene sets had negative enrichment score (i.e. they showed enrichment at the bottom of the ranked list and correlated with group 2); of these, only 1 was significantly enriched at nominal p-value < 1% and 6 were significantly enriched at nominal p-value < 5%. None was significant at FDR < 25%. Genes in core enrichment included IL1 receptor associated proteins, integrins, IL18 receptor, bromodomains and IL11 receptors.

A.

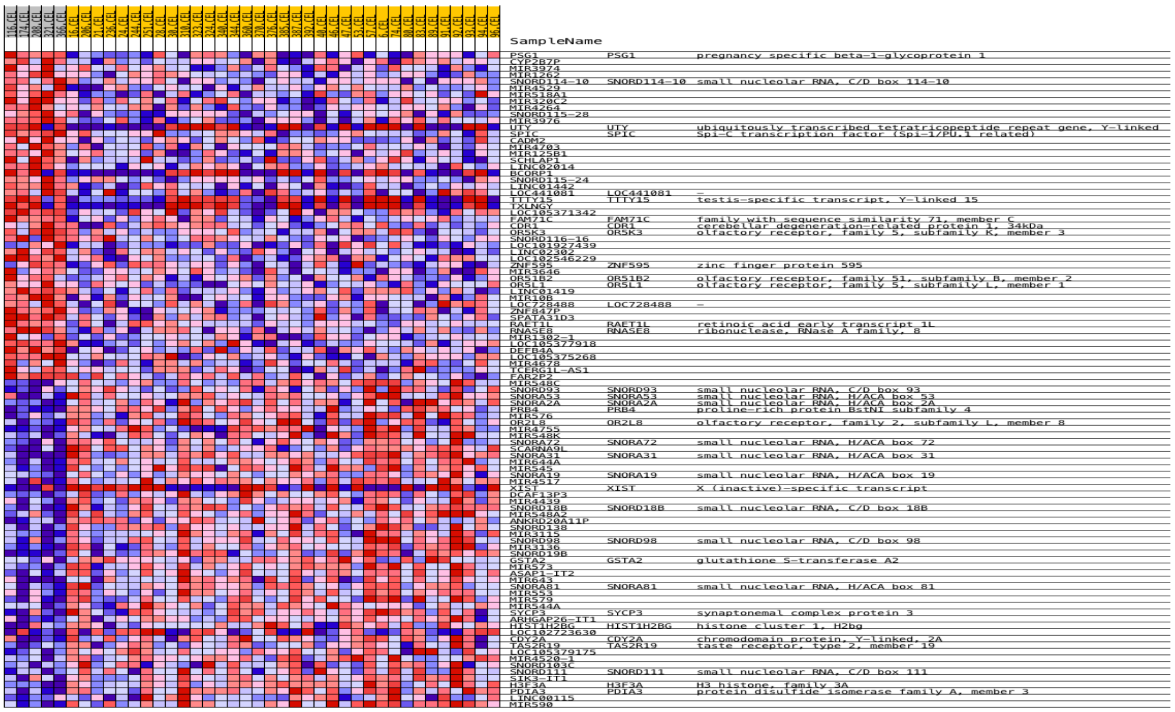

B.

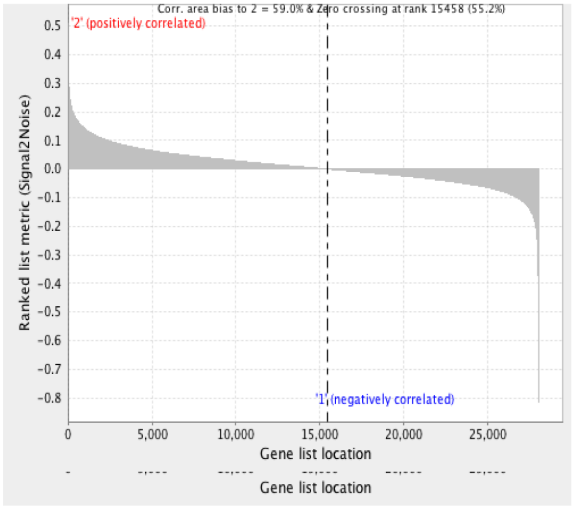

C.

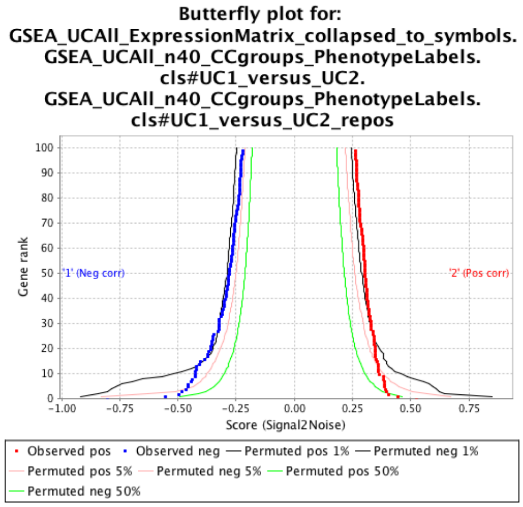

Figure 4.27 Main GSEA findings from the paediatric UC cohort (n=40). Groups as identified through Consensus Clustering. In A. Heatmap of the top 50 features for each phenotype (Consensus Clustering groups 1 vs 2). In B. Plot showing correlation between the ranked genes and groups 1 and 2. In C. Butterfly plot showing the top 100 positive and negative correlations between gene rank and the ranking metric score (i.e. first and last 100 genes in the ranked list). Observed correlations and permuted (1%, 5%, 50%) positive and negative correlations are shown for the top genes. This plot describes the extent to which dataset permutations change the correlation between gene rank and the ranking metric score.

As a next step, we performed WGCNA as an alternative and complementary method to investigate the existence of paediatric specific prognostic signatures in our UC cohort. WGCNA was performed on 38 patients as 2 of them with acute severe onset who needed biologic treatments from the time of diagnosis were excluded from this analysis.

Forty modules were identified in this dataset. Their correlation with the clinical data collected is shown on Figure 4.28 while Figure 4.29 shows an excerpt from Figure 4.28 where only the modules of relevance to disease outcomes are shown.

As shown in Table 4.4, modules yellowgreen [18] and steelblue [36] correlate with multiple outcomes, i.e. treatment with biologics, number of relapses, surgical intervention (colectomy) and severity score.

Moreover, modules yellowgreen and steelblue showed high inverse correlation (< -0.5) with clinical outcome “surgical intervention”. Overall, positive and negative correlation indexes ranged between +0.31 and +0.38, and between -0.29 and -0.59, respectively.

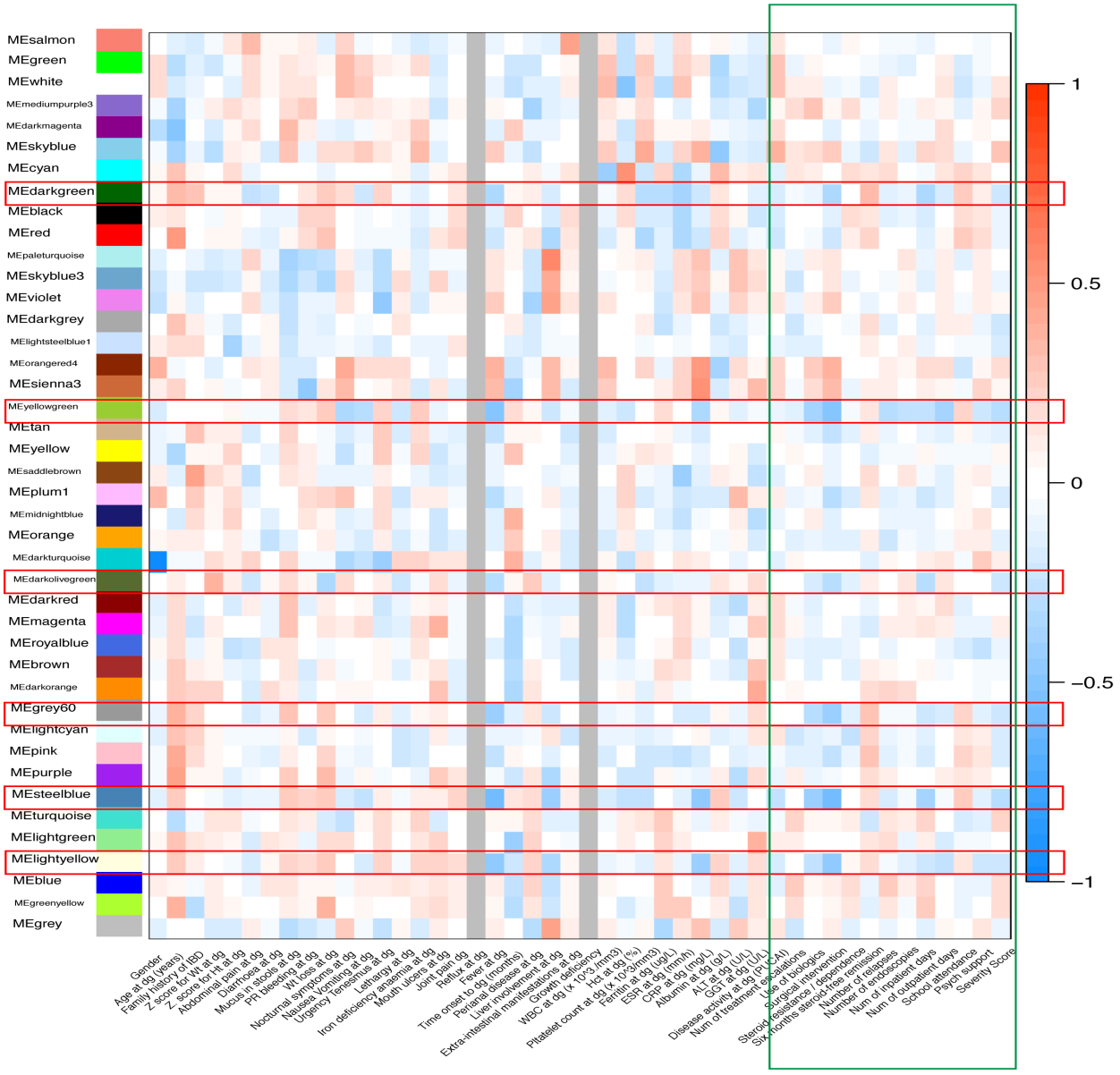

Figure 4.28 WGCNA. Paediatric UC cohort (n=38). Module-trait associations. Each row corresponds to a module eigengene, column to a trait. Each cell contains the corresponding correlation and p-value (colour-coded, numbers not displayed on this plot). The table is colour-coded by correlation according to the colour legend (i.e. 1 = highest direct correlation, -1 = highest inverse correlation). Red frames highlight modules that correlate with outcomes more than they do with clinical parameters at diagnosis. The green frame highlights clinical outcome measures (i.e. number of treatment escalations, surgery, use of biologics etc.)

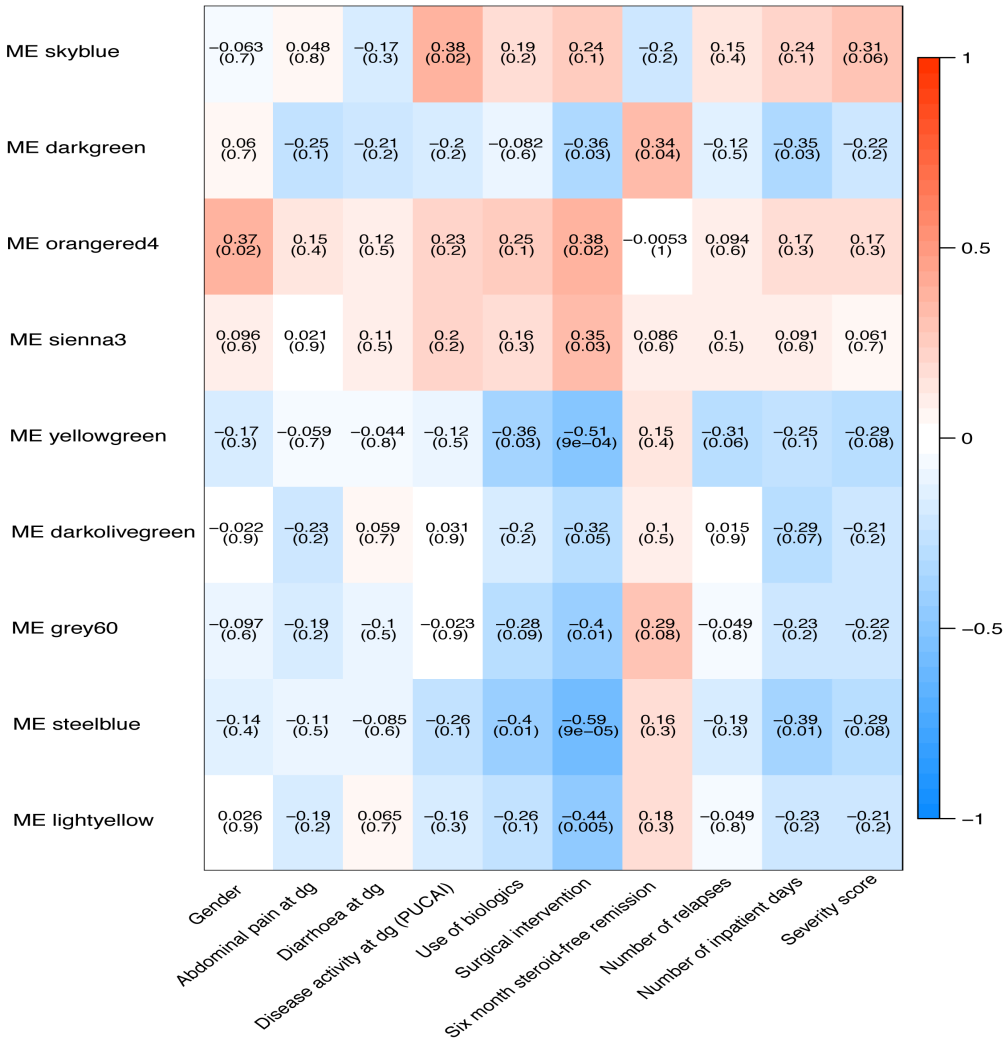

Figure 4.29 WGCNA. Paediatric UC cohort (n=38). Excerpt from Fig. 4.28 displaying modules correlated with clinical outcomes. On the x axis are variables related to the disease at diagnosis (i.e. gender, abdominal pain at diagnosis, diarrhoea and disease activity score at diagnosis (i.e. PUCAI)) followed by variables describing disease outcomes (use of biologics, surgery, steroid resistance, severity score etc.). On the y axis, selected modules are listed (indicated by colour names). The plot shows how these modules correlate more strongly (directly or inversely) with disease outcomes than they do with parameters describing disease at diagnosis.

CLINICAL OUTCOMES	CORRELATION INDEX	P-VALUE
BIOLOGICS		
ME yellowgreen [18]	-0.36	0.03
ME steelblue [36]	-0.4	0.01
RELAPSES		
ME yellowgreen [18]	-0.31	0.06
6 MONTHS STEROID FREE REMISSION		
ME darkgreen [8]	0.34	0.04
INPATIENT DAYS		
ME darkgreen [8]	-0.35	0.03
ME steelblue [36]	-0.39	0.01
SEVERITY SCORE		
ME skyblue [6]	0.31	0.06
ME yellowgreen [18]	-0.29	0.08
ME steelblue [36]	-0.29	0.08
SURGERY		
ME darkgreen [8]	-0.36	0.03
ME orangered4 [16]	0.38	0.02
ME sienna3 [17]	0.35	0.03
ME yellowgreen [18]	-0.51	9e-04
ME orange [26]	-0.32	0.05
ME grey60 [32]	-0.4	0.01
ME steelblue [36]	-0.59	9e-05
ME lightyellow [39]	-0.44	0.005

Table 4.4 WGCNA. Paediatric UC cohort (n=38). Main modules correlating with disease outcomes.

Next, as previously shown in the joint paediatric IBD cohort and in the paediatric CD cohort, we tested the modules identified in this dataset to correlate with disease outcome parameters by subsetting them and by running Consensus Clustering of this selection. Subsequently, we performed survival analysis to compare the groups of patients identified for specific outcomes.

In summary, the signature for “number of unplanned inpatient days” (modules darkgreen and steel blue, 104 probes in total) generated Consensus Clustering groups (Figure 4.30 C) with non-significant differences in disease outcomes, although children in group 2 had fewer treatment escalations and surgical interventions (Kaplan Meier curves in Figure 4.31).

The signature for “use of biologics” (modules yellowgreen and steelblue, 75 probes in total) also generated a non-significant split (Figure 4.32 C shows the Consensus Clustering plots while in Figure 4.33 the Kaplan Meier curve is displayed).

Distinctively, the signature for “surgical intervention” (modules darkgreen, yellowgreen, orange, grey60, steelblue, lightyellow, 345 probes in total), did generate a significant split in outcome between the groups identified, as shown in Figure 4.34 C (Consensus Clustering plots) and in Figure 4.35 (Kaplan Meier curve).

For this specific signature, in view of the significant difference in outcome identified, we also performed GSEA to detect whether these groups would differ in molecular pathways of biological relevance.

As summarised in Figure 4.36, 1700 gene sets had positive enrichment score (i.e. they showed enrichment at the top of the ranked list and correlated with group 1); only 1 of these was significantly enriched at nominal p-value < 1% and 24 were significantly enriched at nominal p-value < 5%. None was significant at FDR < 25%. Genes in the core enrichment included IL23 receptor, chemokine receptors, IL1 receptor, IL2 receptor, IL11 receptor, IL12 receptor, IL32, GABA receptor and TNF receptor.

3172 gene sets had negative enrichment score (i.e. they showed enrichment at the bottom of the ranked list and correlated with group 2); of these, 58 were significantly enriched at nominal p-value < 1% and 158 were significantly enriched at nominal p-value < 5%. None was significant at FDR < 25%. Genes in the core enrichment included IL6 signal transducer, IL6 receptor and integrins.

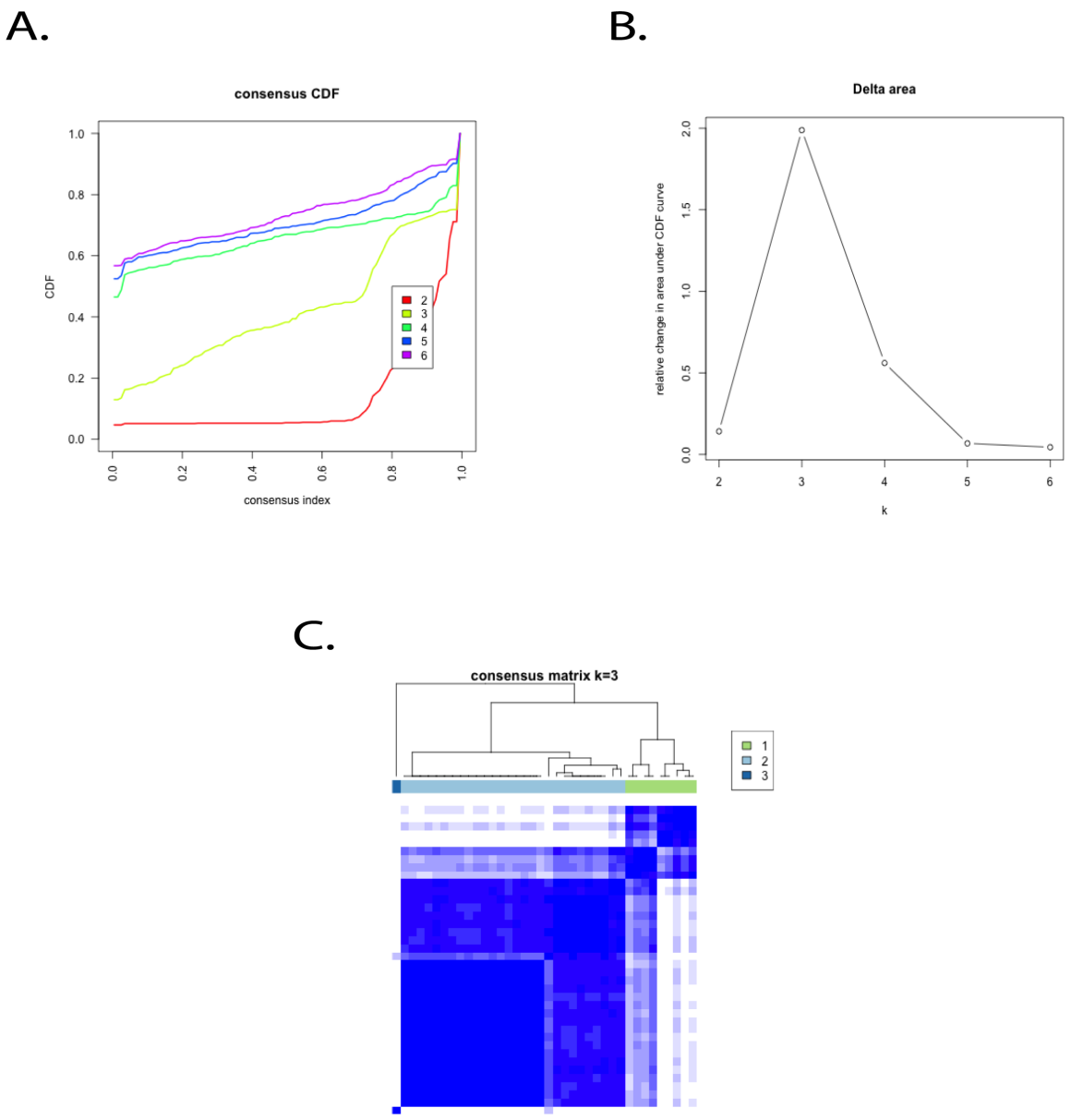

Figure 4.30. Consensus Clustering of a selection of probes included in the WGCNA modules darkgreen and steelblue (104 probes), correlated with "unplanned inpatient days". In A. CDF: Consensus Cumulative Distribution Function, showing at what number of clusters, k, the consensus and cluster confidence reach a maximum. In B. Delta area plot showing the relative change in area under the CDF curve, with no appreciable further increase at k=3. k3 is identified as the strongest clustering option. In C. Consensus Clustering plot for k3: groups 1+3 (n=8, renamed as group 1) vs group 2 (n=30).

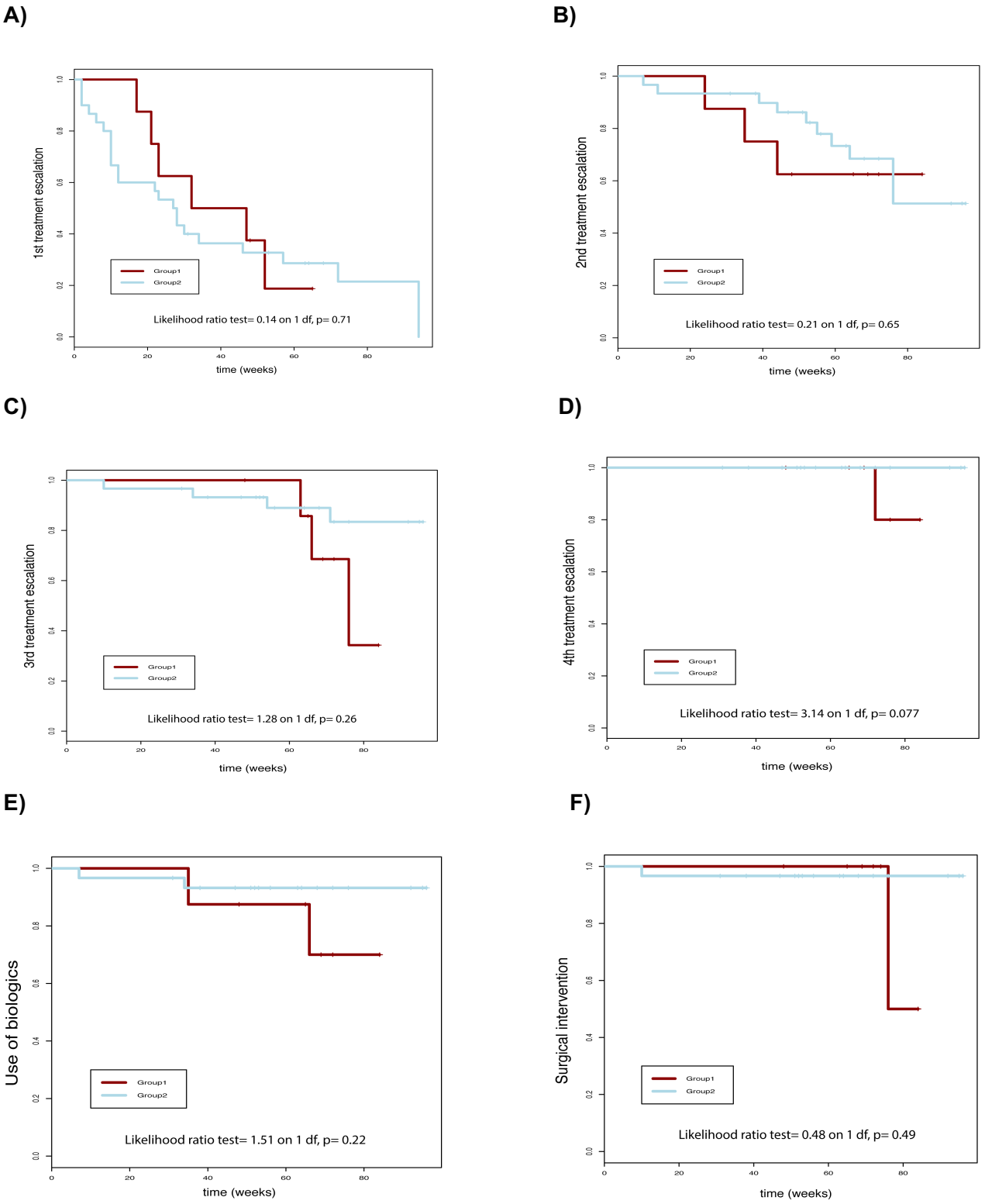

Figure 4.31. Kaplan Meier curves comparing the groups identified in 4.30 C (group 1: n=36 vs group 2 (i.e. 2+3): n=24) for the following outcomes: A) first treatment escalation; B) second treatment escalation; C) third treatment escalation; D) fourth treatment escalation; E) use of biologics; F) surgical intervention.

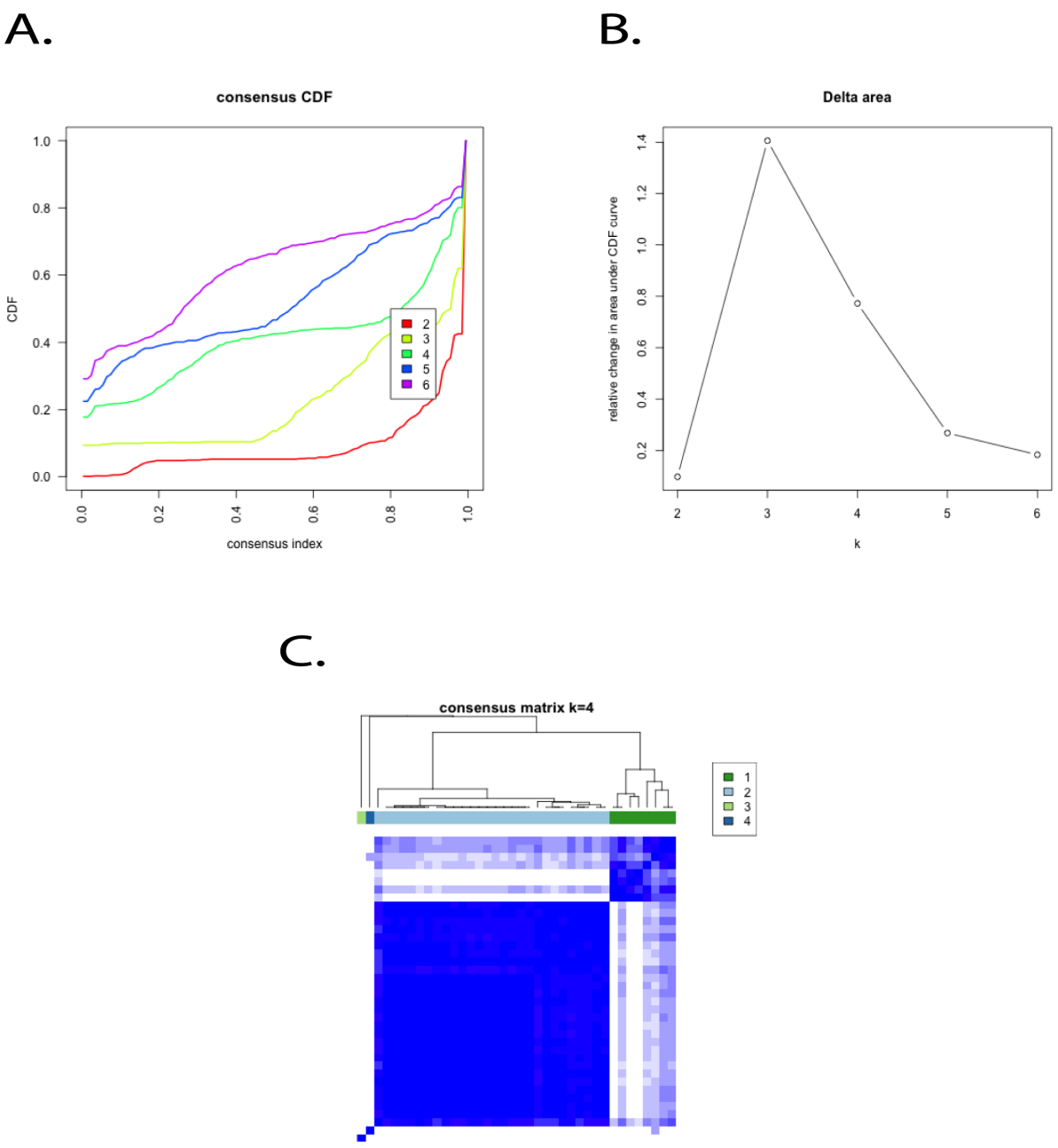

Figure 4.32 Consensus Clustering of a selection of probes included in the WGCNA modules yellowgreen and steelblue (75 probes), correlated with "use of biologics". In A. CDF: Consensus Cumulative Distribution Function, showing at what number of clusters, k, the consensus and cluster confidence reach a maximum. In B. Delta area plot, showing the relative change in area under the CDF curve, with no further appreciable increase at k=3. k3 is identified as the strongest clustering option. k4 was chosen as second-best clustering option, as by choosing k3 only one patient would cluster away from the remainder. In C. Consensus Clustering plot for k4: group 3 (n=8, renamed as group 1) vs groups 1,2 and 4 (n=30, renamed as group 2).

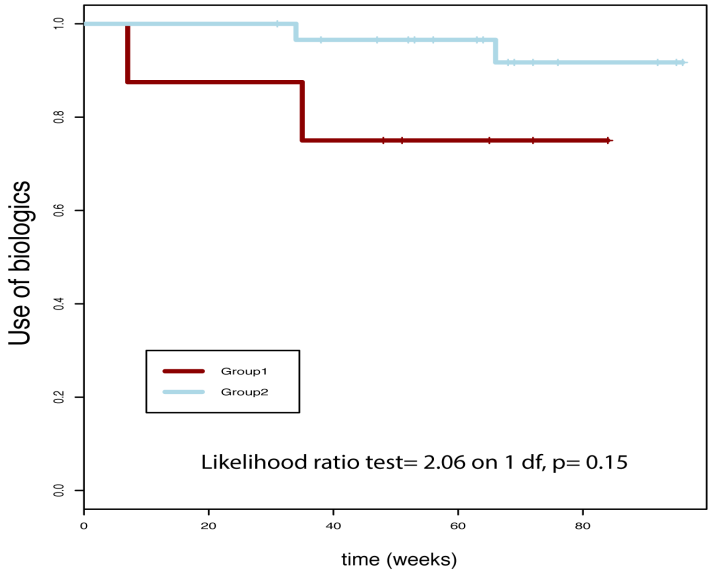

Figure 4.33 Kaplan Meier curves comparing the groups identified in 4.32 C (group 1: n=8 vs group 2 (i.e. 1+2+4): n=30) for the clinical outcome "use of biologics".

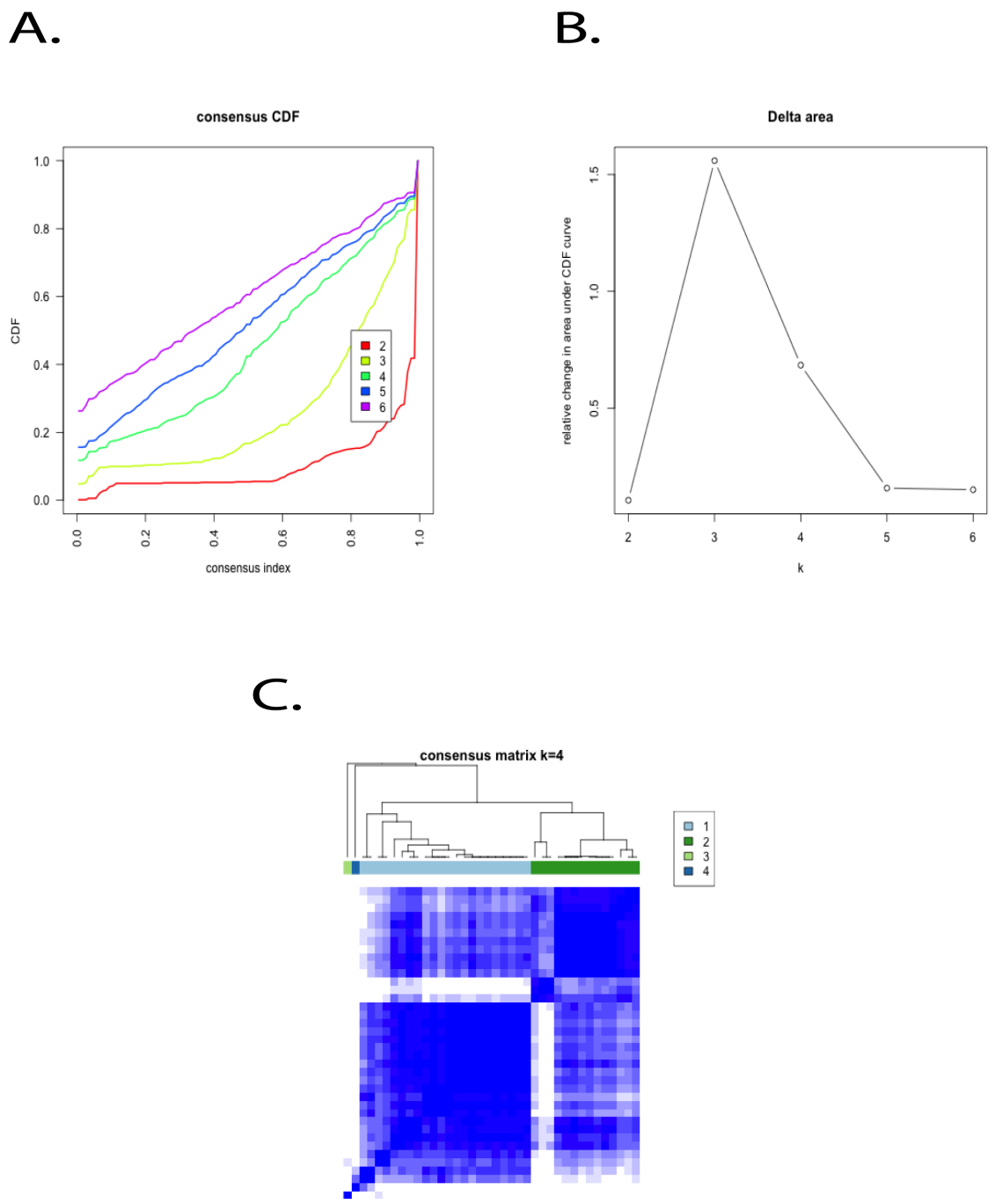

Figure 4.34 Consensus Clustering of a selection of probes included in the WGCNA modules correlated with the clinical variable "surgical intervention" (345 probes). In A. CDF: Consensus Cumulative Distribution Function, showing at what number of cluster, k, the consensus and cluster confidence reach a maximum. In B. Delta area plot, showing the relative change in the area under the CDF curve, with no further increase at k=3. K3 is identified as the strongest clustering option. K4 was chosen as second-best clustering option because k3 would only separate 1 patient out of the remainder. In C. Consensus Clustering plot for k4: group 1 (n=22) vs groups 2+3+4 (n=16, renamed as group 2).

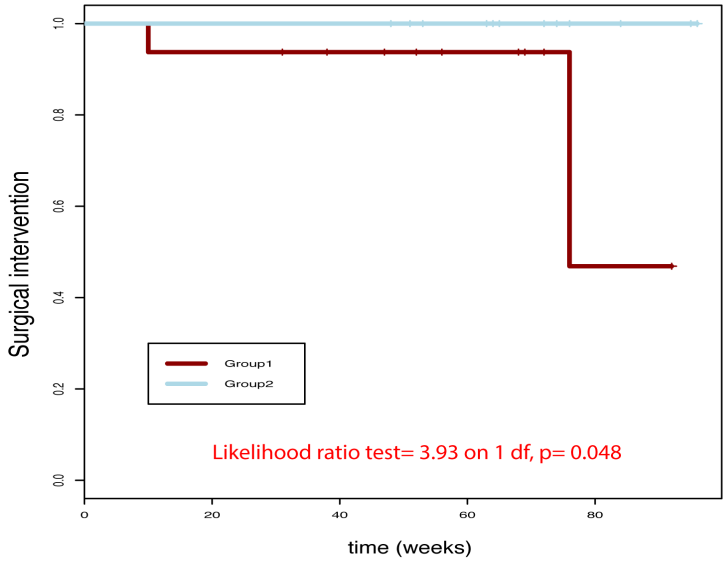

Figure 4.35. Kaplan Meier curves comparing the groups identified in 4.34 C (group 1: n=22 vs group 2 (i.e. 2+3+4): n=16) for the outcome "surgical intervention".

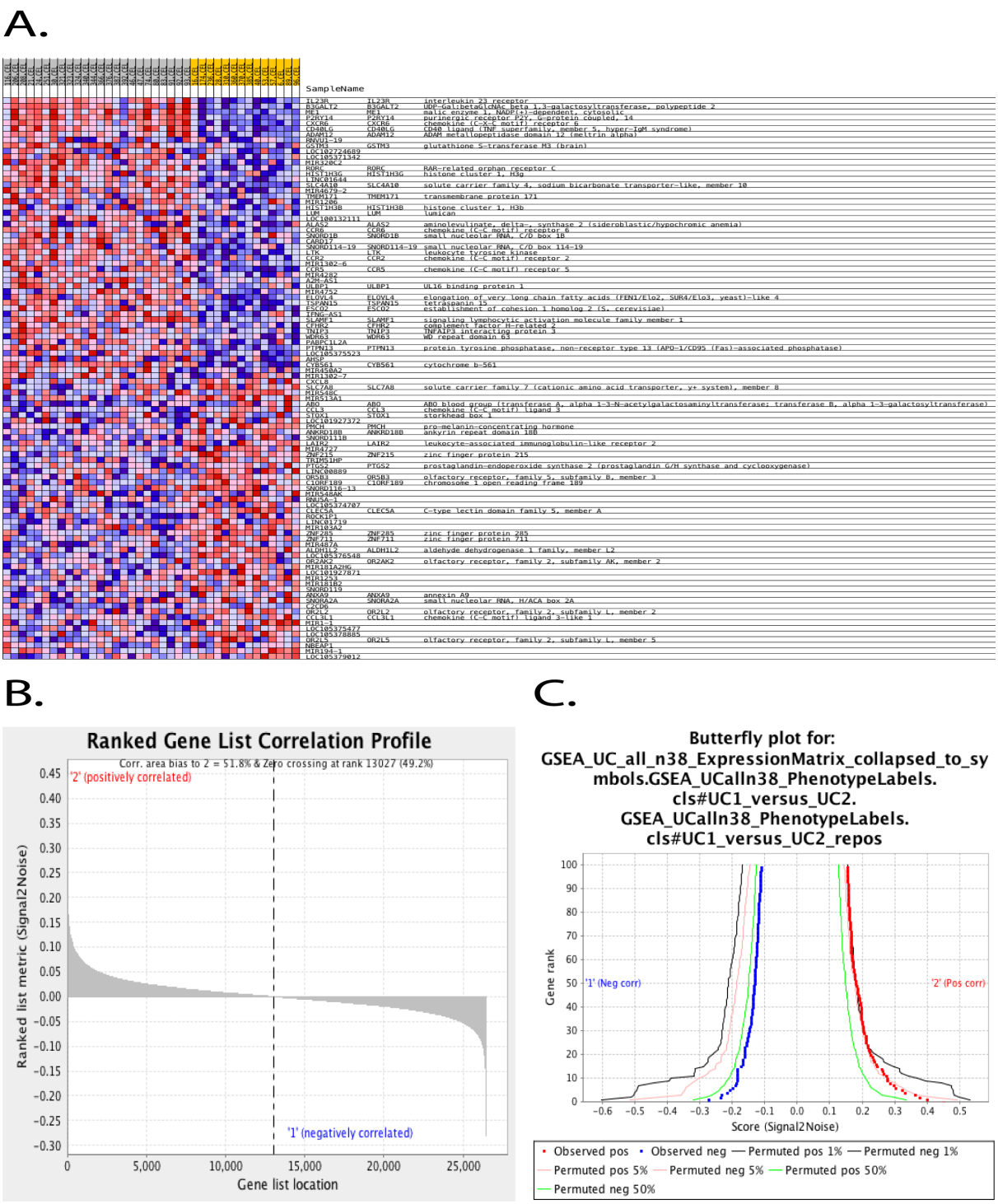

Figure 4.36. GSEA of the paediatric UC cohort (n=38). Groups are based on Consensus Clustering analysis of the selection of genes in WGCNA modules correlated to "surgical intervention". In A. Heatmap of the top 50 features for each phenotype (Consensus Clustering groups 1 vs 2). In B. Plot showing correlation between the ranked genes and groups 1 and 2. In C. Butterfly plot showing the top 100 positive and negative correlations between gene rank and the ranking metric score (i.e. first and last 100 genes in the ranked list). Observed correlations and permuted (1%, 5%, 50%) positive and negative correlations are shown for the top genes. This plot describes the extent to which dataset permutations change the correlation between gene rank and the ranking metric score.

In summary, whilst in this cohort we did not validate any reliable prognostic power of the signatures identified in adult patients [67], the paediatric signatures that emerged from WGCNA (i.e. modules correlated to the event "surgical intervention") did generate groups with significantly different outcomes. Moreover, WGCNA correlation indices of < -0.5 suggest significant strength in the predictive power of these specific signatures.

4.4 Discussion

This chapter aimed to investigate the existence of CD8 "paediatric specific" prognostic signatures, in light of the fact that the adult CD8 prognostic signature and T-cell exhaustion signature did not generate any significant split in outcome in our paediatric cohort, as shown in chapter 3.

In order to identify paediatric specific prognostic signatures, we resorted to the two alternative and complementary methods (i.e. unsupervised clustering analyses and WGCNA) used in the previous chapter.

When analysing CD and UC jointly, neither method showed any significant split in outcomes between the groups of patients identified. Clustering analyses produced a very uneven split between patient groups (90%: 10%), which limited the statistical power of the survival analysis (Kaplan Meier curves) as the milder group only included a limited number of patients (< 10) compared with the remainder clustering together and showing a more severe disease course.

WGCNA of the joint cohort only identified two modules of interest for specific outcomes, both with low correlation indices (< 0.25, > -0.25). In order to further test the prognostic potential of these modules, the corresponding probes were subset from the IBD cohort dataset and Consensus Clustering was performed to identify groups. These groups were then compared for specific outcomes through survival analysis, which failed to show a significant split. This questioned even further the strength of the modules identified. However, it should be pointed out that when testing the module correlated with "surgical intervention" in the joint cohort, the absence of a significant split was likely due to the limited number of events across the cohort. Although all three patients who underwent IBD related surgery did fall in the same Consensus Clustering group, the split in the survival analysis failed to reach significance.

We considered whether the lack of strong correlations could, at least partly, be explained by the fact that CD and UC patients were analysed jointly, given that the two types of IBD are significantly different in terms of indications to specific treatments and in outcome measures, so a separate analysis should be preferred. We therefore went on to investigate the existence of paediatric specific prognostic signatures, in the CD and UC cohorts separately.

Neater results were obtained when looking for CD8 prognostic signatures in the CD and in the UC datasets, with a significant split in some specific outcomes, using both unsupervised clustering (e.g. use of biologics in the paediatric CD cohort) and when applying WGCNA (e.g. surgical intervention

in the paediatric UC cohort). Groups with different outcomes identified by applying WGCNA modules of interest were also compared with GSEA. Top gene sets identified corresponded to those obtained from GSEA of the joint cohort. However, GSEA performed in the split cohort did not always reach FDR < 0.25.

Overall, this part of the analysis failed to identify strong CD8 paediatric specific signatures, although potential modules (signatures) were identified for specific outcomes in the CD and UC cohorts. We speculate that the limitation in the strength of such signatures is likely due to the majority of children developing a severe disease phenotype, with only an extreme minority of patients presenting with mild indolent disease. This hypothesis would be in consistent with the findings discussed in Chapter 3.

CHAPTER 5

Testing CD8 DNA methylation profiles as potential prognostic biomarkers in paediatric CD

5.1 Introduction

DNA methylation is one of the main epigenetic marks that are known to play a key role in regulating gene expression and cellular function in all mammals [55,56]. Its role in regulating cellular function [161] combined with high stability makes DNA methylation signatures an attractive read out for the development of clinical biomarkers [162-165].

In this part of the project we aimed to test the use of genome wide CD8+ T-cell DNA methylation profiles as disease prognostic biomarkers in paediatric IBD.

5.2 Materials and methods

DNA extracted from CD8+ T-cells of 66 children with CD, who were all part of the CD cohort analysed for gene expression (n=67, see section 4.3.2 on page 91), was processed through Epic methylation array. WGCNA was performed to test whether changes in DNA methylation in CD8+ T-cells can be used for outcome prediction.

BioConductor packages used were DMRcate, Minfi, IlluminaHumanMethylationEPICanno.ilm10b2.hg19, IlluminaHumanMethylationEPICmanifest and WGCNA.

Given that methylation data is gender related, the first step of the analysis consisted in checking the dataset for gender prediction using the "getSex" function. As shown in Figure 5.1 A, gender was predicted correctly in this dataset so no further adjustment was required. All samples passed quality control (BioConductor function: getQC) (Figure 5.1 B).

As our dataset was based on one tissue (i.e. blood samples only), the data was normalised by using quantile normalisation (preprocessQuantile function). Removal of SNPs at either the CpG interrogation sites or at the single nucleotide extension was then performed using the functions "dropLociWithSNPs" and "rmSNPandCH'. Data distribution post normalisation is displayed as M and beta values in Figure 5.2.

At this stage, batch correction (ComBat function) and chromosome removal were performed (Figure 5.3).

As a next step prior to performing WGCNA, we filtered out of the total probes (i.e. > 100,000, corresponding to CpGs) the 20% that were most differently methylayed by using the function "genefilter", as explained above (paragraph 2.8.2 on page 51).

At this stage, we went on to perform WGCNA on this methylation dataset. Methods related to WGCNA correspond to what summarised in Chapter 4.2.2 on page 74, other than modules being groups of CpG with similar methylation density. Another expected difference in WGCNA of the methylation data compared to gene expression is a gender related effect, despite chromosome

removal. In particular, the presence of a strong correlation between one (or more) module(s) and the variable “gender” is expected.

Set-up parameters were a soft thresholding power of 18 and minimum module size of 20.

Number and size of the modules identified through WGCNA of 66 children with CD are shown in Table 5.1.

Finally, WGCNA was also performed in a selection of this dataset, where probes corresponding to gene expression signatures of interest identified in the same cohort (Chapter 4.3.2 on page 91) were subset.

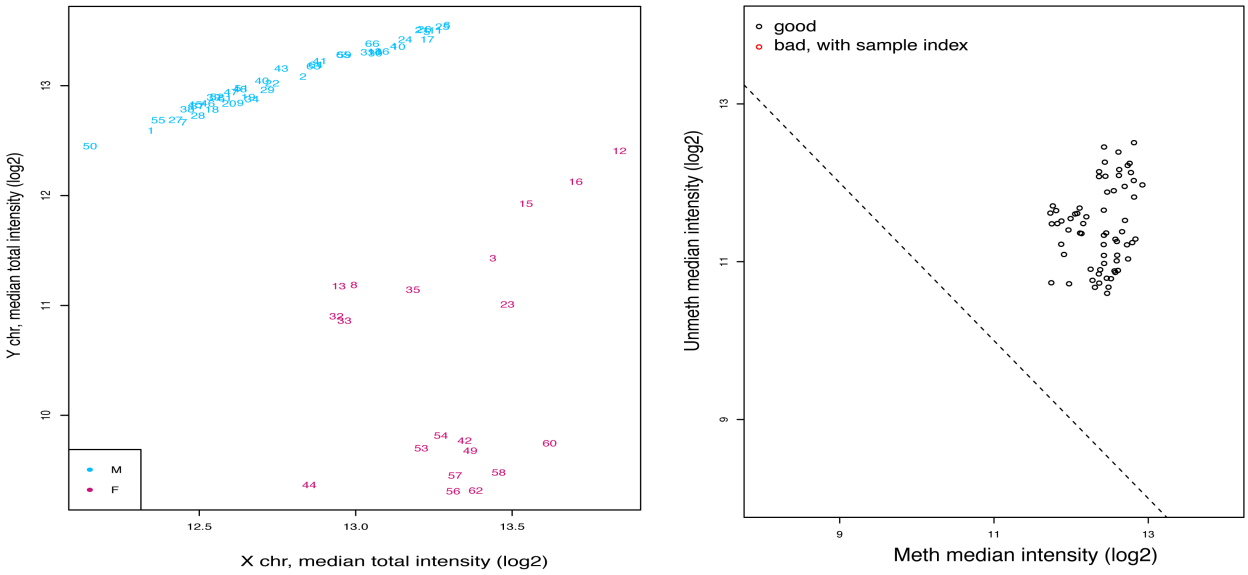

Figure 5.1 In A. Gender prediction of the paediatric methylation data (n=66). MDS plot by gender, on a logarithmic scale. F: female; M: male; x axis and y axis represent X and Y chromosomes. In B. Quality control of CD8 T-cell methylation samples from 66 children with CD.

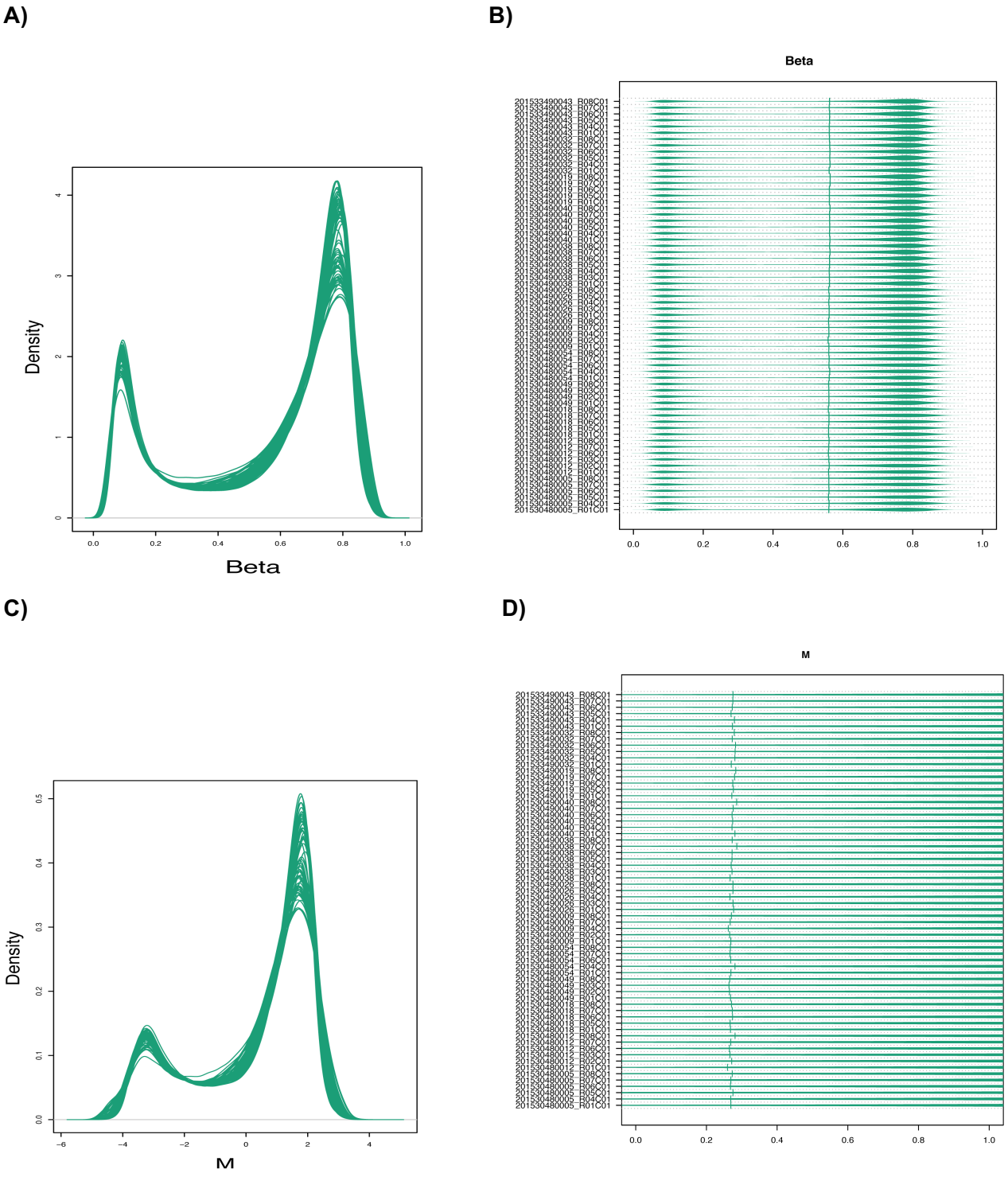

Figure 5.2 CD8+ T-cell methylation data distribution plots. Beta values in A. and B. M values in C. and D. A. and C. are density plots. B. and D. are density bean plots.

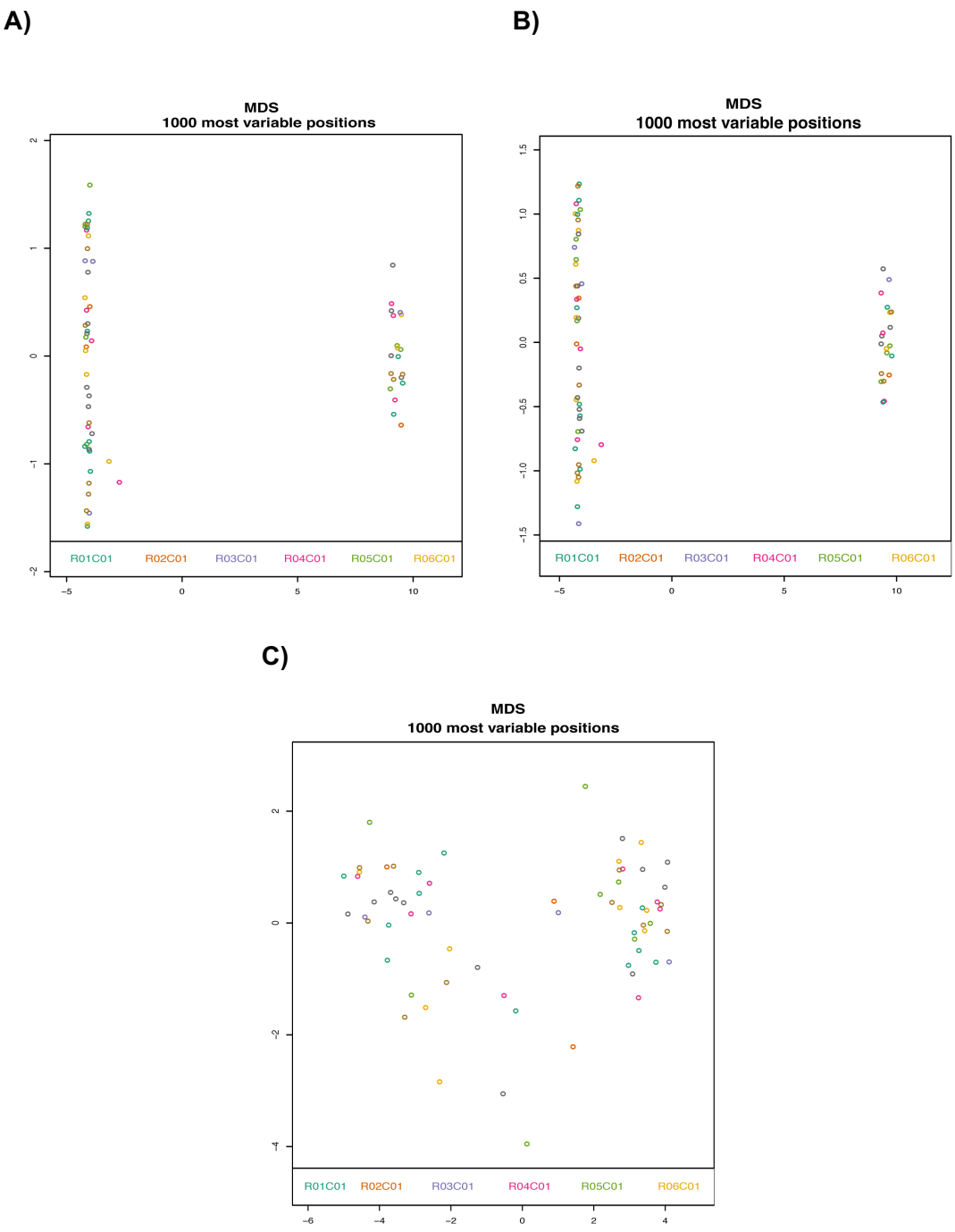

Figure 5.3 CD8+ T-cell methylation data. MDS plots before (A.) and after (B.) batch correction. MDS plot after chromosome removal (C.).

Module Number	Genes in each modules
0	16648
1	34043
2	7362
3	6974
4	6250
5	3020
6	284
7	69
8	49

Table 5.1 WGCNA of methylation data from the paediatric CD cohort (n=66). Module numbers and their size. The label 0 is reserved for genes outside of all modules, so it is not a module per se.

5.3 RESULTS

5.3.1 WGCNA of CD8+ T-cell methylation data from 66 children with CD

First, hierarchical clustering of this dataset was performed to investigate the data distribution and its substructure in groups and subgroups. We noted a relevant split in two main data groups of equal size, which was driven by differences in gender (Fig. 5.4). We then went on with WGCNA to identify 7 modules, which were tested for their correlation with the measured clinical traits.

As shown in Fig. 5.5 (showing correlations between modules and all clinical variables recorded for this patient cohort) and in Fig. 5.6 (an excerpt from Figure 5.5 where only outcome parameters are shown), there was no significant correlation between modules and disease outcomes. Of note, one module (module pink in this dataset) correlated with gender (Figure 5. 5), as expected in methylation datasets.

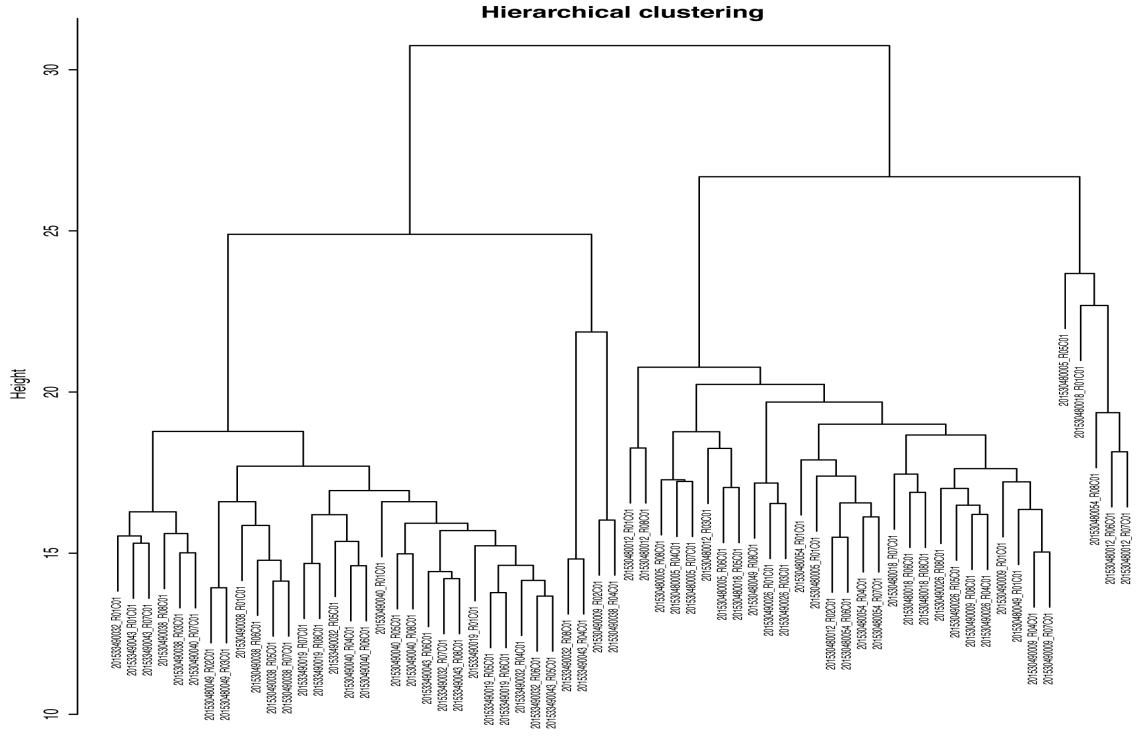

Figure 5.4. Hierarchical clustering of the methylation data in 66 children with CD. Two main clusters and their subgroups are shown.

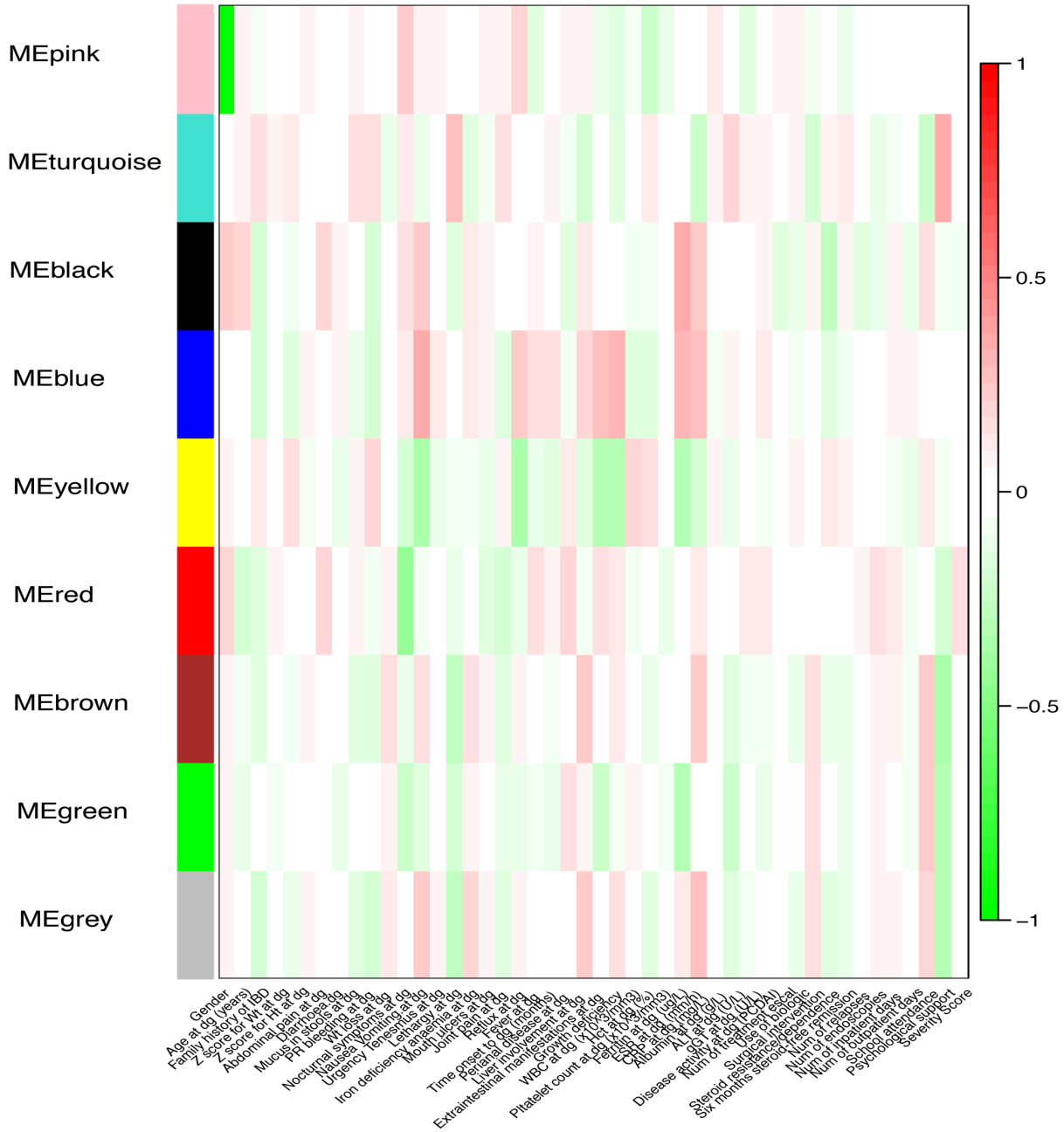

Figure 5.5 WGCNA. Methylation data from 66 children with CD. Module-trait associations. Each row corresponds to a module eigengene, column to a trait. Each cell contains correlation index and p-value (colour-coded, numbers not displayed on this plot). The table is colour-coded by correlation according to the colour legend (i.e. 1 = highest direct correlation, -1 = highest inverse correlation).

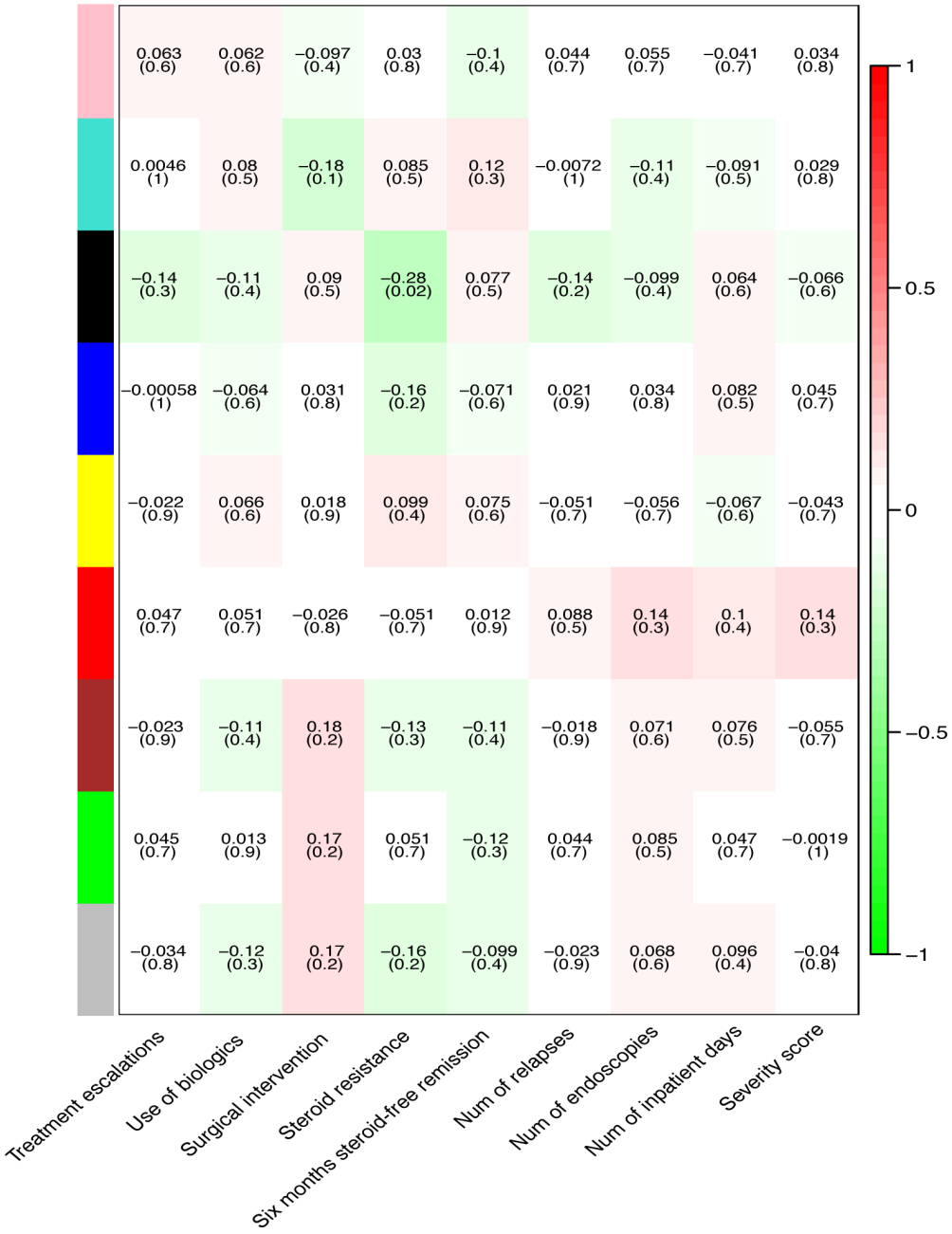

Figure 5.6 WGCNA. Methylation data from 66 children with CD. Excerpt from Figure 5.5 showing the top modules for clinical outcomes. On the x axis are variables related to disease outcomes. On the y axis are selected modules (indicated by colour bars). Each cell contains a correlation index and a p-value (in brackets).

5.3.2 Analysis of a subset of the CD8 methylation data from 66 children with CD: probes correlated with outcomes in the gene expression dataset from the same cohort.

Given the absence of significant correlations from the analysis above, we next resorted to a more supervised approach by subsetting from the methylation dataset those probes corresponding to modules that were significantly correlated with outcomes in the gene expression dataset (from the same patient cohort). This selection included 388,270 probes (across 66 samples). The top 20% of these probes that were most differentially methylated across this cohort were then selected, to obtain a final subset of 77,654 probes / 66 samples.

Fifteen modules were identified and their correlation with measured clinical variables is shown in Figure 5.7 while Figure 5. 8 shows an excerpt from Figure 5.7 where only the modules of relevance to disease outcomes are shown. Correlations for use of biologics (module cyan), surgical intervention (modules salmon and midnightblue) and severity score (modules cyan and midnightblue) were identified, though correlation indexes only ranged between + 0.24 and + 0. 26 for positive correlations, and between – 0.28 and -0.3 for negative correlations.

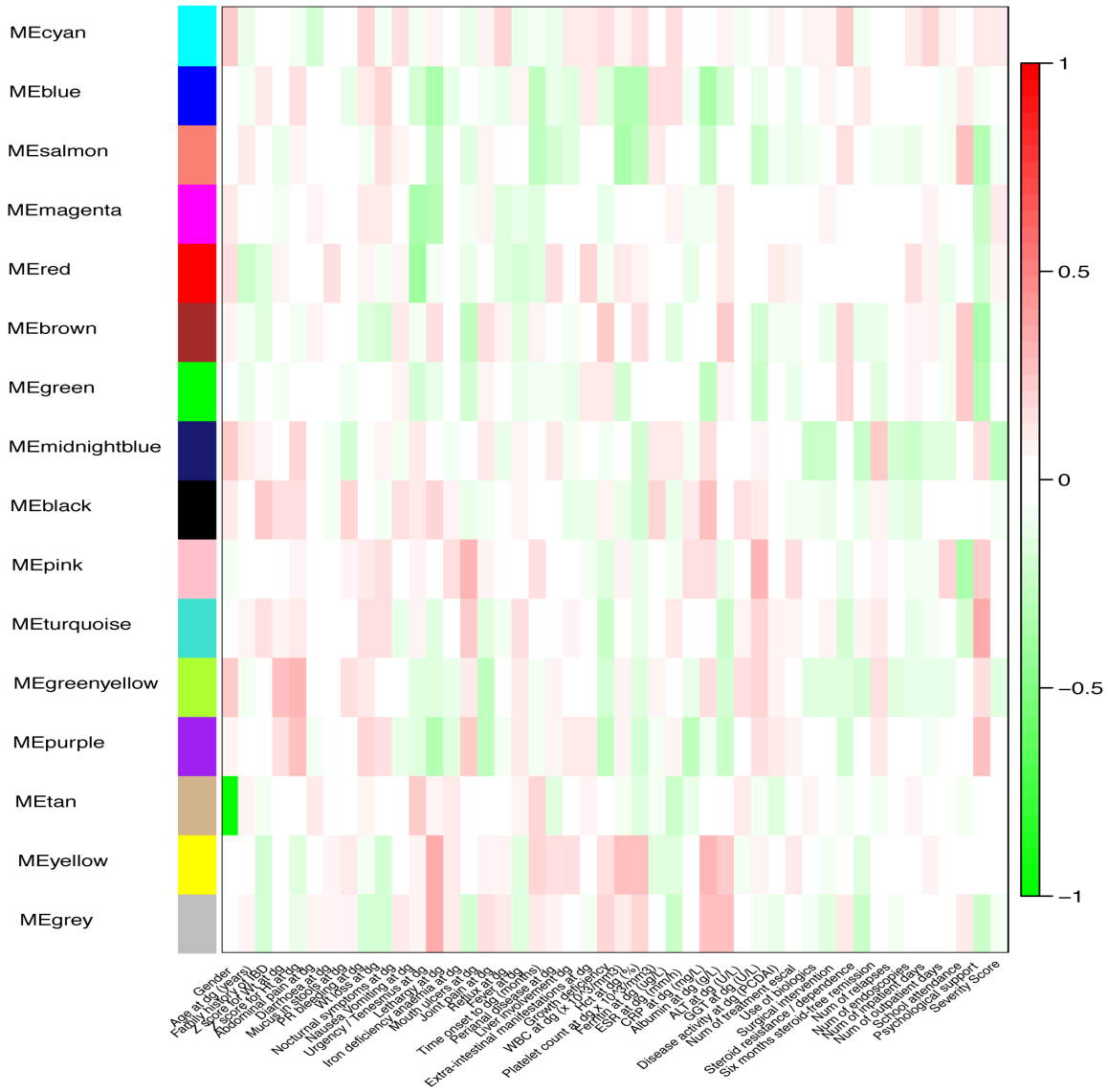

Figure 5.7 WGCNA. Module-trait associations. CD8 methylation data from 66 children with CD: probe selection corresponds to top gene expression WGCNA modules from the same cohort. Each row shows a module eigengene, columns correspond to clinical traits. Each cell contains a correlation index and a p-value (colour-coded, numbers not displayed on this plot). The table is colour-coded by correlation according to the colour legend (i.e. 1 = highest direct correlation, -1 = highest inverse correlation).

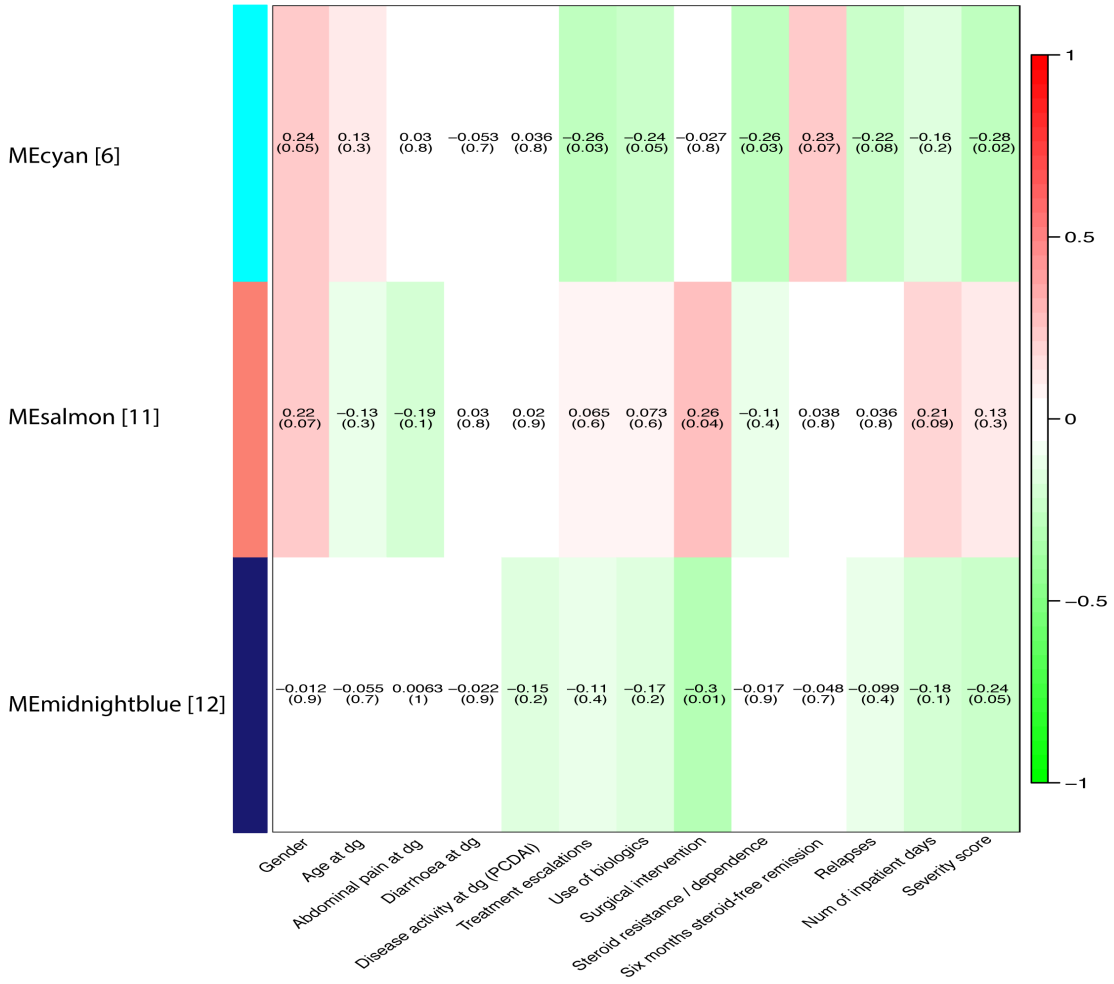

Figure 5.8 WGCNA. Module-trait associations. Selection of modules correlated with clinical outcomes from Figure 5.7. On the x axis are variables related to the disease at diagnosis (i.e. gender, age at diagnosis, abdominal pain at diagnosis, diarrhoea and disease activity score at diagnosis (i.e. PCDAI)) followed by variables describing disease outcomes (use of biologics, surgery, steroid resistance etc.). On the y axis are modules of interest (indicated by numbers and colour names). The plot shows how these modules correlate more strongly (directly or inversely) with disease outcomes than they do with parameters describing disease at diagnosis.

At this stage, in order to test further the prognostic power of the modules identified above, the probes corresponding to each module of interest were subset from this dataset and Consensus Clustering of this selection was performed. Subsequently, survival analysis was performed to compare the groups identified for the specific outcomes of interest.

First, we tested module cyan (21 CpG) correlated to the clinical variables “use of biologics” and “severity score”. Groups identified through Consensus Clustering are shown in Fig. 5.9. Survival analysis showed no significant differences between children in group 1 and 2, in respect to number of treatment escalations, use of biologics and surgical intervention (Fig. 5.10).

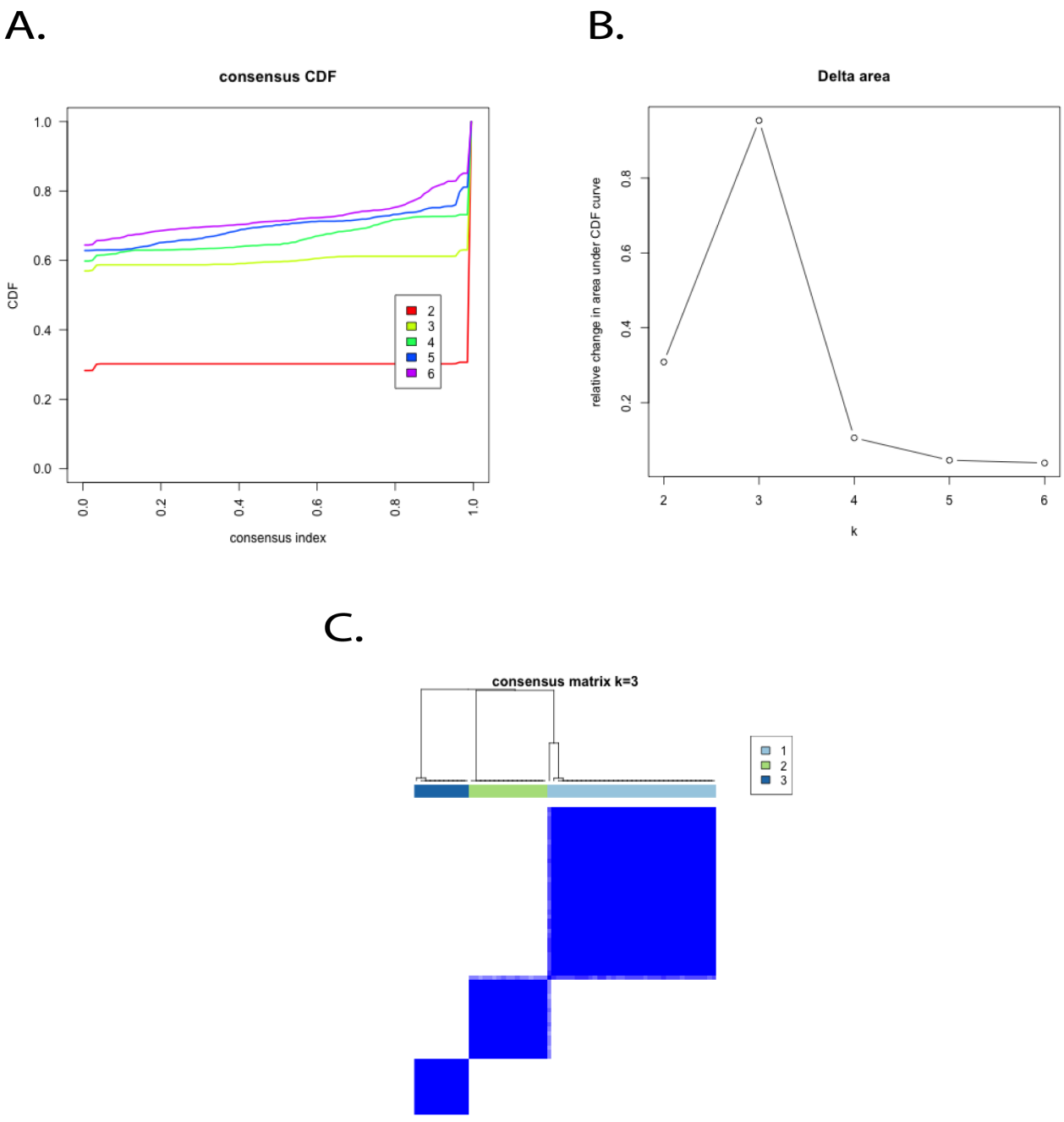

Figure 5.9. Consensus Clustering of a selection of probes included in the WGCNA module cyan (21 CpG) correlated with the clinical variables "use of biologics" and "severity score". In A. CDF: Consensus Cumulative Distribution Function, showing at what number of clusters, k, the consensus and cluster confidence reach a maximum. In B. Delta area plot, showing the relative change in the area under the CDF curve, with no further appreciable increase at k=3. k3 is identified as the strongest clustering option. In C. Consensus Clustering plot for k3: group 1: n=45 vs groups 2 (i.e. 2+3): n=21.

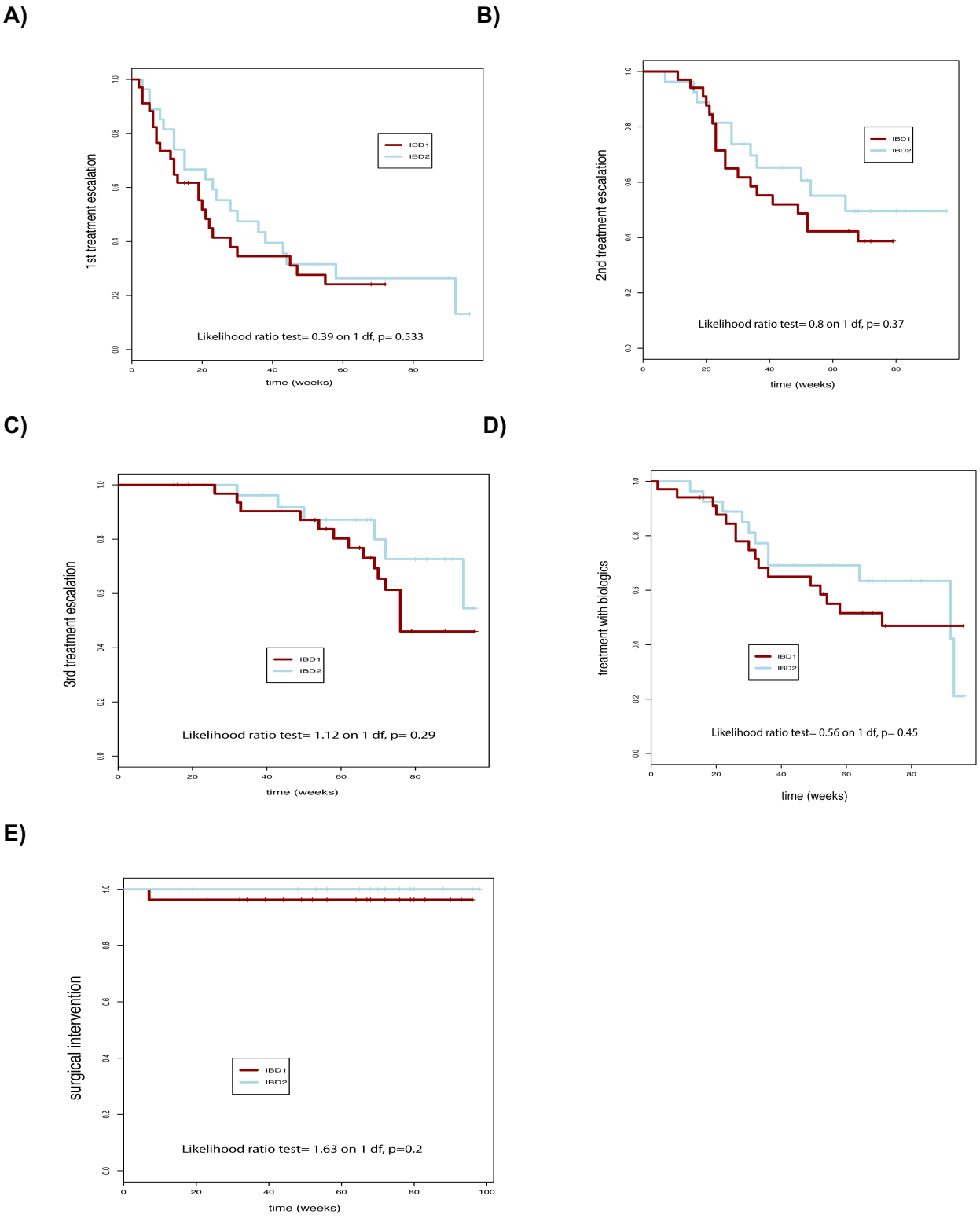

Figure 5.10 Kaplan Meier curves comparing the groups identified in 5.9 C (group 1: n=45 vs groups 2 (i.e. 2+3): n=21) for the following outcomes: A) first treatment escalation; B) second treatment escalation; C) third treatment escalation; D) use of biologics; E) surgical intervention.

We then performed a similar analysis subsetting probes from WGCNA modules salmon and midnightblue, correlated with surgery. Survival analysis failed to identify significant splits between the groups identified through Consensus Clustering.

As a last step, we analysed male and female patients separately, aiming to correct for gender effect. Nevertheless, this did not increase the correlation indexes of the modules identified.

5.4 Discussion

Testing DNA methylation profiles in CD8+ T-cells from our cohort was relevant to this project in view of existing evidence on the role of methylation in regulating gene expression [56] and on changes in methylation described in diseases including IBD [59-65].

We aimed to explore the potential of CD8+ specific DNA methylation profiles in predicting outcome for children with IBD as an alternative parameter endowed with higher stability compared to gene expression [66, 161-164]. The presence of relevant correlations with outcome would also have allowed us to investigate whether different DNA methylation profiles underpin specific changes in gene expression relevant to outcome prediction.

The data analysis shown in this chapter failed to identify significant correlations with disease outcome in our paediatric cohort. Nevertheless, the analysis is still at a preliminary stage and a number of possible limitations must be taken into account when interpreting these results. First, the patient population tested only included 66 children with CD, both males and females. Data breakdown by gender limited the population size even further. Second, so far, we have only applied WGCNA to our methylation data by adjusting the protocol used for gene expression to this specific dataset. The different nature of the methylation dataset may not fit the WGCNA approach extrapolated from the gene expression protocol. There are further analyses that should be undertaken, in particular, supervised differential methylation analysis between groups of children with different disease outcome. Moreover, although WGCNA has been applied to methylation datasets in previous studies [65,165], the use of other computational tools to test for possible correlation between genome wide methylation data and disease outcome should be investigated.

Current plans are to expand our cohort and sample size, adding more patients, including those with UC, and to refine and complete data analysis as discussed above on this larger cohort. Furthermore, as a similar project is being undertaken by our colleague adult gastroenterologists, a combined analysis of CD8+ methylation data from paediatric and adult patients will be available.

CHAPTER 6

Discussion

6.1 Summary and conclusion

The hunt for prognostic biomarkers is one of the most challenging and exciting topics in the study of paediatric and adult autoimmune diseases (including IBD) at present.

Huge progress has been achieved in areas such as oncology, where bench-work has generated reliable genetic and histological predictors that have changed the way in which patients are treated by personalising their care, but a similar approach is still a "work in progress" in complex immune-mediated conditions such as IBD [166].

IBD is a chronic condition for which no cure has yet been developed, so there is no doubt that the discovery of a reliable prognostic biomarker would improve the care of children affected by the disease. However, whether such a discovery would really improve patients' lives is determined by treatment availability. The treatments that are currently available target the immune system on different levels, and aim to achieve remission of the inflammatory status. However, particularly for patients of paediatric age, clinical and endoscopic remission is generally temporary, as children tend to relapse and therefore require accelerated treatment escalation [23,26,124,128]. The majority of children with IBD have shown suboptimal response to treatment, while also being exposed to potentially severe side effects such as infections and malignancy [86-88,111,167].

Increasing evidence suggests that the early, stratified treatment of patients in high-risk groups (i.e. those patients with the severe disease phenotype) is likely to improve the long-term disease outcome [132]. A reliable prognostic biomarker would enable us to advise children and their parents about the likely disease outcome at the point of diagnosis, and hence to propose a tailored, potentially more individualised treatment strategy and/or patient monitoring scheme. Importantly, treatment stratification according to likely disease outcome would avoid the unnecessary exposure of "mild" disease cases to potentially harmful treatment, while still providing sufficiently effective treatment to patients in high-risk groups.

However, treatment availability is currently limited, particularly for paediatric IBD. As shown in Fig. 1.5 on page 33 [89], only a few drugs and/or treatment options (i.e. EEN/steroids, thiopurines, biologics and surgery) are available while dealing with lack or loss of response to treatments.

The use of a "step-up approach" as opposed to a "top down strategy" has been debated for the past two decades. Current data show that, even in countries where a step-up approach is favoured in order to save the more powerful treatment options for a later stage, the majority of children will eventually end up needing second line immunosuppressants and nearly half of them will end up on biologic treatments in the long run. Based on the number of children failing to respond to treatment, it is becoming more and more questionable whether we are indeed able to modify the natural history of IBD [125,127].

It is therefore clear that the search for prognostic biomarkers has to proceed alongside the development of new drugs in order to have enough options available once patients have been stratified for risk at the point of diagnosis.

One of the most promising predictors reported to date has come from work by the group of Prof. Ken Smith (Cambridge Department of Medicine). This group has identified a specific gene expression signature in CD8+ T-cells isolated from peripheral blood that correlates with disease outcome in adult patients with autoimmune diseases (i.e. systemic lupus erythematosus (SLE) and ANCA associate vasculitis (AAV)) as well as adult IBD [67]. E. McKinney from the same group also identified a T-cell related exhaustion signature that is protective towards the development of a severe disease course in adult patients with auto-immune conditions, including IBD [155].

In 2014, we set out to test, for the first time, the use of CD8+ T-cell gene expression profiles as disease prognostic biomarkers in children diagnosed with IBD. Our data from 107 prospectively recruited children did not prove a predictive role of CD8 adult signatures, which may suggest that there are intrinsic differences between children and adults. Moreover, unsupervised clustering analysis of the paediatric data consistently showed a major difference in size between groups of patients identified in our paediatric cohort: when the outcomes for such groups were compared, the fraction of patients in the mild group was approximately 10%, whereas the severe prognostic group made up 80–90% of the sample. This uneven split limited the power of our survival analyses and differed to the 40/60 split identified in the previous study on adult patients.

IBD is a complex condition with a wide phenotypic spectrum, so age-related differences in gene expression profiles are likely, and previous studies have shown that children tend to develop a severe disease phenotype more often (and earlier) than adult patients. A common theme throughout our findings is that IBD in the paediatric population is less heterogeneous than that in the adult population: the majority of paediatric patients appear to suffer from moderate or severe forms of the disease and therefore fall into the same prognostic group.

By comparing the clinical data collected to the information available from the adult study, we were able to provide evidence that paediatric IBD is a disease subgroup where the vast majority of patients fall into the moderate/severe group (Fig. 3.9 on page 69).

Of particular interest are our findings related to the investigation of T-cell exhaustion in children. Exhaustion genes expressed in adults were mostly down-regulated in our paediatric cohort and vice versa. This may suggest that children go on to develop a severe disease course because their T-cells are not exhausted.

Because it was not possible to apply the prognostic power of adult signatures to the paediatric population, the second part of our work was based on testing for the existence of paediatric-specific signatures that could serve as prognostic biomarkers in children with IBD. Significant correlations were obtained by analysing CD and UC separately: signatures from specific WGCNA modules

generated noteworthy differences in use of biologics in CD and in surgical intervention in UC between the groups identified.

GSEA based on the groups identified using the above signatures highlighted the presence of pathways including IL7, TNF-alpha and interferon, amongst others which are less known to play a role in IBD. However, the reliability of the paediatric signatures identified is such that further validation is required, as the correlation indexes ranged between ± 0.2 and ± 0.4 for most of the clinical outcomes investigated.

Interestingly, the findings emerging from our study suggest that a smaller focus should be placed on the use of prognostic biomarkers in paediatric IBD. In fact, as the majority of children seem to fall in the severe prognostic group, one should recommend a top-down approach to enable prompt effective treatment in anticipation of further complications. Our results may question the worth of a biomarker for predicting the overall disease course in paediatric IBD, but the focus should remain on developing predictors of response to treatments, particularly in view of the development of new drugs on the horizon. A major interest in predicting the response to IBD treatment has recently arisen, and promising data is emerging [168].

In summary, this prospective study performed on a large cohort and over an adequate follow-up time, has increased our understanding of paediatric (and adult) IBD by confirming that patients of paediatric age follow a more severe disease course, which makes the identification and validation of prognostic biomarkers particularly challenging. Paediatric IBD appears to be a unique entity with a more severe phenotype.

Importantly, our findings pave the way to further investigation on the process of T-cell exhaustion in children. Exploring mechanisms that induce exhaustion of T lymphocytes might provide future preventative therapeutic options for paediatric patients diagnosed with IBD.

6.2 Strengths and limitations

The main strength of this work is the prospective recruitment of a large cohort of treatment-naïve paediatric patients and the thorough collection of detailed clinical information from the same operator over a 1.5-year follow-up period.

The consistent results found by using two complementary bioinformatics analyses, i.e. unsupervised clustering and WGCNA, are also an element of strength in supporting our findings and conclusion.

The single-centre setting of the work is arguably a limitation, as it allowed a reliable, consistent, single-operator-based collection of detailed clinical data, which was fundamental for the aim of this specific study.

Another limitation in this study was that the comparison between the paediatric and the adult gene expression data was managed by keeping the two cohorts separate. In fact, merging data from different versions of the gene expression array (Affymetrix Human Gene 1.0 and 2.0 ST, respectively) was not achievable. Nevertheless, we are planning to use whole blood samples collected in PAX tubes from a group of children from the same paediatric cohort to test the adult prognostic signature through a RT-PCR essay. This approach will allow us to bypass the issue of the different arrays and will be used as a validation step of our findings.

In respect to limitations, this 4-year project acts as an example of the huge amount of translational work that is required for the development and/or testing of prognostic biomarkers. The availability of patients and samples, the prospective collection of clinical data including strict patient monitoring during follow-up (as shown in Appendix 2 on page 176), laboratory techniques (e.g. cell separation, extraction of nucleic acids, microarray), and the availability of bioinformatics skills for appropriate up-to-date analyses all made this experience complex and challenging.

One relevant hurdle in collecting clinical information was the identification of which parameters would reflect disease severity in a paediatric population. In fact, using the number of treatment escalations as in the adult study would be limiting in paediatric patients who mostly have more than two escalations. We therefore collected information on the use of biologics, IBD-related surgical intervention and IBD-related inpatient admissions in order to expand the outcome range and increase the chance of identifying a split between the more severe patients and the milder ones. In the absence of a summary score for disease severity in the paediatric literature to date, we also created scores for the purpose of this study, although they could not be weighted or validated (chapter 2.2.1 on page 45).

In summary, the complexity mentioned above must be taken into account when setting up translational research studies aimed to develop disease biomarkers. We foresee that in the near future, more advanced and automated electronic clinical databases will alleviate the need for manual data collection. Moreover, new computational tools are likely to be implemented to match high throughput data with corresponding clinical information.

6.3 Future work

We are currently using whole blood samples collected in PAX tubes from a group of 79 children enrolled in this study to test the adult prognostic signature through a RT-PCR assay, as a validation step of the work presented in this thesis. We aim to verify whether the majority of these children would correspond to the adult severe prognostic group, as expected from the findings of this study. If this were to be the case, the limited role of CD8+ gene expression signatures as disease prognostic biomarkers in paediatric patients would be corroborated.

Additionally, we aim to complete and improve the preliminary work on CD8+ DNA methylation showed in chapter 5. Relevant findings have recently been published on the role of DNA methylation profiles in intestinal epithelial cells as diagnostic biomarkers for paediatric IBD, with specific changes in methylation reflecting the type of IBD diagnosis and its distribution [64,65].

No data on DNA methylation profiles in CD8+ T-cell has been shown so far, to our knowledge. CD8+ methylation samples from a larger cohort are now available in our laboratory, hence we aim to conduct further bioinformatics analysis aimed to test this parameter as a potential prognostic biomarker in children with IBD.

Future investigation should focus on T-cell exhaustion signatures. Findings from this study suggest that CD8+ T-cells in children might be not exhausted which may therefore predispose the patients to a more severe disease course. If such a theory were to be proved by further experiments, this would potentially pave the way towards preventative therapeutic options based on inducing T-cell exhaustion in paediatric-onset IBD.

Finally, throughout the course of this project we have collected blood samples at different time points during the patients' follow-up, i.e. when patients were being treated and were either achieving remission or going through a relapse of their IBD. Analysis of gene expression (and methylation) profiles from these samples and correlation with clinical data has the potential to measure the stability of these profiles over time and their correlation with disease activity and/or response to treatments.

References

1. Ruel, J., Ruane, D., Mehandru, S., Gower-Rousseau, C., Colombel, J.F. IBD across the age spectrum - is it the same disease? *Nat Rev Gastroenterol Hepatol.* **11(2)**, 88-98 (2014).

2. Levine, A., Koletzko, S., Turner, D., Escher, J.C., Cucchiara, S., de Ridder, L., *et al*. European Society of Pediatric Gastroenterology, Hepatology, and Nutrition. ESPGHAN revised porto criteria for the diagnosis of inflammatory bowel disease in children and adolescents. *J Pediatr Gastroenterol Nutr*. **58(6)**, 795-806 (2014).

3. Aujnarain, A., Mack, D.R., Benchimol, E.I. The role of the environment in the development of pediatric inflammatory bowel disease. *Curr Gastroenterol Rep.* **15(6),** 326 (2013).

4. Sauer, C.G., Kugathasan, S. Pediatric inflammatory bowel disease: highlighting pediatric differences in IBD. *Med Clin North Am.* **94,** 35-52 (2010).

5. Marx, G., Seidman, E.G., Martin, S.R., Deslandres, C. Outcome of Crohn's disease diagnosed before two years of age. *J Pediatr.* **140,** 470-3 (2002).

6. Cannioto, Z., Berti, I., Martellossi, S., Bruno, I., Giurici, N., Crovella, S., Ventura, A. IBD and IBD mimicking enterocolitis in children younger than two years of age. *Eur J Pediatr.* **168**, 149-155 (2009).

7. Abraham, B.P., Mehta, S., El-Serag, H.B. Natural history of pediatric-onset inflammatory bowel disease: a systematic review. *J Clin Gastroenterol.* **46(7)**, 581-9 (2012).

8. Vaisman, N., Dotan, I., Halack, A., Niv, E. Malabsorption is a major contributor to underweight in Crohn's disease patients in remission. *Nutrition.* **22(9)**, 855-9 (2006).

9. Shamir, R., Phillip, M., Levine, P.A. Growth Retardation in Pediatric Crohn's Disease: Pathogenesis and Interventions. *Inflamm Bowel Dis.* **13,** 620-28 (2007).

10. Heuschkel, R., Salvestrini, C., Beattie, R.M., Hildebrand, H., Walters, T., Griffiths, A. Guidelines for the management of growth failure in childhood inflammatory bowel disease. *Inflamm Bowel Dis.* **14(6)**, 839-49 (2008).

11. Griffiths, A.M. Growth retardation in early-onset inflammatory bowel disease: should we monitor and treat these patients differently? *Dig Dis.* **27(3)**, 404-11 (2009).

12. Walters, T.D., Griffiths, A.M. (2008). Growth impairment in pediatric inflammatory bowel disease. In P. Mamula, J.E. Markowitz, R.N. Baldassano (Eds. Springer Publ), *Pediatric Inflammatory Bowel Diseases*. (pp. 103-14). New York, NY.

13.Levine, A., Griffiths, A., Markowitz, J., Wilson, D.C., Turner, D., Russell, R.K., *et al*. Pediatric modification of the Montreal classification for inflammatory bowel disease: the Paris classification. *Inflamm Bowel Dis.* **17(6)**, 1314-21 (2011).

14.Burisch, J., Munkholm, P. Inflammatory bowel disease epidemiology. *Curr Opin Gastroenterol.* **29(4)**, 357-62 (2013).

15.Burisch, J., Pedersen, N., Čuković-Čavka, S., Brinar, M., Kaimakliotis, I., Duricova, D., *et al*. EpiCom-group. East-West gradient in the incidence of inflammatory bowel disease in Europe: the ECCO-EpiCom inception cohort. *Gut.* **63(4)**, 588-97 (2014).

16.Cosnes, J., Gower-Rousseau, C., Seksik, P., Cortot, A. Epidemiology and natural history of inflammatory bowel diseases. *Gastroenterology.* **140(6)**, 1785-94 (2011).

17.Leichtner, A.M., Higuchi, L (2004). Epidemiology of ulcerative colitis. In Walker, Goulet, Kleinman, Sherman, Schneider, Sanderson (Eds. BC Decker Int Publ), Pediatric Gastrointestinal Disease. (p. 826).

18.Bousvaros, A., Sylvester, F., Kugathasan, S., Szigethy, E., Fiocchi, C., Colletti, R., *et al*. Challenges in pediatric inflammatory bowel disease. *Inflamm Bowel Dis.* **12(9)**, 885-913 (2006).

19.Ananthakrishnan, A.N. Epidemiology and risk factors for IBD. *Nat Rev Gastroenterol Hepatol.* **12(4)**, 205-17 (2015).

20.Ng, S.C., Bernstein, C.N., Vatn, M.H., Lakatos, P.L., Loftus, E.V. Jr, Tysk, C., *et al*. Epidemiology and Natural History Task Force of the International Organization of Inflammatory Bowel Disease (IOIBD). Geographical variability and environmental risk factors in inflammatory bowel disease. *Gut.* **62(4)**, 630-49 (2013).

21.Benchimol, E.I., Kaplan, G.G., Otley, A.R., Nguyen, G.C., Underwood, F.E., Guttmann, A., Jones, J.L., *et al.* Rural and Urban Residence During Early Life is Associated with Risk of Inflammatory Bowel Disease: A Population-Based Inception and Birth Cohort Study. *Am J Gastroenterol*. **112(9)**, 1412-1422 (2017).

22.Baumgart, D.C., Bernstein, C.N., Abbas, Z., Colombel, J.F., Day, A.S., D'Haens, G., *et al.* IBD around the world: comparing the epidemiology, diagnosis, and treatment: proceedings of the World Digestive Health Day 2010 - Inflammatory Bowel Disease Task Force meeting. *Inflamm Bowel Dis.* **17(2)**, 639-44 (2011).

23.Cosnes, J., Cattan, S., Blain, A., Beaugerie, L., Carbonnel, F., Parc, R., *et al.* Long-term evolution and disease behavior of Crohn's disease. *Inflamm Bowel Dis.* **8(4)**, 244-50 (2002).

24. Benchimol, E.I., Guttmann, A., Griffiths, A.M., Rabeneck, L., Mack, D.R., Brill, H., et al. Increasing incidence of paediatric inflammatory bowel disease in Ontario, Canada: evidence from health administrative data. *Gut.* **58(11)**, 1490-7 (2009).

25.Bernstein, C.N., Wajda, A., Svenson, L.W., MacKenzie, A., Koehoorn, M., Jackson, M., *et al.* The epidemiology of inflammatory bowel disease in Canada: a population-based study. *Am J Gastroenterol.* **101 (7)**, 1559-68 (2006).

26.Rocchi, A., Benchimol, E.I., Bernstein, C.N., Bitton, A., Feagan, B., Panaccione, R., et al. Inflammatory bowel disease: a Canadian burden of illness review. *Can J Gastroenterol.* **26(11)**, 811-7 (2012).

27.Mayberry, J.F., Lobo, A., Ford, A.C., Thomas, A. NICE clinical guideline (CG152): the management of Crohn's disease in adults, children and young people. *Aliment Pharmacol Ther.* **37(2)**, 195-203 (2013).

28.Molodecky, N.A., Soon, I.S., Rabi, D.M., Ghali, W.A., Ferris, M., Chernoff, G., *et al.* Increasing incidence and prevalence of the inflammatory bowel diseases with time, based on systematic review. *Gastroenterology* **142 (1)**, 46-54 (2012).

29.Day, A.S., Ledder, O., Leach, S.T., Lemberg, D.A. Crohn's and colitis in children and adolescents. *World J Gastroenterol.* **18(41)**, 5862-69 (2012).

30.Sawczenko, A., Sandhu, B.K., Logan, R.F., Jenkins, H., Taylor, C.J., Mian, S., *et al.* Prospective survey of childhood inflammatory bowel disease in the British Isles. *Lancet.* **357**, 1093e42001 (2001).

31.Benchimol, E.I., Fortinsky, K.J., Gozdyra, P., Van den Heuvel, M., Van Limbergen, J., Griffiths, A.M. Epidemiology of pediatric inflammatory bowel disease: a systematic review of international trends. *Inflamm Bowel Dis.* **17(1)**, 423-39 (2011).

32.Guariso, G., Gasparetto, M., Visonà Dalla Pozza, L., D'Incà, R., Zancan, L., Sturniolo, G., *et al*. Inflammatory bowel disease developing in paediatric and adult age. *J Pediatr Gastroenterol Nutr.* **51(6)**, 698-707 (2010).

33.Bernstein CN. New insights into IBD epidemiology: Are there any lessons for treatment? *Dig Dis.* **28(3),** 406-10 (2010).

34.Van Assche, G., Dignass, A., Panes, J., Beaugerie, L., Karagiannis, J., Allez, M., *et al.* European Crohn's and Colitis Organisation (ECCO). The second European evidence-based consensus on the diagnosis and management of Crohn's disease: Definitions and diagnosis. *J Crohns Colitis.* **4**, 7–27 (2010).

35.Dignass, A., Eliakim, R., Magro, F., Maaser, C., Chowers, Y., Geboes, K., *et al.* Second European evidence-based Consensus on the diagnosis and management of ulcerative colitis: Definitions and diagnosis. *J Crohn`s Colitis.* **6(10)**, 965-90 (2012).

36.Kronman, M.P., Zaoutis, T.E., Haynes, K., Feng, R., Coffin, S.E. Antibiotic exposure and IBD development among children: a population-based cohort study. *Pediatrics.* **130(4)**, e794-8032012.

37.Chouraki, V., Savoye, G., Dauchet, L., Vernier-Massouille, G., Dupas, J.L., Merle, V., *et al.* The changing pattern of Crohn's disease incidence in northern France: a continuing increase in the 10- to 19-year-old age bracket (1988-2007). *Aliment Pharmacol Ther.* **33(10)**, 1133-42 (2011).

38.Jussila, A., Virta, L.J., Salomaa, V., Mäki, J., Jula, A., Färkkilä, M.A. High and increasing prevalence of inflammatory bowel disease in Finland with a clear North-South difference. *J Crohns Colitis.* **7(7)**, e256-62 (2013).

39.Gower-Rousseau, C., Vasseur, F., Fumery, M., Savoye, G., Salleron, J., Dauchet, L., *et al.* Epidemiology of inflammatory bowel diseases: new insights from a French population-based registry (EPIMAD). *Dig Liver Dis*. **45(2)**, 89-94 (2013).

40.Ravikumara, M., Sandhu, B.K. Epidemiology of inflammatory bowel diseases in childhood. *Indian J Pediatr.* **73**, 717–21 (2006).

41.Oliva-Hemker, M., Fiocchi, C. Etiopathogenesis of inflammatory bowel disease: the importance of the pediatric perspective. *Inflamm Bowel Dis.* **8**, 112-28 (2002).

42.Jostins, L., Ripke, S., Weersma, R.K., Duerr, R.H., McGovern, D.P., Hui, K.Y., *et al.* Host-microbe interactions have shaped the genetic architecture of inflammatory bowel disease. *Nature.* **491(7422)**, 119-24 (2012).

43.Huang, H., Fang, M., Jostins, L., Umicevic Mirkov, M., Boucher, G., Anderson, C.A., *et al.* International Inflammatory Bowel Disease Genetics Consortium. Fine-mapping inflammatory bowel disease loci to single-variant resolution. *Nature*. **547(7662),** 173-178 (2017).

44.Lees, C.W., Barrett, J.C., Parkes, M., Satsangi, J. New IBD genetics: common pathways with other diseases. *Gut*. **60(12),** 1739-53 (2011).

45.Lee, J.C., Biasci, D., Roberts, R., Gearry, R.B., Mansfield, J.C., Ahmad, T., *et al.* UK IBD Genetics Consortium. Genome-wide association study identifies distinct genetic contributions to prognosis and susceptibility in Crohn's disease. *Nat Genet.* **49(2),** 262-268 (2017).

46.Christodoulou, K., Wiskin, A.E., Gibson, J., Tapper, W., Willis, C., Afzal, N.A., et al. Next generation exome sequencing of paediatric inflammatory bowel disease patients identifies rare and novel variants in candidate genes. *Gut.* **62(7)**, 977-84 (2013).

47.Scherr, R., Essers, J., Hakonarson, H., Kugathasan, S. Genetic determinants of pediatric inflammatory bowel disease: is age of onset genetically determined? *Dig Dis.* **27,** 236-9 (2009).

48.Schirmer, M., Smeekens, S.P., Vlamakis, H., Jaeger, M., Oosting, M., Franosa, E.A. Linking the Human Gut Microbiome to Inflammatory Cytokine Production Capacity. *Cell.* **167(4)**, 1125-1136.e8 (2016)

49.Horst, R., Jaeger, M., Smeekens, S.P., Oosting, M., Swertz, M.A., Kumar, V., *et al.* Host and Environmental Factors Influencing Individual Human Cytokine Responses. Cell. **167(4)**, 1111-1124.e13 (2016).

50.Sartor, R.B. Mechanisms of disease: pathogenesis of Crohn's disease and ulcerative colitis. *Nat Clin Pract Gastroenterol Hepatol.* **3(7)**, 390-407 (2006).

51.Lepage, P., Häsler, R., Spehlmann, M.E., Rehman, A., Zvirbliene, A., Begun, A., *et al.* Twin study indicates loss of interaction between microbiota and mucosa of patients with ulcerative colitis. *Gastroenterology.* **141(1)**, 227-36 (2011).

52.Nimmo, E.R., Prendergast, J.G., Aldhous, M.C., Kennedy, N.A., Henderson, P., Drummond, H.E., *et al.* Genome-wide methylation profiling in Crohn's disease identifies altered epigenetic regulation of key host defense mechanisms including the Th17 pathway. *Inflamm Bowel Dis.* **18(5)**, 889-99 (2012).

53.Liu, A., La Cava, A. Epigenetic dysregulation in systemic lupus erythematosus. *Autoimmunity.* **47(4)**, 215-9 (2014).

54.Costa-Reis, P., Sullivan, K.E. Genetics and epigenetics of systemic lupus erythematosus. *Curr Rheumatol Rep.* **15(9)**, 369 (2013).

55.Okano, M., Bell, D. W., Haber, D. A., Li, E. DNA methyltransferases Dnmt3a and Dnmt3b are essential for de novo methylation and mammalian development. *Cell.* **99,** 247–57 (1999).

56.Esteller, M. Epigenetic gene silencing in cancer: the DNA hypermethylome. *Hum Mol Genet*. **16**, R50–9 (2007).

57.Portela, A., Esteller, M. Epigenetic modifications and human disease. *Nat Biotechnol.* **28**, 1057–1068 (2010).

58.Kohli, R.M., Zhang, Y. TET enzymes, TDG and the dynamics of DNA demethylation. *Nature.* **502,** 472–9 (2013).

59.Zelic, R., Fiano, V., Grasso, C., Zugna, D., Pettersson, A., Gillio-Tos, A., *et al.* Global DNA hypomethylation in prostate cancer development and progression: a systematic review. *Prostate Cancer Prostatic Dis.* **18(1),** 1-12 (2015).

60.Van Dijk, S.J., Molloy, P.L., Varinli, H., Morrison, J.L., Muhlhausler, B.S. Epigenetics and human obesity. *Int J Obes (Lond).* **39**, 85–97 (2015).

61.Kuratomi, G., Iwamoto, K., Bundo, M., Kusumi, I., Kato, N., Iwata, N., *et al.* Aberrant DNA methylation associated with bipolar disorder identified from discordant monozygotic twins. *Mol Psychiatry.* **13(4)**, 429–41 (2008).

62.De Jager, P.L., Srivastava, G., Lunnon, K., Burgess, J., Schalkwyk, L.C., Yu, L., *et al.* Alzheimer's disease: early alterations in brain DNA methylation at ANK1, BIN1, RHBDF2 and other loci. *Nat Neurosci.* **17(9)**, 1156–63 (2014).

63.Lin, S.Y., Hsieh, S.C., Lin, Y.C., Lee, C.N., Tsai, M.H., Lai, L.C., *et al.* A whole genome methylation analysis of systemic lupus erythematosus: hypomethylation of the IL10 and IL1R2 promoters is associated with disease activity. *Genes Immun.* **13(3)**, 214–20 (2012).

64.Kraiczy, J., Nayak, K., Ross, A., Raine, T., Mak, T.N., Gasparetto, M., *et al.* Assessing DNA methylation in the developing human intestinal epithelium: potential link to inflammatory bowel disease. *Mucosal Immunol.* **9(3)**, 647-58 (2016).

65.Howell, K.J., Kraiczy, J., Nayak, K.M., Gasparetto, M., Ross, A., Lee, C., *et al.* DNA methylation and transcription patterns in intestinal epithelial cells from pediatric patients with inflammatory bowel disease differentiate disease subtypes and associate with outcome. *Gastroenterology.* **154(3),** 585-98 (2018).

66.Youngblood, B., Hale, J.S., Kissick, H.T., Ahn, E., Xu, X., Wieland, A., Araki, K. Effector CD8 T cells dedifferentiate into long-lived memory cells. *Nature.* **552(7685)**, 404-409 (2017).

67.Lee, J.C., Lyons, P.A., McKinney, E.F., Sowerby, J.M., Carr, E.J., Bredin, F., et al. Gene expression profiling of CD8+ T cells predicts prognosis in patients with Crohn disease and ulcerative colitis. *The Journal of Clinical Investigation.* **121(10),** 4170-9 (2011).

68.Golubovskaya, V., Wu, L. Different Subsets of T Cells, Memory, Effector Functions, and CAR-T Immunotherapy. Cancers. 8(36), 1-12 (2016).

69.Muller, S., Lory, J., Corazza, N., Griffiths, G.M., Z'graggen, K., Mazzucchelli, L., et al. Activated CD4+ and CD8+ cytotoxic cells are present in increased numbers in the intestinal mucosa from patients with active inflammatory bowel disease. Am J Pathol. **152(1)**, 261–268 (1998).

70.Probert, C.S., Chott, A., Saubermann, L.J., Stevens, A.C., Balk, S.P., Blumberg, R.S. Prevalence of an ulcerative colitis-associated CD8+ T cell receptor beta-chain CDR3 region motif and its association with disease activity. J Clin Immunol. **21(2)**, 126–134 (2001).

71.Hegazy AN, West NR, Stubbington M JT, Wendt E, Suijker K IM, Datsi A, et al. Circulating and tissue-resident CD4+ T cells with reactivity to intestinal microbiota are abundant in healthy individuals and function is altered during inflammation. Gastroenterology. **153(5)**, 1320-37 (2017).

72.Kontoyiannis D, Boulougouris G, Manoloukos M, Armaka M, Apostolaki M, Pizarro T, et al. Genetic dissection of the cellular pathways and signaling mechanisms in modeled tumor necrosis factor-induced Crohn'slike inflammatory bowel disease. J Exp Med. **196(12)**, 1563–74 (2002).

73.Nancey, S., Holvoet, S., Graber, I., Joubert, G., Philippe, D., Martin, S. et al. CD8+ cytotoxic T cells induce relapsing colitis in normal mice. Gastroenterology. **131(2)**, 485–496 (2006).

74. McKinney, E.F., Lyons, P.A., Carr, E.J., Hollis, J.L., Jayne, D.R., Willcocks L.C., et al. A CD8+ T cell transcription signature predicts prognosis in autoimmune disease. *Nat Med.* **16(5),** 586–591 (2010).

75. Turner, D., Levine, A., Escher, J.C., Griffiths, A.M., Russell, R.K., Dignass, A., et al. European Crohn's and Colitis Organization; European Society for Paediatric Gastroenterology, Hepatology, and Nutrition. Management of Paediatric Ulcerative Colitis: Joint ECCO and ESPGHAN Evidence-based Consensus Guidelines. *J Pediatr Gastroenterol Nutr.* **55(3),** 340-61 (2012).

76. Aomatsu, T., Imaeda, H., Matsumoto, K., Kimura, E., Yoden, A., Tamai, H., *et al.* Faecalchitinase 3-like-1: a novel biomarker of disease activity in paediatric inflammatory bowel disease. *Aliment Pharmacol Ther.* **34(8)**, 941-8 (2011).

77. Aomatsu, T., Yoden, A., Matsumoto, K., Kimura, E., Inoue, K., Andoh, A., *et al.* Fecal calprotectin is a useful marker for disease activity in pediatric patients with inflammatory bowel disease. *Dig Dis Sci.* **56(8)**, 2372-7 (2011).

78. Valette, P.J., Rioux, M., Pilleul, F., Saurin, J.C., Fouque, P., Henry, L. Ultrasonography of chronic inflammatory bowel diseases. *Eur Radiol.* **11(10),** 1859-66 (2001).

79. Thomson, M., Rao, P., Berger, L., Rawat, D. Graded compression and power Doppler ultrasonography versus endoscopy to assess paediatric Crohn disease activity pre- and post-treatment. *J Pediatr Gastroenterol Nutr.* **54(3),** 404-8 (2012).

80. Giles, E., Barclay, A.R., Chippington, S., Wilson, D.C. Systematic review: MRI enterography for assessment of small bowel involvement in paediatric Crohn's disease. *Aliment Pharmacol Ther*. **37(12),** 1121-31 (2013).

81. Sanka, S., Gomez, A., Set, P., Rimareva, N., Davies, R.J., Rolfe, P., *et al.* Use of small bowel MRI enteroclysis in the management of paediatric IBD. *J Crohn`s Colitis.* **6(5),** 550-6 (2012).

82. Feakins, R.M. Ulcerative colitis or Crohn's disease? Pitfalls and problems. *Histopathology.* **64(3)**, 317-35 (2014).

83. D'Haens, G., Baert, F., Caenepeel, P., Vergauwe, P., Tuynman, H., De Vos, M. North-Holland Gut Club. Early combined immunosuppression or conventional management in patients with newly diagnosed Crohn's disease: an open randomised trial. *Lancet.* **371(9613),** 660–667 (2008).

84.D' Haens, G.R. Top-down therapy for IBD: rationale and requisite evidence. *Nat Rev Gastroenterol Hepatol.* **7(2)**, 86–92 (2010).

85.Rogler, G. Top-down or step-up treatment in Crohn's disease? *Dig Dis.* **31(1),** 83-90 (2013).

86.Keane, J., Gershon, S., Wise, R.P., Mirabile-Levens, E., Kasznica, J., Schwieterman, W.D., *et al.* Tuberculosis associated with infliximab, a tumor necrosis factor alpha-neutralizing agent. *N Engl J Med.* **345(15)**, 1098–1104 (2001).

87.Fromont, A., De Seze, J., Fleury, M.C., Maillefert, J.F., Moreau, T. Inflammatory demyelinating events following treatment with anti-tumor necrosis factor. *Cytokine.* **45(2),** 55–57 (2009).

88.Siegel, C.A., Marden, S.M., Persing, S.M., Larson, R.J., Sands, B.E. Risk of lymphoma associated with combination anti-tumor necrosis factor and immunomodulator therapy for the treatment of Crohn's disease: a meta-analysis. *Clin Gastroenterol Hepatol*. **7(8),** 874–881 (2009).

89.Aloi, M., Nuti, F., Stronati, L., Cucchiara, S. Advances in the medical management of paediatric IBD. Nat Rev Gastroenterol Hepatol. 11(2), 99-108 (2014).

90.Alhagamhmad, M.H., Day, A.S., Lemberg, D.A., Leach, ST. An update of the role of nutritional therapy in the management of Crohn's disease. *J Gastroenterol.* **47(8),** 872-82 (2012).

91.Shamir, R. Nutritional aspects in inflammatory bowel disease. *J Pediatr Gastroenterol Nutr.* **48,** S86-S88 (2009).

92.Berni Canani, R., Terrin, G., Borrelli, O., Romano, M.T., Manguso, F., Coruzzo, A., *et al.* Short- and long-term therapeutic efficacy of nutritional therapy and corticosteroids in paediatric Crohn's disease. *Dig Liver Dis.* **38(6)**, 381-7 (2006).

93.Day, A.S., Whitten, K.E., Sidler, M., Lemberg, D.A. Systematic review: nutritional therapy in paediatric Crohn's disease. *Aliment Pharmacol Ther.* **27(4),** 293-307 (2008).

94.Soo, J., Bushra, A.M., Turner, J.M., Persad, R., Wine, E., Siminosky, K., *et al.* Use of Exclusive Enteral Nutrition Is Just as Effective as Corticosteroids in Newly Diagnosed Pediatric Crohn's Disease. *Dig Dis Sci.* **58(12)**, 3584-91 (2013).

95.Whitten, K.E., Leach, S.T., Bohane, T.D., Woodhead, H.J., Day, A.S. Effect of exclusive enteral nutrition on bone turnover in children with Crohn's disease. *J Gastroenterol.* **45(4),** 399-405 (2010).

96.Gupta, K., Noble, A., Kachelries, K.E., Albenberg, L., Kelsen, J.R., Grossman, A.B., *et al.* A Novel Enteral Nutrition Protocol for the Treatment of Pediatric Crohn's Disease. *Inflamm Bowel Dis.* **19,** 1374-78 (2013).

97.Roberts, R.L., Barclay, M.L. Update on thiopurine pharmacogenetics in inflammatory bowel disease. *Pharmacogenomics.* **16,** 891-903. (2015)

98.Chande, N., Patton, P.H., Tsoulis, D.J., Thomas, B.S., MacDonald, J.K. Azathioprine or 6-mercaptopurine for maintenance of remission in Crohn's disease. *Cochrane Database Syst Rev.* **10,** CD000067 (2015).

99.Gordon, M., Taylor, K., Akobeng, A.K., Thomas, A.G. Azathioprine and 6-mercaptopurine for maintenance of surgically-induced remission in Crohn's disease. *Cochrane Database Syst Rev.* **8,** CD010233 (2014).

100.Benmassaoud, A., Xie, X., AlYafi, M., Theoret, Y., Bitton, A., Afif, W., *et al.* Thiopurines in the Management of Crohn's Disease: Safety and Efficacy Profile in Patients with Normal TPMT Activity-A Retrospective Study. *Can J Gastroenterol Hepatol*. **2016,** 1034834 (2016).

101.McDonald, J.W., Wang, Y., Tsoulis, D.J., MacDonald, J.K., Feagan, B.G. Methotrexate for induction of remission in refractory Crohn's disease. *Cochrane Database Syst Rev*. **8,** CD003459 (2014).

102.Patel, V., Wang, Y., MacDonald, J.K., McDonald, J.W., Chande, N. Methotrexate for maintenance of remission in Crohn's disease. *Cochrane Database Syst Rev.* **8,** CD006884 (2014).

103.Kammermeier, J., Morris, M.A., Garrick, V., Furman, M., Rodrigues, A., Russell, R.K. BSPGHAN IBD Working Group. Management of Crohn's disease. *Arch Dis Child.* **101,** 475-480 (2016).

104.Sandborn, W.J., Feagan, B.G., Rutgeerts, P., Hanauer, S., Colombel, J-F, Sands, B.E., *et al.* GEMINI 2 Study Group. Vedolizumab as Induction and Maintenance Therapy for Crohn's Disease. *N Engl J Med.* **369,** 711-721 (2013).

105.Singh, N., Rabizadeh, S., Jossen, J., Pittman, N., Check, M., Hashemi, G. *et al.* Multi-Center Experience of Vedolizumab Effectiveness in Pediatric Inflammatory Bowel Disease. *Inflamm Bowel Dis*. **22,** 2121-26 (2016).

106.Amiot, A., Peyrin-Biroulet, L. Current, new and future biological agents on the horizon for the treatment of inflammatory bowel diseases. *Therap Adv Gastroenterol.* **8(2),** 66-82 (2015).

107.Sharma, S., Eckert, D., Hyams, J.S., Mensing, S., Thakkar, R.B., Robinson, A.M., *et al.* Pharmacokinetics and exposure-efficacy relationship of adalimumab in pediatric patients with moderate to severe Crohn's disease: results from a randomized, multicenter, phase-3 study. *Inflamm Bowel Dis.* **21,** 783-792 (2015).

108.Russell, R.K., Wilson, M.L., Loganathan, S., Bourke, B., Kiparissi, F., Mahdi, G., *et al.* A British Society of Paediatric Gastroenterology, Hepatology and Nutrition survey of the effectiveness and safety of adalimumab in children with inflammatory bowel disease. *Aliment Pharmacol Ther.* **33(8),** 946-53 (2011).

109.Hyams, J., Crandall, W., Kugathasan, S., Griffiths, A., Olson, A., Johanns, J., *et al.* REACH Study Group. Induction and maintenance infliximab therapy for the treatment of moderate-to-severe Crohn's disease in children. *Gastroenterology*. **132,** 863-873 (2007).

110.Ruemmele, F.M., Lachaux, A., Cézard, J.P., Morali, A., Maurage, C., Giniès, J.L., *et al.* Groupe Francophone d'Hépatologie, Gastroentérologie et Nutrition Pédiatrique. Efficacy of infliximab in pediatric Crohn's disease: a randomized multicenter open-label trial comparing scheduled to on demand maintenance therapy. *Inflamm Bowel Dis.* **15,** 388-394 (2009).

111.Dziechciarz, P., Horvath, A., Kierkuś, J. Efficacy and Safety of Adalimumab for Paediatric Crohn's Disease: A Systematic Review. *J Crohns Colitis.* **10,** 1237-44 (2016).

112.Papamichael, K., Van Stappen, T., Jairath, V., Gecse, K., Khanna, R., D' Haens, G. Review article: pharmacological aspects of anti-TNF biosimilars in inflammatory bowel diseases. *Aliment Pharmacol Ther.* **42,** 1158-69 (2015).

113.Hyams, J.S., Griffiths, A., Markowitz, J., Baldassano, R.N., Faubion, W.A. Jr, Colletti, R.B., *et al.* Safety and efficacy of adalimumab for moderate to severe Crohn's disease in children. *Gastroenterology.* **143,** 365-374 (2012).

114.Puthoor, P.R., de Zoeten, E.F. Pediatric Ulcerative Colitis: The Therapeutic Road to Infliximab. *Biol Ther.* **3,** 1-14 (2013).

115.Cleynen, I., Boucher, G., Jostins, L., Schumm, L.P., Zeissig, S., Ahmad, T., *et al.* International Inflammatory Bowel Disease Genetics Consortium. Inherited determinants of Crohn's disease and ulcerative colitis phenotypes: a genetic association study. *Lancet.* **387(10014),** 156-67 (2016).

116.Pfefferkorn, M.D., Marshalleck, F.E., Saeed, S.A., Slpawski, J.B., Lindeln, B.C., Weston, B.F. NASPGHAN clinical report on the evaluation and treatment of pediatric patients with internal penetrating Crohn's Disease: intraabdominal abscess with and without fistula. *J Pediatr Gastroenterol Nutr*. **57 (3),** 394-400 (2013).

117. Rubio, A., Pigneur, B., Garnier-Lengliné, H., Talbotec, C., Schmitz, J., Canioni, D., et al. The efficacy of exclusive nutritional therapy in paediatric Crohn's disease, comparing fractionated oral vs. continuous enteral feeding. *Aliment Pharmacol Ther.* **33(12),** 1332-9 (2011).

118.Heuschkel, R. Enteral nutrition should be used to induce remission in childhood Crohn's disease. *Dig Dis.* **27(3),** 297-305 (2009).

119.Vasseur, F., Gower-Rousseau, C., Vernier-Massouille, G., Dupas, J.L., Merle, V., Merlin, B., *et al.* Nutritional Status and Growth in Pediatric Crohn's Disease: A Population-Based Study. *Am J Gastroenterol*. **105,** 1893-900 (2010).

120.Gerasimidis, K., McGrogan, P., Edwards, C.A. The aetiology and impact of malnutrition in paediatric inflammatory bowel disease. *J Hum Nutr Diet.* **24(4),** 313-26 (2011).

121.Xavier, R.J., Podolsky, D.K. Unravelling the pathogenesis of inflammatory bowel disease. *Nature.* **448(7152),** 427–34 (2007).

122.Powrie, F. T cells in inflammatory bowel disease: protective and pathogenic roles. *Immunity*. **3(2),** 171–174 (1995).

123.Vernier-Massouille, G., Balde, M., Salleron, J., Turck, D., Dupas, J.L., Mouterde, O., *et al.* Natural history of pediatric Crohn's disease: a population-based cohort study. *Gastroenterology.* **135,** 1106-13 (2008).

124.Van Assche, G., Vermeire, S., Rutgeerts, P. The potential for disease modification in Crohn's disease. *Nat Rev Gastroenterol Hepatol.* **7(2),** 79-85 (2010).

125.Sninsky, C.A. Altering the natural history of Crohn's disease? *Inflamm Bowel Dis.* **7,** S34-9 (2001).

126.Kovács, J., Nagy, A., Szabó, A., Lorincz, M. To grow up with Crohn's disease. *Orv Hetil.* **152(14),** 546-54 (2011).

127.Vermeire, S., van Assche, G., Rutgeerts, P. Review article: Altering the natural history of Crohn's disease-evidence for and against current therapies. *Aliment Pharmacol Ther.* **25(1),** 3-12 (2007).

128.Gower-Rousseau, C., Dauchet, L., Vernier-Massouille, G., Tilloy, E., Brazier, F., Merle, V., *et al.* The natural history of pediatric ulcerative colitis: a population-based cohort study. *Am J Gastroenterol.* **104(8),** 2080-8 (2009).

129.Ricart, E., García-Bosch, O., Ordás, I., Panés, J. Are we giving biologics too late? The case for early versus late use. *World J Gastroenterol.* **14(36),** 5523-7 (2008).

130.Hyams, J.S. (2008). Natural history of pediatric ulcerative colitis. In P. Mamula, J.E. Markowitz, R.N. Baldassano (Eds. Springer Publ), *Pediatric Inflammatory Bowel Diseases*. (pp. 75-79). New York, NY.

131.Falaiye, T.O., Mitchell, K.R., Lu, Z., Saville, B.R., Horst, S.N., Moulton, D.E., *et al.* Outcome Following Infliximab Therapy for Pediatric Patients Hospitalized With Refractory Colitis-Predominant Inflammatory Bowel Disease. *J Pediatr Gastroenterol Nutr.* **58(2),** 213-9 (2014).

132.Peyrin-Biroulet, L., Sandborn, W., Sands, B.E., Reinisch, W., Bemelman, W., Bryant, R.V., *et al*. Selecting Therapeutic Targets in Inflammatory Bowel Disease (STRIDE): Determining Therapeutic Goals for Treat-to-Target. *Am J Gastroenterol*. **110(9),** 1324-38 (2015).

133.Siegel, C.A., Whitman, C.B., Spiegel, B.M.R., Feagan, B., Sands, B., Loftus, E.V. Jr, *et al.* Development of an index to define overall disease severity in IBD. *Gut.* **67(2),** 244-54 (2018).

134.Lichtenstein, G.R. Emerging prognostic markers to determine Crohn's disease natural history and improve management strategies: a review of recent literature. *Gastroenterol Hepatol*. **6(2),** 99-107 (2010).

135.Siegel, C.A., Siegel, L.S., Hyams, J.S., Kugathasan, S., Markowitz, J., Rosh, J.R., *et al.* Real-time tool to display the predicted disease course and treatment response for children with Crohn's disease. *Inflamm Bowel Dis.* **17(1),** 30-8 (2011).

136.Florholmen, J., Fries, W. Candidate mucosal and surrogate biomarkers of inflammatory bowel disease in the era of new technology. *Scand J Gastroenterol.* **46(12),** 1407-17 (2011).

137.Cohen-Dolev, N., Sladek, M., Hussey, S., Turner, D., Veres, G., Koletzko, S., *et al.* Differences in Outcomes Over Time With Exclusive Enteral Nutrition Compared With Steroids in Children With Mild to Moderate Crohn's Disease: Results From the GROWTH CD Study. *J Crohns Colitis.* **12(3),** 306-312 (2018).

138.Allez, M., Lémann, M. Role of endoscopy in predicting the disease course in inflammatory bowel disease. *World J Gastroenterol.* **16(21),** 2626- 32 (2010).

139.Buning, C., Genschel, J, Buhner, S., Kruger, S., Kling, K., Dignass, A., *et al.* Mutations in the NOD2/CARD15 gene in Crohn's disease are associated with ileocecal resection and are a risk factor for reoperation. *Aliment Pharmacol Ther.* **19(10),** 1073–78 (2004).

140.Ahmad, T., Armuzzi, A., Neville, M., Bunce, M., Ling, K.L., Welsh, K.I., *et al.* The contribution of human leucocyte antigen complex genes to disease phenotype in ulcerative colitis. *Tissue Antigens*. **62(6),** 527–535. (2003).

141.Haritunians, T., Taylor, K.D., Targan, S.R., Dubinsky, M., Ippoliti, A., Kwon, S., *et al.* Genetic predictors of medically refractory ulcerative colitis. *Inflamm Bowel Dis*. **16(11),** 1830-40 (2010).

142.Seow, C.H., Stempak, J.M., Xu, W., Lan, H., Griffiths, A.M., Greenberg, G.R., *et al.* Novel anti-glycan antibodies related to inflammatory bowel disease diagnosis and phenotype. Am J Gastroenterol. **104(6),** 1426–34 (2009).

143.Ferrante, M., Henckaerts, L., Joossens, M., Pierik, M., Joossens, S., Dotan, N., *et al.* New serological markers in inflammatory bowel disease are associated with complicated disease behaviour. *Gut.* **56(10),** 1394–1403 (2007).

144.Dubinsky, M.C., Kugathasan, S., Mei, L., Picornell, Y., Nebel, J., Wrobel, I., *et al.* Western Regional Pediatric IBD Research Alliance; Pediatric IBD Collaborative Research Group; Wisconsin Pediatric IBD Alliance. Increased immune reactivity predicts aggressive complicating Crohn's disease in children. *Clin Gastroenterol Hepatol.* **6(10),** 1105-11 (2008).

145.Lichtenstein, G.R., Targan, S.R., Dubinsky, M.C., Rotter, J.I., Barken, D.M., Princen, F., *et al.* Combination of genetic and quantitative serological immune markers are associated with complicated Crohn's disease behavior. Inflamm Bowel Dis. **17(12),** 2488-96 (2011).

146.Hagiwara, S.I., Okayasu, I., Fujiwara, M., Matsuura, M., Ohnishi, H., Ito, S., *et al.* Prostaglandin E-major Urinary Metabolite as a Biomarker for Paediatric Ulcerative Colitis Activity. *J Pediatr Gastroenterol Nutr.* **64(6),** 955-61 (2017).

147.Bessissow, T., Lemmens, B., Ferrante, M., Bisschops, R., Van Steen, K., Geboes, K., *et al.* Prognostic value of serologic and histologic markers on clinical relapse in ulcerative colitis patients with mucosal healing. *Am J Gastroenterol.* **107(11),** 1684-92 (2012).

148.Schechter, A., Griffiths, C., Gana, J.C., Shaoul, R., Shamir, R., Shteyer, E., *et al.* Early endoscopic, laboratory and clinical predictors of poor disease course in paediatric ulcerative colitis. *Gut.* **64(4),** 580-8 (2015).

149.Hyams, J.S., Davis, S., Mack, D.R., Boyle, B., Griffiths, A.M., LeLeiko, N.S., *et al.* Factors associated with early outcomes following standardized therapy in children with ulcerative colitis (PROTECT): a multiple inception cohort study. *Lancet Gastroenterol Hepatol.* **2(12),** 855-868 (2017).

150.Gasparetto, M., Wong-Spracklen, V., Torrente, F., Howell, K., Brennan, M., Noble-Jamieson, G., *et al.* Early Treatment Response Predicts Outcome in Paediatric Ulcerative Colitis. *J Pediatr Gastroenterol Nutr*. **67(2),** 217-220 (2018).

151.Wenger, S., Nikolaus, S., Howaldt, S., Bokemeyer, B., Sturm, A., Preiss, J.C., *et al.* Predictors for subsequent need for immunosuppressive therapy in early Crohn's disease. *J Crohns Colitis*. **6(1),** 21-8 (2012).

152.Beaugerie, L., Seksik, P., Nion-Larmurier, I., Gendre, J.P., Cosnes, J. Predictors of Crohn’s disease. *Gastroenterology*. **130(3),** 650–56 (2006).

153.Loly, C., Belaiche, J., Louis, E. Predictors of severe Crohn’s disease. *Scand J Gastroenterol.* **43(8),** 948–954 (2008).

154.Lasson, A., Simren, M., Stotzer, P.O., Isaksson, S., Ohman, L., Strid, H. Fecal calprotectin levels pfound a role for faecal calprotectinredict the clinical course in patients with new onset of ulcerative colitis. *Inflamm Bowel Dis.* **19(3),** 576-81 (2013).

155.McKinney, E.F., Lee, J.C., Jayne, D.R., Lyons, P.A., Smith, K.G. T-cell exhaustion, co-stimulation and clinical outcome in autoimmunity and infection. *Nature*. **523(7562),** 612-6 (2015).

156.Zilbauer, M., Rayner, T.F., Clark, C., Coffey, A.J., Joyce, C.J., Palta, P., *et al.* Genome-wide methylation analyses of primary human leukocyte subsets identifies functionally important cell-type specific hypomethylated regions. *Blood.* **122(25),** e52-60 (2013).

157.Monti, S., Tamayo, P., Mesirov, J., Golub, T. Consensus Clustering: A Resampling-Based Method for Class Discovery and Visualization of Gene Expression Microarray Data. *Machine Learning*. **52,** 91-118 (2003).

158. https://cran.r-project.org/web/packages/sigclust

159.Langfelder, P., Horvath, S. WGCNA: an R package for weighted correlation network analysis. *BMC Bioinformatics.* **9,** 559 (2008).

160.Zhang, B., Horvath, S. A General Framework for Weighted Gene Co-Expression Network Analysis. *Stat Appl Genet Mol Biol.* **4,** Article 17 (2005).

161.Feil, R., Fraga, M. F. Epigenetics and the environment: emerging patterns and implications. *Nat Rev Genet.* **13**, 97–109 (2011).

162.Tapp, H. S., Commane, D.M., Bradburn, D.M., Arasaradnam, R., Mathers, J.C., Johnson, I.T., et al. Nutritional factors and gender influence age-related DNA methylation in the human rectal mucosa. *Aging Cell*. **12**, 148–55 (2013).

163.Cedar, H. & Bergman, Y. Programming of DNA methylation patterns. *Annu Rev Biochem*. **81**, 97–117 (2012).

164.Bocker, M. T., Hellwig, I., Breiling, A., Eckstein, V., Ho, A.D., Lyko, F. Genome-wide promoter DNA methylation dynamics of human hematopoietic progenitor cells during differentiation and aging. *Blood*. **117**, e182-9 (2011).

165.Nardone, S., Sams, D.S., Zito, A., Reuveni, E., Elliott, E. Dysregulation of Cortical Neuron DNA Methylation Profile in Autism Spectrum Disorder. *Cereb Cortex.* **1; 27(12),** 5739-5754 (2017).

166.Mamdani, H., Ahmed, S., Armstrong, S., Mok, T., Jalal, S.I. Blood-based tumor biomarkers in lung cancer for detection and treatment. *Transl Lung Cancer Res.* **6(6)**, 648-660 (2017).

167.Conrad, M.A., Stein, R.E., Maxwell, E.C., Albenberg, L., Baldassano, R.N., Dawany, N., et al. Vedolizumab Therapy in Severe Pediatric Inflammatory Bowel Disease. Inflamm Bowel Dis. **22**, 2425–2431. (2016).

168.West, N.R., Hegazy, A.N., Owens, B.M.J., Bullers, S.J., Linggi, B., Buonocore, S., *et al.* Oxford IBD Cohort Investigators. Oncostatin M drives intestinal inflammation and predicts esponse to tumor necrosis factor-neutralizing therapy in patients with inflammatory bowel disease. Nat Med. **23(5)**, 579-589 (2017).

169.Anne Segonds-Pichon. Introduction to Statistics with R. *Babraham Bioinformatics.* (2015).

Appendix 1. Definition, measurement units and normal values of the main clinical items collected

- IBD diagnosis: The sub-classification of the IBD-U as CD-like or UC-like was based on the combination of disease localisation (e.g. the involvement of any tract of the small bowel would be more consistent with CD, with the exception of backwash ilieitis in patients with UC) and of the histological findings [2];
- Diarrhoea at diagnosis: defined by the World Health Organisation as having three or more loose or liquid stools per day; diarrhoea is defined as chronic when symptoms last more than 14 days;
- Stool consistency at diagnosis: scores 1 to 7, as defined by the Bristol Stool Scale;
- Moderate-severe abdominal pain, defined as > 5 on VAS Scale;
- Weight loss at diagnosis: defined as an involuntary loss ≥ 10% of the weight reported before the symptom onset;
- Fever at diagnosis: defined as T> 37.5 ^C with no detection of infections;
- Iron deficiency anaemia at diagnosis: definition based on the combination of clinical signs and symptoms, RBC count, haematocrit, haemoglobin, MCV, reticulocytes, ferritin levels. Haemoglobin thresholds as defined by World Health Organisation: 11 g/dL for children < 5 years of age, 11.5 g/dL for children aging 5-10 years, 12 g/dL for children aging 12 – 15 years;
- Perianal disease at diagnosis (fissures, fistulae, abscesses) defined on the basis of clinical assessment ± pelvis MRI);
- Extraintestinal manifestations (EIMs) at diagnosis: joint pain, hepato-biliary disorders (diagnostic work-up based on clinical evidence of liver enlargment and/or jaundice, liver function tests, serology, imaging ± ERCP), pancreatitis (diagnostic work-up based on clinical assessment, measurement of pancreatic enzymes, imaging), skin manifestations (erythema nodosum, pyoderma gangrenosum), eye manifestation (uveitis, epi-scleritis);
- Mouth ulcers: considered when detected at diagnosis or during the recent months prior to diagnosis;
- Scores of IBD activity at diagnosis and at follow-up: Paediatric Crohn's Disease Activity Index (PCDAI) and Paediatric Ulcerative Colitis Activity Index (PUCAI) [34-35];
- Disease localisation at diagnosis and at follow-up: defined according to the Paris classification for IBD [13] (Appendix 6 on page 1208), on the basis of endoscopy, histology and small bowel MRI results;
- White Blood Cells (WBC) at diagnosis and at follow-up (x 10^3/mm3, n.v. ages 5 to 12 years: males 4.5-10.5, females 4.7-10.3; ages 12 to 16 years: males 4.5-10, females 4.8-10.1);
- Haemoglobin (Hb) at diagnosis and at follow-up (g/dL, n.v. ages 5 to 12 years: males 11-13.3, females 10.9-13.3; ages 12 to 16 years: males 11.5-14.8, females 11.2-13.6);

- Mean Corpuscolar Volume (MCV) at diagnosis and at follow-up (fL, n.v. boys: 78 – 98, girls: 78 – 102);
- Haematocrit (Htc) at diagnosis and at follow-up (%. n.v. ages 5-12 years: males 32.7-39.3, females 33-39.6; ages 12-18 years: males 34.8-43.9, females 34-40.7);
- Platelet count at diagnosis and at follow-up (x 10^3/mm3, n.v. ages 5 to 12 years: males 194-364, females 183-369; ages 12 to 18 years: males 165-332, females 185-335);
- C-reactive protein (CRP) at diagnosis and at follow-up (mg/L, n.v. < 6);
- Erythrocyte sedimentation rate (ESR) at diagnosis and at follow-up (mm/h, n.v. < 8 mm/h);
- Albumin at diagnosis and at follow-up (g/L, n.v. ages 5 to 6 years: 35-52; ages 7 to 9 years: 37-56; ages 9 to 19 years: 37-56);
- Faecal calprotectin at diagnosis and at follow-up (mcg/g, threshold for significance 300).

Appendix 2. Clinical Database used as a .csv file to align clinical data to gene expression data in the WGCNA.

Case Number	Gender	Diagnosis	Age at diagnosis	Family history of IBD	Z score for Weight at diagnosis
6.CEL	1	0	12	0	-0.817
10.CEL	1	1	15	0	-2.469
13.CEL	1	1	13	0	-0.441
16.CEL	0	0	13	1	-0.364
19.CEL	1	1	10	0	-1.255
21.CEL	0	0	14	0	-0.824
24.CEL	0	0	14	0	1.795
26.CEL	1	1	13	0	-1.71
28.CEL	0	0	14	0	1.208
30.CEL	1	0	12	0	0.7
34.CEL	0	1	13	0	0.729
40.CEL	1	0	14	1	-0.872
44.CEL	1	1	13	0	-1.254
46.CEL	0	0	11	0	1.367
47.CEL	1	0	13	0	-0.491
49.CEL	1	1	10	0	-0.239
50.CEL	1	1	8	1	0.45
51.CEL	1	1	13	0	-1.13
53.CEL	0	0	7	1	-0.372
57.CEL	1	0	12	0	0.066
58.CEL	0	1	13	0	0.935
59.CEL	0	1	8	0	-1.437
61.CEL	1	1	15	0	0.848
70.CEL	1	1	13	1	-0.029
72.CEL	1	1	7	0	-0.981
74.CEL	1	0	14	1	-0.757
76.CEL	1	1	14	0	0.328
77.CEL	0	1	14	0	-0.381
78.CEL	1	1	14	0	-0.53
80.CEL	0	0	14	0	-0.316
82.CEL	1	1	14	1	-0.427
83.CEL	1	0	13	1	0.779
84.CEL	1	1	17	0	-0.28

89.CEL	0	0	10	0	-0.234
90.CEL	1	1	9	1	-0.633
91.CEL	0	0	6	1	2.16
92.CEL	0	0	9	0	0.674
93.CEL	1	0	9	0	-0.16
95.CEL	1	1	6	0	-0.12
96.CEL	0	0	15	0	0.175
97.CEL	1	1	13	0	-1.91
98.CEL	0	1	15	0	-0.98
102.CEL	0	1	11	0	-0.37
104.CEL	1	1	15	0	-1.65
105.CEL	1	1	13	0	-2.09
106.CEL	1	1	11	0	-0.02
112.CEL	1	1	13	0	0.95
116.CEL	1	0	8	0	1
173.CEL	1	1	13	1	0.76
174.CEL	1	0	14	0	-0.56
193.CEL	1	1	14	1	0.4
199.CEL	1	1	13	0	-2.03
205.CEL	1	1	14	1	0.64
206.CEL	0	0	15	0	1.65
208.CEL	1	0	12	0	-0.27
209.CEL	0	1	13	1	-1
217.CEL	1	1	14	0	0.73
219.CEL	1	1	11	0	1.52
227.CEL	1	1	13	0	-2.33
232.CEL	0	1	15	0	-2.65
236.CEL	0	0	11	1	-0.21
246.CEL	1	1	13	1	-0.43
249.CEL	1	1	13	1	-1.49
251.CEL	0	0	11	0	1
270.CEL	1	1	12	0	-0.68
272.CEL	1	1	15	1	-1.66
273.CEL	0	1	9	0	2.27
277.CEL	1	1	11	1	-0.07
279.CEL	1	1	12	0	1.38
280.CEL	0	1	15	1	1.69
282.CEL	0	1	12	0	-0.76
289.CEL	1	1	10	0	0.39

290.CEL	0	1	15	0	-2.75
301.CEL	1	1	7	0	1.08
307.CEL	0	1	15	0	-0.26
310.CEL	1	0	11	0	0.88
318.CEL	0	1	10	0	-1.04
319.CEL	0	1	9	0	-1.12
320.CEL	1	1	11	0	-0.429
321.CEL	0	0	13	0	-0.69
323.CEL	1	0	15	1	-0.67
324.CEL	1	0	11	1	1.12
330.CEL	0	1	15	1	-0.85
335.CEL	0	1	14	1	-1.04
340.CEL	1	0	15	0	-0.73
344.CEL	1	0	15	0	0.69
348.CEL	0	1	11	0	-1.4
352.CEL	0	1	15	0	-0.24
354.CEL	1	1	15	0	-2.21
358.CEL	1	1	13	0	-1.79
359.CEL	1	1	13	0	-0.5
360.CEL	0	0	8	0	-1.36
366.CEL	1	0	12	1	1.03
370.CEL	0	0	14	1	-1.209
376.CEL	0	0	15	0	1.03
385.CEL	1	0	5	0	-3.08
387.CEL	1	0	14	0	2.01
392.CEL	0	0	15	0	0.68

Z score for Height at diagnosis	Abdominal pain at diagnosis	Diarrhoea at diagnosis	Mucus in stools at diagnosis	Per rectal bleeding at diagnosis	Weight loss at diagnosis
-1.155	1	1	0	0	1
0.988	1	1	0	0	1
1.368	1	1	0	1	1
0.26	0	1	1	1	1
-0.111	1	1	1	1	1
0.317	1	1	0	0	0
0.779	1	1	0	1	0
-1.572	0	1	0	1	1
0.316	1	1	1	1	0
0.7	1	1	1	1	0
0.617	1	1	0	1	0
0.357	1	0	0	1	1
-1.164	1	1	0	0	0
-0.437	1	0	0	1	0
0.465	1	1	0	1	0
1.234	1	1	0	0	1
0.3	1	0	0	1	0
-0.27	1	0	0	1	1
-0.864	1	1	0	1	0
0.615	1	1	0	1	0
1.464	0	1	0	1	0
-1.838	1	1	0	0	0
1.159	1	1	0	0	1
1.83	1	1	1	1	1
-1.485	0	0	0	0	1
-0.412	0	1	0	1	0
-0.334	1	0	0	1	0
0.351	1	1	1	0	0
0.646	1	1	1	1	0
-0.854	0	0	0	1	0
1.728	1	1	0	1	0
-1.141	0	1	0	1	0
0.381	1	0	0	1	1
-0.451	1	1	0	0	0
-1.726	1	1	0	1	0
2.306	1	1	1	1	0

1.009	1	1	1	1	0
-1.987	1	1	0	1	0
0.723	0	1	0	0	1
-0.369	1	1	0	1	1
-0.77	1	0	0	0	1
0.07	1	1	0	1	1
0.58	1	1	0	1	0
-0.2	1	1	0	1	1
-1.6	1	1	0	0	1
0.79	1	1	0	0	0
-0.82	1	0	0	1	0
1.56	1	1	0	1	0
0.25	1	0	0	0	0
-0.85	1	1	0	1	1
-0.15	1	1	0	1	0
-0.73	1	1	1	0	1
1.36	0	0	0	0	0
-0.17	0	1	0	1	0
-0.99	0	0	0	1	0
-0.77	1	1	0	1	0
1.07	1	1	0	1	1
1.32	1	1	1	0	0
-1.8	1	0	0	0	0
-0.75	0	1	1	1	1
-0.14	1	1	1	1	0
-0.03	1	1	1	1	0
0.13	1	1	1	1	1
0.48	1	1	0	1	0
0.18	1	1	0	0	0
-1.03	1	1	0	1	1
0.93	1	0	0	1	0
0.31	1	1	0	0	0
0.83	0	1	0	1	0
1.5	1	1	1	0	1
0.25	1	0	0	0	1
1.41	1	0	0	0	1
-2.24	1	1	1	0	1
-0.02	1	1	0	1	0
-0.02	1	1	0	0	1

1.43	1	1	0	1	0
0.49	1	1	0	1	1
0.2	1	0	0	0	1
0.568	1	1	0	0	1
-0.86	1	1	0	1	0
-0.03	1	1	0	1	0
0.93	1	1	1	1	0
0.36	1	0	0	1	1
-0.75	1	1	0	1	1
-0.1	0	1	0	1	0
0.69	1	1	1	1	0
-0.88	1	0	0	0	0
-0.14	1	0	1	1	0
-0.85	1	1	0	1	1
-0.81	1	1	0	1	1
-0.45	0	1	1	1	0
0.04	1	1	0	1	0
0.14	0	1	0	1	1
-0.168	1	1	0	1	0
1.28	1	0	0	1	1
-1.49	0	0	0	1	1
0.91	0	1	0	1	0
0.23	1	1	1	1	1

Nocturnal symptoms at diagnosis	Nausea / vomiting at diagnosis	Urgency / tenesmus at diagnosis	Lethargy at diagnosis	Iron deficiency anaemia at diagnosis	Mouth ulcers at diagnosis
0	0	1	1	0	0
0	0	0	1	1	1
0	0	0	0	0	1
0	0	0	0	1	0
0	0	0	0	1	0
1	0	0	0	0	0
1	0	0	0	0	1
0	0	0	0	0	1
0	0	0	0	0	0
1	1	1	0	0	0
0	0	1	0	1	1
1	0	1	0	0	0
1	0	1	1	0	0
0	0	0	0	0	0
0	0	0	0	0	0
0	0	0	0	0	0
0	0	0	1	0	0
0	1	0	0	0	1
0	0	0	0	0	0
1	0	1	0	0	0
0	0	0	0	0	0
0	1	1	1	0	1
0	1	0	1	0	0
0	0	0	0	0	0
0	0	0	0	0	0
0	0	1	0	0	0
0	0	1	0	0	0
1	0	0	1	0	0
0	0	0	0	0	0
0	0	0	0	0	0
1	0	0	0	0	0
0	0	0	0	0	0
0	0	0	1	1	1
1	0	0	1	0	0
0	0	0	0	0	0

0	0	1	0	0	0
0	0	0	0	0	0
1	0	0	0	0	0
1	0	0	1	0	0
0	0	0	0	0	0
0	0	0	0	0	0
1	0	1	0	0	0
0	0	0	1	0	0
0	0	0	0	0	0
0	0	1	1	0	0
0	0	0	0	0	0
0	0	0	0	1	0
1	0	0	0	1	0
1	1	0	0	0	0
0	0	0	0	0	0
0	0	0	1	0	0
0	1	0	0	0	0
0	1	1	0	0	0
0	0	0	1	1	0
0	0	0	0	0	0
0	1	0	1	0	0
0	0	0	0	0	0
0	0	1	1	0	0
0	1	0	1	0	0
0	1	1	1	0	1
0	0	0	1	0	0
0	0	0	1	1	0
1	0	1	0	0	0
0	0	1	0	1	0
0	0	0	1	0	1
1	0	0	1	1	0
0	0	0	0	0	1
1	1	0	1	0	0
0	0	0	1	0	1
0	1	0	0	0	0
1	0	0	1	0	0
0	0	0	1	0	0
1	1	1	1	1	0
1	0	1	0	0	0

0	0	0	0	0	0
0	1	0	0	0	0
0	0	0	0	0	0
0	1	0	1	1	0
0	0	0	1	1	0
0	0	0	0	0	0
0	0	1	0	0	0
1	0	1	0	0	0
0	1	1	0	1	0
0	1	0	1	0	0
1	0	1	0	0	0
0	0	0	0	0	0
0	0	0	0	0	1
0	0	0	1	1	0
0	1	0	1	1	0
1	0	0	1	1	0
0	0	0	0	0	0
0	0	0	1	1	0
1	0	1	0	0	0
0	0	1	0	0	0
0	0	0	0	0	0
0	0	1	0	1	0
0	0	1	0	0	0
0	0	0	0	1	0

Joint pain at diagnosis	Fever at diagnosis	Time onset to diagnosis	Perianal disease at diagnosis	Liver involvement at diagnosis	EIM at diagnosis
0	0	3	0	0	0
0	0	1	1	0	0
1	1	2	0	0	0
0	0	2	0	0	0
0	0	1	0	0	0
0	0	1	0	0	0
0	0	1	0	0	0
0	0	2	1	0	0
1	0	2	0	0	0
0	0	1	0	0	0
0	0	3	0	0	0
0	0	1	0	0	0
0	0	3	0	1	1
0	0	3	0	0	0
0	0	3	0	0	1
0	0	3	0	1	0
0	0	3	0	0	0
1	0	2	0	0	1
0	0	3	0	0	0
0	0	1	0	0	0
0	0	3	0	0	0
1	1	1	0	0	1
0	0	3	0	0	0
0	0	1	0	0	0
0	0	3	1	0	0
0	0	3	1	0	0
0	0	2	0	0	0
0	0	1	0	0	1
1	0	3	0	0	1
0	0	3	0	0	0
0	0	2	0	0	1
0	0	1	0	0	0
0	0	3	1	0	0
0	1	2	0	1	0
0	0	3	0	0	0

0	0	3	0	0	0
0	0	2	0	0	0
0	0	1	0	0	0
0	0	1	1	1	0
0	0	2	0	0	0
0	0	2	0	0	1
0	0	1	1	1	0
1	0	1	0	0	0
0	0	3	0	0	0
0	0	1	0	0	0
0	0	1	0	0	0
1	0	2	0	0	1
0	0	2	0	1	0
0	0	1	0	0	0
0	0	1	0	0	0
0	0	3	1	0	0
0	0	1	0	0	0
1	0	3	0	0	1
0	0	2	0	0	0
0	0	1	0	0	0
0	0	1	0	0	0
0	0	1	0	0	0
0	0	2	0	0	0
0	0	3	0	0	1
1	0	1	0	0	1
0	0	2	0	0	0
0	0	1	0	0	0
0	0	2	0	0	0
0	0	3	0	0	0
1	0	1	0	0	0
0	0	1	0	0	0
0	0	2	0	0	0
1	0	1	1	0	1
0	0	2	0	1	0
0	0	2	0	0	0
0	0	2	0	0	0
0	0	2	0	0	0
0	0	2	0	0	0
0	0	3	0	0	0

0	0	2	0	0	0
0	1	1	0	0	0
0	0	3	0	1	0
0	0	2	0	0	0
0	0	1	0	0	0
0	0	3	0	0	0
0	0	3	0	0	0
0	0	1	0	0	0
0	1	3	0	0	0
0	0	3	1	0	0
0	0	1	0	0	0
0	0	1	0	0	0
0	0	3	0	0	1
1	0	1	1	0	1
0	0	1	0	0	0
0	0	2	0	0	0
0	0	3	0	0	0
0	0	2	0	0	0
0	0	2	0	0	0
0	0	2	0	1	0
0	0	3	0	0	0
0	0	2	0	0	0
0	0	1	0	0	0
0	0	1	0	0	0

Growth deficiency at diagnosis	White Cell Count at diagnosis (x 10^3 / mm3)	Haematocrit at diagnosis (%)	Platelets at diagnosis (x 10^3 / mm3)	Ferritin at diagnosis (ug / L)	ESR at diagnosis (mm / h)
0	8.6	30.9	460	15	38
0	12.3	36.8	579	12.4	25
0	5.5	41.7	366	39.2	30
0	7.3	32.6	341	33.4	8
1	12.3	24.7	796	1.8	47
0	7.7	36.2	633	2.5	17
0	7.2	34.7	226	16.7	19
0	9.8	36.6	538	40.2	25
0	9.3	38	277	23.7	11
0	10.6	37.5	397	4.6	9
0	5.7	32.2	304	21.3	8
0	7.2	39.5	280	3.6	16
0	7.9	26.8	538	20	49
0	7.4	34.1	273	14	7
0	8.8	34.6	376	13.7	18
0	10.8	39.9	303	15	18
0	8.7	39	309	66.2	6
1	6.7	35.6	328	99.5	13
0	11.3	33.6	427	15	9
0	6.9	35.6	409	21	16
0	5.9	37.6	259	15	15
1	22.3	26.3	613	156.8	35
0	8.2	37.5	464	10	16
0	10.5	33.4	442	11.9	13
1	12.8	37.7	400	39	8
0	9	39	251	6.1	4
0	6.8	36.1	350	10.3	33
0	8.7	29.2	483	6.5	32
0	9	37.3	187	7.7	11
0	6.7	37.3	309	3.6	14
0	9.3	38.1	490	269.8	79
0	7.7	41.6	186	27.9	4
1	6	33.9	421	10	30
0	21.2	31.2	574	7	65

0	7.4	37	340	10	6
0	8.6	33	330	6.5	12
0	8.1	41.1	256	36.5	5
0	14.8	20.8	348	2.5	54
1	13.2	33.2	475	5.1	19
0	8.7	34.2	289	12.5	18
0	14.5	35.2	692	8.8	25
0	6	30	371	28.7	10
0	8.5	29	336	1	6
0	8	35.2	380	15	10
0	12.6	37.8	541	155.8	5
0	8.4	36.6	463	10.4	10
0	8.1	37.8	342	17.6	16
0	8.1	39.5	369	14.6	29
0	16.5	31.5	693	118.6	29
0	9.2	29	267	14.6	10
0	10.1	37.3	334	132.6	33
0	11.6	37.2	710	66	17
0	5.3	45	296	17	4
0	9.4	36.5	394	4.6	10
0	8.2	34.8	273	6	7
0	7.5	32.3	548	14	34
0	6	31.2	610	22	47
0	10.9	38.4	322	34.9	13
0	7.3	30.3	356	31.4	35
0	3.6	40.3	304	95	42
0	8.1	37	299	12.3	5
0	8	35.4	367	15	12
1	8.2	36.3	503	56.5	10
0	11.8	34	576	6.7	44
0	8.4	40.3	266	6.2	5
0	12.6	34.2	364	146.1	17
0	6.6	36.4	374	15	22
0	9.1	35.7	482	96	19
0	5.8	31.4	386	5.7	54
0	6.2	36.8	228	15	6
0	7.1	38.8	494	42.4	39
1	12.8	37.5	537	86	43
1	13.4	37	82	10.8	82

0	8.2	41	547	15	9
0	7.8	39.5	373	62.1	7
0	6.3	42.5	656	15	9
0	8.1	41.2	420	10.7	1
0	9.1	33	523	30.7	39
0	6.5	38.7	279	12.9	26
0	6.8	33.1	359	11.3	16
0	6.8	37.5	373	5.7	5
0	10.5	34	503	5.9	16
0	5.5	31.8	359	26.6	33
0	5.1	35.1	527	9.6	19
0	5.2	43.6	325	9	15
0	6.1	44.4	220	84.5	5
0	7.8	40.2	243	27.6	10
1	11.8	34.6	290	18	25
0	7.4	34.1	476	73.4	30
1	12.3	36	645	72.9	42
0	8	34.2	366	19	16
0	8.6	27.6	721	15	32
0	13	35	307	4.6	9
0	4.7	34.4	339	23.6	32
0	5.5	29.9	283	3.1	28
0	6.8	32	409	15	29
0	4.7	42.5	245	20.4	4
0	9	24.5	532	19.5	44

CRP at diagnosis (mg/L)	Albumin at diagnosis (g/L)	ALT at diagnosis (U/L)	GGT at diagnosis (U/L)	Disease activity at diagnosis (PCDAI/PUCAI)	Number of treatment escalations
1	39	27	24	22.5	1
71	27	14	60	42.5	1
3	36	46	21	30	0
1	33	19	20	30	3
22	21	15	26	55	3
6	33	17	21	40	0
7	41	41	58	45	1
31	30	17	16	35	3
2	41	18	21	35	3
30	31	18	31	55	1
30	28	24	14	37.7	2
4	34	16	21	45	2
64	25	25	60	50	5
2	40	21	25	35	3
3	43	40	29	30	3
3	41	257	147	25	0
4	41	19	11	20	2
56	19	10	23	40	3
5	36	23	18	35	1
1	37	15	19	45	0
1	44	10	10	12.5	0
101	27	16	11	47.5	4
49	30	27	40	30	0
23	27	12	7	37.5	1
1	31	12	7	17.5	0
1	45	15	18	22.5	2
18	37	11	9	20	1
41	26	9	14	42.5	2
12	36	13	9	25	0
1	40	9	7	17.5	0
150	35	10	13	27.5	0
4	39	15	20	20	1
53	29	16	13	40	0
128	30	28	24	52.5	3
1	30	12	6	30	4

3	38	21	14	45	1
4	46	19	14	30	1
1	35	8	9	45	1
5	34	27	197	35	3
8	38	9	9	30	3
14	29	10	10	27.5	2
20	27	15	10	37.5	3
4	41	15	27	32.5	3
34	41	15	10	30	3
48	32	8	11	35	2
21	36	10	11	25	0
19	31	18	7	25	1
4	35	54	28	50	1
40	40	8	42	15	2
4	37	10	8	20	0
23	36	19	54	25	3
23	32	11	10	25	0
2	39	15	15	15	1
4	39	18	15	30	1
4	38	15	7	20	2
33	27	9	10	40	1
30	35	9	13	35	1
20	34	20	30	35	2
79	26	8	14	30	1
84	26	5	11	32.5	1
4	43	21	12	15	1
7	41	13	12	30	3
12	29	11	34	45	4
4	32	11	9	25	1
17	39	14	8	27.5	1
101	24	8	16	37.5	3
15	38	17	10	17.5	0
8	30	24	18	35	4
4	37	66	129	45	0
4	46	15	17	25	1
37	39	11	12	35	2
22	33	10	8	32.5	2
74	38	17	15	35	1
4	38	31	20	15	0

4	42	12	18	25	0
4	35	12	10	55	3
4	35	14	16	55	2
29	27	10	36	32.5	3
11	30	16	15	35	1
6	39	10	12	50	0
8	34	13	12	40	0
6	37	17	7	60	4
4	35	11	12	35	3
18	19	8	8	37.5	4
12	45	18	17	50	0
4	44	22	34	50	2
4	39	17	12	15	0
8	32	42	26	22.5	2
28	30	40	48	35	2
74	31	8	17	35	1
10	36	11	14	20	2
10	37	15	11	45	1
4	38	19	10	50	0
4	39	19	31	45	1
4	38	15	7	40	1
5	36	13	8	45	1
4	43	26	12	40	0
3	37	9	18	65	1

Use of biologics	Surgical intervention	Steroid resistance / dependency	6 months steroid free remission	Number of relapses	Number of endoscopies
0	0	0	0	1	1
0	0	0	0	2	2
0	0	0	0	0	1
0	0	0	1	3	2
1	0	0	0	3	2
0	0	0	1	1	1
0	0	0	0	2	2
1	0	0	1	4	2
0	0	1	0	3	1
0	0	0	1	2	1
0	0	0	0	3	1
0	0	0	1	2	1
1	0	0	0	4	3
0	0	1	0	4	4
0	0	1	1	3	3
0	0	0	1	0	1
0	0	0	1	1	3
1	0	1	1	3	2
0	0	0	1	1	1
0	0	0	1	0	1
0	0	0	1	0	2
1	0	1	0	4	3
0	0	0	1	0	1
0	0	0	0	1	2
0	0	0	1	0	1
0	0	0	1	2	2
0	0	0	1	1	2
1	0	0	0	2	2
0	0	0	0	0	1
0	0	0	1	0	1
0	0	0	1	0	1
0	0	0	1	2	2
0	0	0	1	1	1
1	1	0	0	4	2
1	0	1	0	4	4
0	0	0	1	1	1

0	0	0	0	1	1
0	0	0	0	1	2
1	0	1	1	3	3
1	0	1	0	3	2
1	0	1	0	2	2
1	0	0	0	2	2
1	0	0	0	3	2
1	0	1	0	4	4
1	0	1	0	2	2
0	0	0	1	0	1
1	0	1	1	1	3
0	0	0	0	1	2
0	1	0	1	1	2
0	0	0	1	0	1
1	0	1	0	3	2
0	0	0	1	0	1
0	0	0	0	1	1
0	0	0	1	1	2
0	0	0	0	2	3
0	0	0	1	1	2
0	0	0	1	1	1
0	0	0	0	3	3
0	0	0	0	1	1
1	0	0	0	1	2
0	0	0	1	1	2
1	0	1	0	3	2
1	0	1	0	4	3
0	0	0	1	0	1
0	0	0	1	0	1
1	0	1	0	4	2
0	0	0	1	0	1
1	0	1	1	3	2
0	0	0	1	0	1
0	0	0	1	0	1
1	0	1	0	2	2
0	0	0	0	3	2
0	0	0	1	1	3
0	0	0	1	0	1
0	0	0	1	0	1

1	1	1	0	4	2
1	0	1	0	3	3
1	0	1	0	3	2
0	0	0	1	1	1
0	0	0	1	0	1
0	0	0	1	0	1
1	0	0	0	4	1
1	0	1	0	4	3
1	0	1	0	4	2
0	0	0	1	0	1
0	0	1	1	2	1
0	0	0	1	0	1
0	0	0	0	2	1
0	0	0	0	2	1
1	0	0	0	1	2
0	0	0	0	1	2
0	0	0	0	1	1
0	0	0	1	0	1
0	0	0	1	1	1
0	0	0	0	1	1
0	0	0	0	1	1
0	0	0	1	0	1
0	0	0	0	1	1

Number of unplanned inpatient days	Num of outpatient days	Severity Score	School attendance	Psychological support
0	11	2	1	1
0	13	1	1	1
0	9	0	1	0
5	15	4	1	1
10	15	6	0	1
0	9	0	1	1
0	16	2	1	1
0	23	5	1	1
0	11	4	0	0
0	17	1	1	0
0	13	1	1	0
0	6	3	1	0
7	24	6	0	1
0	22	4	0	1
0	15	2	1	0
0	10	0	1	0
0	17	1	0	0
3	15	5	0	1
0	5	0	1	0
0	7	0	1	0
0	9	0	1	0
12	24	6	0	0
0	13	0	1	0
0	18	0	1	0
0	12	1	1	0
1	7	1	1	0
1	9	0	1	0
0	13	3	1	0
0	6	0	1	0
0	4	0	1	0
0	5	0	1	0
0	6	0	1	0
0	6	1	1	0
8	15	10	0	1
	6	5	1	0

0	5	2	1	0
0	8	2	1	0
0	9	2	0	0
0	18	5	1	0
0	11	6	1	1
0	17	3	1	0
2	18	5	0	1
5	8	6	1	0
20	21	6	1	0
0	15	3	0	0
0	8	0	1	0
0	10	2	0	1
0	8	2	0	0
18	12	5	0	1
0	5	0	1	0
6	11	7	1	1
0	9	0	1	0
0	10	0	1	0
0	11	0	1	0
0	12	3	1	0
0	10	0	1	1
0	8	0	1	0
10	13	3	1	0
0	18	0	1	0
0	13	2	1	0
0	13	0	1	1
0	18	4	1	0
12	17	6	0	1
5	9	2	0	1
0	11	0	1	0
10	21	6	0	0
0	6	0	0	0
0	13	5	0	0
0	9	0	1	0
0	8	0	1	0
0	17	3	0	1
0	13	1	1	0
4	14	1	0	0
0	7	0	0	1

0	5	0	1	0
17	15	10	0	1
11	18	5	0	1
7	16	6	1	0
0	13	0	0	1
0	13	0	1	1
0	12	0	1	0
5	11	8	0	1
2	19	4	0	1
0	15	5	1	0
0	8	0	1	0
0	11	1	1	0
0	4	0	1	0
0	9	3	0	1
3	8	2	0	0
2	18	3	0	1
0	12	1	1	1
4	11	3	1	0
0	8	0	1	1
0	9	0	1	0
3	12	2	1	1
0	8	1	1	0
0	8	0	1	1
7	6	4	0	0

Appendix 2 Legend: 0= event never happened; 1= event has happened; Gender: 0=female, 1=male; Diagnosis: 0=UC, 1=CD; CRP: C-reactive protein; ESR: erythrocyte sedimentation rate; time onset-diagnosis: 1= < 3 months, 2= 3-6 months, 3= > 6 months.

Appendix 3. Protocols for CD8+ T cell separation (including MACS) (A), and preparation of samples for purity assessment (FACS) (B)

Recipes

1. *MACs Running Buffer (1 X PBS, 2mM EDTA, 0.5% BSA)*
   4ml 0.5M EDTA
   50ml 10% BSA Stock
   Make up to 1 litre with 1xPBS. Filter Sterilise.

2. *MACs Rinsing buffer (1xPBS 2mM EDTA)*
   996ml 1xPBS
   4ml 0.5M EDTA
   Filter Sterilise.

3. *MACs Cleaning Solution (70% Ethanol)*
   700ml absolute ethanol
   300ml MilliQ water

4. *Red Blood Cell Lysis Buffer*
   0.155M NH_4Cl [8.29g]
   12mM $NaHCO_3$ [1.0g]
   0.1M 0.5M EDTA [200µl]
   Make up to 1 litre with distilled water (Store at 4ºC)

5. *4% Sodium Citrate Solution*
   40g of sodium citrate made up to 1l with sterile MilliQ water.

6. *FACs Fixative solution (only use when don't have access to FACs)*
   12.5ml 40% formaldehyde
   10g glucose
   5ml 2% Azide
   Make up to 500ml with sterile PBS. Filter sterilise and store at room temperature.

A) CD8+ T cell separation from samples of peripheral blood

1. Set up ficoll gradient tubes (as indicated below): Pipette 15ml of Histopaque 1077 into the falcon tubes

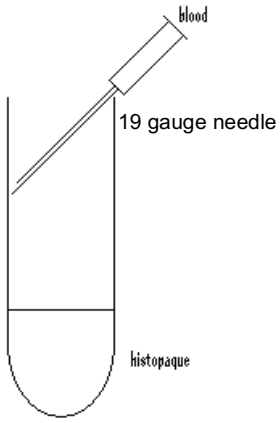

Age of the patient	No. of falcon tube with Ficoll
5-10 years	1
10-16	2

2. Collect appropriate volume of whole blood into 1x 50 ml Falcon tubes containing 4% sodium citrate solution and mix well by inversion.

Age of the patient	Volume of Blood (ml)	Volume of 4% sodium citrate (1ml/10ml of blood)
5-10 years	10	1
10-16	25	2.5

3. Aliquot 500ul of whole blood for DNA extraction. Put on ice. Store at -80C at the end of the protocol.

4. Transfer the rest of the blood to T25 flask. Add appropriate volume of rinsing buffer at room temperature (RT) and mix well.

Age of the patient	Volume of Blood (ml)	Volume of rinsing buffer(ml)
5-10 years	10	5
10-16	25	12.5

5. Pipette diluted blood into syringe sitting in ficoll gradient tube with 19 gauge (yellow) needle with bevelled edge positioned as in diagram above. Ensure each tube has the same volume. Layer no more than 35ml diluted blood over the histopaque.

6. Centrifuge at 1900 rpm for 20 minutes at RT with the brake off.

Blood cell separation

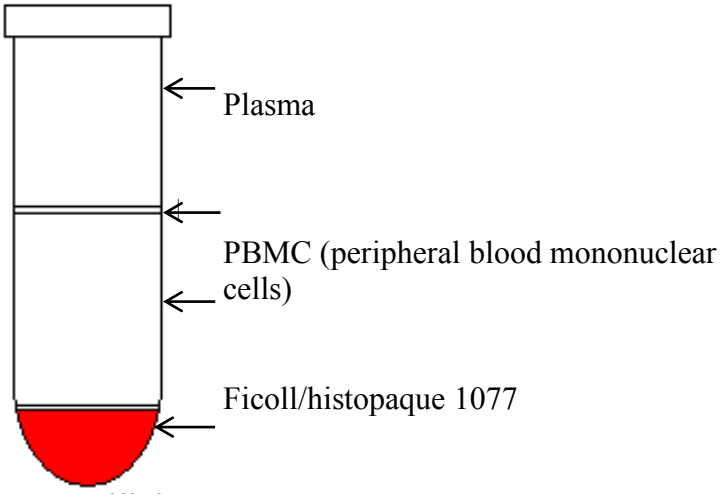

7. Using a 5ml pipette transfer the plasma (top layer) from tube into a 15ml Falcon tube (maximum 3ml/tube), taking care not to disturb PBMC interface. Store at - 80ºC.
8. Using a plastic Pasteur pipette remove the PBMC interface and transfer to a fresh 50 ml tube sitting on ice. Collect most of the Ficoll and the plasma layer. Make the volume up to 50 ml with rinsing buffer chilled to 4°C and mix by inversion.
9. Centrifuge at 2000 rpm for 10 minutes at 4ºC with the brake on.
10. Whilst PBMC tubes are spinning: using a pastette carefully remove any remaining ficoll layer from red blood cell pellet; dispose of the ficoll in the jar of virkon. Add 25 ml chilled red cell lysis buffer to the pellet. Mix well by inversion and incubate on ice for 30 minutes.
11. Proceed to CD8+ T cell isolation and granulocyte separation protocol.

$CD8^+$ T cell (from PBMC) isolation

12. Decant the supernatant from the PBMC tube into Virkon jar and disperse the cell pellets by flicking the tubes.
13. Re-suspend each cell pellet in 25 ml rinsing buffer chilled to 4°C.
14. Pool two tubes into one 50 ml Falcon tube
15. Centrifuge 1000-1250rpm for 7-10 minutes at 4ºC with the brake on (soft spin which leaves the platelets in suspension).
16. Decant the supernatant, disperse the cell pellets by flicking and re-suspend in 25 ml rinsing buffer chilled to 4°C.
17. Centrifuge 1000-1250rpm for 7-10 minutes at 4ºC with the brake on.
18. Decant the supernatant, disperse the cell pellet by flicking and re-suspend in a final volume of 10 ml chilled running buffer.
19. Remove a 5 ul aliquot of cells for PBMC count and dilute 20 fold with 95 ul trypan blue in a 0.5 ml eppendorf. Use haemocytometer for counting the number of live cells (white).

Total cell number:

Number counted x Dilution factor x 10^4 x Total volume of the cell suspension

20. Aliquot 20 ul for FACS analysis into 0.5 ml eppendorf labelled with 8p (unstained), 8p (CD8-APC), 8p (CD3-PE) and 8p (double stained) and keep on ice.
21. Centrifuge the PBMC at 1250 rpm for 7 minutes at 4ºC.
22. Decant supernatant and resuspend the pellet in 80 µl running buffer per 10^7 cells. [total no. cells / 10^7 = ___ x 80 ul = ___ ul running buffer].
23. Add 20 µl of CD8 microbeads per 10^7 cells. [volume running buffer/4 = ul microbeads].
24. Incubate in the fridge for 20-30 minutes.
25. After incubation add up to 5 ml of running buffer.
26. Centrifuge 1250 rpm for 7 minutes at 4ºC.
27. Decant supernatant and re-suspend the cell pellet in 600 µl running buffer.
28. Place CD8+ labelled cells on the autoMACS and place clean 15 ml Falcon tubes under the positive [CD8+ tube] and negative [CD8- tube] outlet ports.
29. Select cell separation programme. Positive fraction eluted will be $CD8^+$ T cells and the negative fraction eluted is the $CD8^-$ unlabelled flow through.
30. Run quickRINSE programme to clean autoMACS prior to next purification.
31. Remove a 5 ul aliquot of $CD8^-$ cells and dilute 20 fold with 95ul trypan blue in a 0.5 ml eppendorf and count the live cells using the haemocytometer.
32. Take 5 ul of positive fraction and dilute 2 fold with trypan blue, then count the live cells.
33. Optional: Remove 20ul aliquot of both the positive and negative fraction (8+, 8-) and keep on ice until the end of this protocol for FACS.
34. Centrifuge the cell suspension at 1250 rpm for 7mins at 4ºC.
35. Proceed to RNA preparation.

Granulocyte Separation

36. After 30 mins on ice, centrifuge the tube of lysed red blood cells at 1250 rpm for 7 mins at 4ºC, with brake.
37. Decant supernatant into virkon jar and disperse the pellet by flicking.
38. Add 25 ml chilled red cell lysis buffer to each tube and mix well by inversion.
39. Centrifuge 1250 rpm for 7 minutes at 4ºC.
40. Decant the supernatant into virkon jar and disperse the cell pellet.
41. Re-suspend each pellet in 25 ml chilled rinsing buffer. (Pool contents of both tubes).
42. Centrifuge 1250 rpm for 7 minutes at 4ºC.
43. Decant the supernatant into virkon jar and disperse the cell pellet by flicking.
44. Re-suspend the pellet in 10 ml chilled running buffer.
45. Remove a 5 ul aliquot of cells for granulocyte count and dilute 20 fold with 95 ul trypan blue in a 0.5 ml eppendorf: use haemocytometer for counting the number of live cells (white).

    Total cell number:

    Number counted x Dilution factor x 10^4 x Total volume of the cell suspension

46. Collect 20 ul aliquot for FACS analysis in tubes labelled with: Granulocytes (unstained), Granulocytes (CD15-FITC), Granulocytes (CD16-PE), Granulocytes (double stained).
47. Centrifuge granulocytes at 1250 rpm for 7 mins at 4ºC.
48. Proceed to RNA preparation.
49. Decant supernatant and disperse the cell pellet in appropriate volume of RLT Plus buffer to each sample:

    Note: Add 10ul of β–ME per 1ml of RLT Plus; make fresh each time

    300 µl <5x10^6 cells

    600 µl – 5x10^6 – 1x10^7 cells
50. Pipette thoroughly to mix and load samples onto Qiagen QIAshredder spin columns (maximum 700 µl). Centrifuge for 2 minutes at 14800 rpm.
51. Discard the column and store the flow-through at -80ºC for RNA/DNA extraction.

B) Sample Preparation for FACS

52. Add 200 ul of running buffer to each cell fraction and transfer to appropriately labelled FACS tubes.
53. Centrifuge the samples at 1250 rpm for 7mins at 4ºC.
54. Decant supernatant, disperse the cell pellet by dragging tubes along hedgehog holder and add the appropriate antibody cocktail to each tube (see table below). [Antibodies stored @ 4°, in dark. Keep on ice whilst using.]

Tube	Cells	Antibodies (20 µl of each)	
1	Unstained 8p	-	-
2	CD8p (CD8-APC)	-	CD8-APC
3	CD8p (CD3-PE)	CD3-PE	-
4	CD8p(double stained	CD3-PE	CD8-APC
5	CD8 +ve	CD3-PE	CD8-APC
6	CD8 -ve	CD3-PE	CD8-APC
7	Unstained granulocytes	-	-
8	Granulocytes(CD15-FITC),	CD15-FITC	-
9	Granulocytes (CD16-PE)	-	CD16-PE
10	Granulocytes (double stained)	CD15-FITC	CD16-PE

[One antibody is a selection marker specific for the cell type, the second antibody is used to check the purity of selected cells, i.e. it is non-specific and reacts with other cell types]

55. Incubate for 20 minutes at 4ºC.
56. Add 1 ml running buffer to each tube and centrifuge at 1250 rpm for 7mins at 4ºC. [Washes off excess antibody]
57. Decant the supernatant, disperse the cell pellet and add 300µl of FACs fixing buffer to each tube, cover with para-film and store in the fridge until ready to use.

Appendix 4. Paediatric Crohn's Disease Activity Index (PCDAI) [34]

ITEM POINTS
Abdominal pain None 0 Mild (brief episodes, not interfering with activities) 5 Moderate/severe (frequent or persistent, affecting with activities) 10
Stools 0-1 liquid stools, no blood 0 2-5 liquid or up to 2 semi-formed with small blood 5 Gross bleeding, >6 liquid stools or nocturnal diarrhoea 10
Patient functioning, general well-being (Recall, 1 week) No limitation of activities, well 0 Occasional difficulties in maintaining age appropriate activities, below par 5 Frequent limitation of activities, very poor 10
EXAMINATION
Weight Weight gain or voluntary weight loss 0 Involuntary weight loss 1-9% 5 Weight loss >10% 10
Height < 1 channel decrease (or height velocity > -SD) 0 > 1<2 channel decrease (or height velocity < -1SD> -2SD) 5 > 2 channel decrease (or height velocity < -2SD) 10
Abdomen No tenderness, no mass 0 Tenderness, or mass without tenderness 5 Tenderness, involuntary guarding, definite mass 10

Peri-rectal disease None, asymptomatic tags 0 1-2 indolent fistula, scant drainage, tenderness of abscess 5 Active fistula, drainage, tenderness or abscess 10
Extra-intestinal manifestations **Fever > 38.5 x 3 days in week, arthritis, uveitis, erythema nodosum, or pyoderma gangrenosum** None 0 One 5 Two 10
LABORATORY
Hct (%) < 10yrs: > 33 0; 28-33 5; < 28 10 11-14 (male): > 35 0; 30-34 5; < 30 10 15-19 (male): > 37 0; 32-36 5; < 32 10 11-19 (female): > 37 0; 32-36 5; < 32 10
ESR (mm/hr) < 20 0 20-50 2.5 > 50 5
Albumin (g/L) >35 0 31-34 5 <30 10

Appendix 4. Legend

Disease severity is defined by the following scores:

- severe: 40 or above
- moderate: 30-39
- mild: 10-29
- remission (disease not active): below 10

Appendix 5. Paediatric Ulcerative Colitis Activity Index (PUCAI) [35]

Item	Category/Points
Abdominal pain	No pain = 0 Pain can be ignored = 5 Pain cannot be ignored = 10
Rectal bleeding	None = 0 Small amount only, in less than 50% of stools = 10 Small amount with most stools =20 Large amount (50% of the stool content) = 30
Stool consistency of most stools	Formed = 0 Partially formed = 5 Completely unformed = 10
Number of stools per 24 hours	0-2 = 0 points 3-5 = 5 points 6-8 = 10 points >8 = 15 points
Nocturnal stools (any episode causing wakening)	no = 0 points yes = 10 points
Activity Level	No limitation of activity = 0 Occasional limitation of activity = 5 Severe restricted activity = 10
	Sum of PUCAI (0-85)

Appendix 5. Legend

Disease severity is defined by the following scores:

- severe: 65 or above;
- moderate: 35-64;
- mild: 10-34;
- remission (disease not active): below 10.

Appendix 6. Paris Classification for Paediatric IBD [13]

Crohn's Disease	
Age A1	• A1a <10 years; • A1b >10 <17 years.
Location (macroscopic only)	• L1 distal 1/3 ileum, ileum +cecum • L2 colon • L3 ileocolon • L4a upper disease proximal to Treitz, L4b distal to Treitz
Behaviour	• B1 non stricturing non-penetrating • B2 stricturing • B3 penetrating • B2,3 both stricturing and penetrating
Growth	• G0 no evidence of growth delay • G1 growth delay
Ulcerative Colitis	
Location (macroscopic only)	• E1 Proctitis • E2 Left sided • E3 Extensive • E4 Pancolitis
Disease activity	• S0 Never Severe • S1 Severe at any time (PUCAI ≥ 65)

Appendix 6. Legend

PUCAI: Paediatric Ulcerative Colitis Activity Index (see Appendix 4)

Appendix 7. Power Calculations

Patients were recruited in two consecutive phases, so the data was initially collected and analysed from a first group of 45 children (discovery cohort) and subsequently from a second group of 67 (validation).
The group size of our validation cohort exceeded the 50 cases recommended as per power calculations performed on the preliminary data obtained by the discovery cohort.

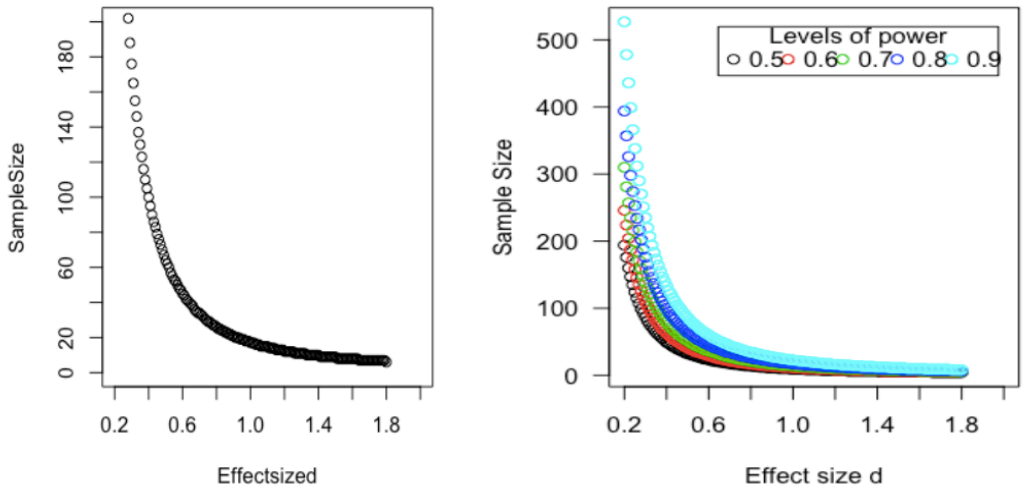

Figure A7. Power calculations to detect size of validation cohort based on preliminary results from the discovery cohort (n=45)

Power calculations were performed using the package "pwr" on R bioconductor.
The definition of power is the probability of detecting a specified effect at a specified significance level [169].
“Specified effect” refers to the effect size which can be the result of an experimental manipulation or the strength of a relationship between 2 variables. This effect size is ‘specified’ because prior to the power analysis we should set the size of the effect we expect to see. The ‘probability of detecting’ it refers to the ability of a test to detect an effect of a specified size. The recommended power is generally 0.8 which means we have an 80% chance of detecting an effect if one genuinely exists [169].
The main output of a power analysis is the estimation of a sufficient sample size.
For this study, we based on preliminary results from WGCNA in our discovery cohort (n=43). As explained above, WGCNA provides a measure of the correlation between modules (groups of genes with similar gene expression level) and clinical outcomes. Preliminary results from the WGCNA in our discovery cohort of 43 children with IBD showed top correlation index between modules and outcomes around 0.5. Aiming to reach an ideal correlation index of 0.8 in a larger cohort, we used a delta of 0.3 (30%) in our settings. Power was 0.8 and p-value < 0.05.
As shown in Figure, the sample size estimated for our validation cohort was around 50 samples.